

Morphology and molecular analyses reveal three new species of Botryosphaerales isolated from diseased plant branches in China

Lu Lin¹, Yukun Bai¹, Meng Pan¹, Chengming Tian¹, Xinlei Fan¹

¹ *The Key Laboratory for Silviculture and Conservation of Ministry of Education, Beijing Forestry University, Beijing 100083, China*

Corresponding author: Xinlei Fan (xinleifan@bjfu.edu.cn)

Academic editor: C. Sharma Bhunjun | Received 25 February 2023 | Accepted 10 April 2023 | Published 26 April 2023

Citation: Lin L, Bai Y, Pan M, Tian C, Fan X (2023) Morphology and molecular analyses reveal three new species of Botryosphaerales isolated from diseased plant branches in China. MycoKeys 97: 1–19. <https://doi.org/10.3897/mycokeys.97.102653>

Abstract

The Botryosphaerales represents an ecologically diverse group of fungi, comprising endophytes, saprobes, and plant pathogens. In this study, taxonomic analyses were conducted based on morphological characteristics and phylogenetic analyses of multi-gene sequence data from four loci (ITS, LSU, *tef1- α* , and *tub2*). Thirteen isolates obtained from Beijing and Yunnan Province were identified as seven species of Botryosphaerales, including *Aplosporella javeedii*, *Dothiorella alpina*, *Phaeobotryon aplosporum* and *Ph. rhois*, and three previously undescribed species, namely *Aplosporella yangqingensis*, *Dothiorella baihuashanensis*, and *Phaeobotryon platycladi*. Additionally, the new records of *Dothiorella alpina* from the host species *Populus szechuanica*, *Phaeobotryon aplosporum* from *Juglans mandshurica*, and *Phaeobotryon rhois* from *Populus alba* var. *pyramidalis* are included.

Keywords

Aplosporella, dieback, *Dothiorella*, *Phaeobotryon*, phylogeny, taxonomy

Introduction

The Botryosphaerales C.L. Schoch, Crous & Shoemaker is an ecologically diverse fungal order comprising endophytes, saprobes, and plant pathogens (Schoch et al. 2006; Ekanayaka et al. 2016; Phillips et al. 2019). Slippers et al. (2013) provided molecular

and morphological evidence to show that the Botryosphaeriales included six families (Aplosporellaceae Slippers, Boissin & Crous, Botryosphaeriaceae Theiss. & Syd., Melanopsaceae A.J.L. Phillips, Slippers, Boissin & Crous, Phyllostictaceae Fr., Planistromellaceae M.E. Barr, and Saccharataceae Slippers, Boissin & Crous). Then, Wyka and Broders (2016) introduced Septorioideaceae Wyka & Broders., Yang et al. (2017) introduced two new families (Endomelanconiopsisaceae Tao Yang & Crous and Pseudofusicoccumaceae Tao Yang & Crous). However, Phillips et al. (2019) argued that only six families (Aplosporellaceae, Botryosphaeriaceae, Melanopsaceae, Phyllostictaceae, Planistromellaceae and Saccharataceae) could be accepted in Botryosphaeriales, with reducing Endomelanconiopsisaceae, Pseudofusicoccumaceae, and Septorioideaceae to the synonymy under Botryosphaeriaceae, Phyllostictaceae, and Saccharataceae, respectively. In the present study, thirteen isolates were classified as three genera (*Aplosporella* Speg., *Botryosphaeria* Ces. & De Not., and *Phaeobotryon* Theiss. & Syd.) in two families (Aplosporellaceae and Botryosphaeriaceae).

Aplosporellaceae was introduced by Slippers et al. (2013) to accommodate two genera viz. *Aplosporella* and *Bagnisiella* Speg. However, Slippers et al. (2013) suggested that *Aplosporella* and *Bagnisiella* should be synonymized based on their close phylogenetic relationships and their remarkably similar multiloculate sporocarps. Ekanayaka et al. (2016) agreed with this and provided evidence that the sexual morph of *Aplosporella thailandica* Ekanayaka, Dissanayaka, Q. Zhao & K.D. Hyde resembles *Bagnisiella*. Phillips et al. (2019) formally placed *Bagnisiella* as a synonym of *Aplosporella*. Sharma et al. (2017) introduced *Alanomyces* Roh. Sharma in Aplosporellaceae based on four loci phylogeny. Therefore, two genera (*Alanomyces* and *Aplosporella*) can be accepted in Aplosporellaceae. The morphological characters of *Aplosporellaceae* are multiloculate ascostromata, septate pseudoparaphyses, aseptate and ellipsoid to ovoid ascospores, and ellipsoid to subcylindrical and hyaline to pigmented conidia (Slippers et al. 2013; Phillips et al. 2019).

Botryosphaeriaceae was introduced by Theissen and Sydow (1918) for three genera (*Botryosphaeria*, *Phaeobotryon*, and *Dibotryon* Theiss. & Syd.). Over the years the family and genera have undergone several taxonomic revisions and updates. Currently, the Botryosphaeriaceae has approximately 100 verified species in 24 genera, according to DNA sequence data (Phillips et al. 2013; Slippers et al. 2013; Yang et al. 2017; Xiao et al. 2021; Zhang et al. 2021). *Botryosphaeria* has uniloculate and clustered ascostromata and septate pseudoparaphyses (Phillips et al. 2019). In the phylogenetic tree of Botryosphaeriaceae, hyaline or colored conidia or ascospores are distributed randomly (Slippers et al. 2013). A large number of new species have been described in recent years, which indicated that the diversity of Botryosphaeriaceae was worthy of further exploration (Bezerra et al. 2021; Zhang et al. 2021; Sun et al. 2022).

With the modern taxonomic approaches applying, more than 30 novel species have been identified in the last five years (Zhang et al. 2021; Rathnayaka et al. 2022; Sun et al. 2022; Wang et al. 2023). Considering the important economic status of Botryosphaeriales, a survey to explore more hidden species of Botryosphaeriales was considered imperative. Thus, a survey on the diversity of Botryosphaeriales on diseased branches was conducted in Beijing and Yunnan Province from 2021 to 2022. In this

study, we introduce three new species, in which *Aplosporella yanqingensis* and *Phaeobotryon platycladi* were collected from *Platycladus orientalis* and *Dothiorella baihuashanensis* were collected from *Juniperus chinensis* in China. Moreover, the newly discovered *Dothiorella alpina* from *Populus szechuanica*, *Phaeobotryon aplosporum* from *Juglans mandshurica*, and *Ph. rhois* from *Populus alba* var. *pyramidalis* are featured.

Materials and methods

Fungal isolation

Fresh specimens (woody branches and twigs with canker or dieback symptoms) were randomly collected in Beijing and Yunnan Province from the summer of 2021 to the autumn of 2022. The specimens were packed in kraft paper bags and transferred to the laboratory for fungal isolation following Jiang et al. (2022). Isolates were obtained by removing the spore mass from conidiomata to sterilised distilled water using sterilised needle, and generating single spore colonies on potato dextrose agar (PDA: 200 g potatoes, 20 g dextrose, 20 g agar per L) at 25 °C in the dark. After three to five days, hyphal tips were transferred to new PDA plates twice to obtain a pure culture. The cultures are deposited in the China Forestry Culture Collection Center (CFCC; <http://www.cfcc-caf.org.cn/>), and the specimens in this study are deposited in the Museum of the Beijing Forestry University (BJFC).

Morphology

Morphological observations were conducted based on conidiomata produced on infected plant tissues. The conidiomata were manually sectioned using a double-edged blade and examined under a dissecting microscope for macroscopic and microscopic characterization, while conidiomata structure and size were imaged with a Leica stereomicroscope (M205) (Leica Microsystems, Wetzlar, Germany). Conidia and other microstructures were selected randomly for observation using a Nikon Eclipse 80i microscope (Nikon Corporation, Tokyo, Japan) equipped with a Nikon digital sight DSRi2 high-definition colour camera with differential interference contrast (DIC). Fifty conidia were measured per species, and 30 measurements were taken of other morphological structures. Colony characters i.e. colours and texture on PDA and MEA (malt extract agar; 30 g malt extract, 5 g mycological peptone, 15 g agar per L) at 25 °C were observed and noted over 14 days. The colony colours were determined based on the colour charts of Rayner (1970).

DNA extraction, amplification and sequencing

The fresh mycelium from PDA was scraped and put it in a 1.5 mL centrifuge tube for genomic DNA extraction which used the modified CTAB (cetyltrimethylammonium bromide) method (Doyle and Doyle 1990). For initial species confirmation, the

internal transcribed spacer (ITS) region was sequenced using the primer pairs ITS1/ITS4 (White et al. 1990) for all isolates. The BLAST tool (<https://blast.ncbi.nlm.nih.gov/Blast.cgi>) was used to compare the resulting sequences with those in GenBank. After confirmation to the genus level, additional partial loci were amplified, including the nuclear ribosomal large subunit (LSU), the partial translation elongation factor 1-alpha (*tef1- α*), and partial beta-tubulin (*tub2*) using the primer pairs LR0R/LR5 (Vilgalys and Hester 1990), EF1-728F/EF1-986R (Carbone and Kohn 1999), and Bt2a/Bt2b (Glass and Donaldson 1995), respectively. The additional combination of T1 and Bt2b (Glass and Donaldson 1995; O'Donnell and Cigelnik 1997) was used in case of amplification failure of the primer Bt2a and Bt2b. The genes used in different genera and the amplification conditions are listed in Table 1. The PCR mixture for all regions consisted of 1 μ L DNA template, 1 μ L each 10 μ M primer, 10 μ L T5 Super PCR Mix (containing Taq polymerase, dNTP and Mg²⁺, Beijing TisingKe Biotech Co., Ltd., Beijing, China), and 7 μ L sterile water. PCR products were electrophoresed in 1% agarose gel and the DNA was sequenced by the SinoGenoMax Company Limited (Beijing, China). The forward and reverse reads were edited and assembled with Seqman v. 7.1.0 in the DNASTAR Lasergene core suite software (DNASTAR Inc., Madison, Wisconsin USA). All sequences generated in this study were submitted to GenBank (Suppl. material 1).

Phylogenetic analyses

The sequences obtained in this study were supplemented with additional sequences obtained from GenBank (Suppl. material 1) based on BLAST searches and from relevant published literature on the related genera (Bezerra et al. 2021; Wijayawardene et al. 2021; Xiao et al. 2021; Zhang et al. 2021; Peng et al. 2023). The individual data-sets of each gene region were aligned separately using MAFFT v. 6.0 (Kato and Standley 2013) and trimmed at both terminal ends in MEGA v. 6.0 (Tamura et al. 2013). Maximum Likelihood (ML) analyses were conducted for the single gene sequence data sets (ITS and *tef1- α* regions for *Aplosporella*; ITS, *tef1- α* , and *tub2* regions for *Dothiorella*; ITS, LSU, and *tef1- α* regions for *Phaeobotryon*). Then the combined data set of each genus of all gene regions were used for multi-gene phylogenetic analyses including Maximum Likelihood (ML) and Bayesian Inference (BI) analyses. *Alanomyces indica* (CBS 134264), *Lasiodiplodia americana* (CFCC 50065), and *Alanphillipsia aloecicola* (CBS 138896) were selected as the outgroup taxa for *Aplosporella*, *Dothiorella*, and *Phaeobotryon* analyses respectively.

Table 1. Genes used in this study with PCR primers and optimal annealing temperature.

Locus	PCR primers	PCR: thermal cycles: (Annealing temp. in bold)	Genus
ITS	ITS1/ITS4	(95 °C: 30 s, 51 °C : 30 s, 72 °C: 1 min) × 35 cycles	<i>Aplosporella</i> , <i>Dothiorella</i> , <i>Phaeobotryon</i>
LSU	LR0R/LR5	(95 °C: 45 s, 55 °C : 45 s, 72 °C: 1 min) × 35 cycles	<i>Phaeobotryon</i>
<i>tef1-α</i>	EF1-728F/EF1-986R	(95 °C: 15 s, 55 °C : 20 s, 72 °C: 1 min) × 35 cycles	<i>Aplosporella</i> , <i>Dothiorella</i> , <i>Phaeobotryon</i>
<i>tub2</i>	Bt2a/Bt2b	(95 °C: 30 s, 55 °C : 30 s, 72 °C: 1 min) × 35 cycles	<i>Dothiorella</i>
	T1/Bt2b		

Maximum Likelihood (ML) analyses were conducted using PhyML v. 3.0 (Guindon et al. 2010), employing a GTR model of site substitution with 1000 bootstrap replicates (Stamatakis 2014). Bayesian Inference (BI) analyses were conducted based on the DNA dataset from the results of the MrModeltest v. 2.4 (Nouri et al. 2004) using a Markov Chain Monte Carlo (MCMC) algorithm in MrBayes v. 3.1.2 (Ronquist and Huelsenbeck 2003). Two MCMC chains were run from random trees for 1,000,000 generations, resulting in a total of 10,000 trees. The first 25% of trees sampled were discarded as the burn-in phase of each analysis. The posterior probabilities (BPP) were calculated from the remaining trees (Rannala and Yang 1996). Phylogenetic trees were shown using FigTree v. 1.4.4 (Rambaut 2018) and processed by Adobe Illustrator 2019.

Results

Phylogenetic analyses

The BLAST results indicated that the 13 isolates in this study resided in *Aplosporella*, *Dothiorella*, and *Phaeobotryon*. Datasets for the three genera, the number of characters of each gene with gaps and the substitution models used for BI analyses are provided in Table 2. The topologies of BI analyses did not significantly differ from the ML analyses.

Species of *Aplosporella*

Five isolates clustered into two phylogenetic groups for the individual genes (ITS and *tef1- α*), as well as the combined gene dataset (Fig. 1). In ML analysis based on the combined gene dataset, the matrix had 221 distinct alignment patterns. Estimated base frequencies are as follows: A = 0.211117, C = 0.277509, G = 0.253698, T = 0.257676; substitution rates: AC = 3.242352, AG = 4.568839, AT = 2.135067, CG = 2.137396, CT = 5.690231, GT = 1.000000; gamma distribution shape parameter: α = 0.217402. The isolates CFCC 58330, 58329, and 58412 resided in a clade with *Aplosporella javeedii* (ML/BI = 98/1.00), while the isolates CFCC 58791 and 58792 formed an individual clade distinct from the other species in *Aplosporella* (ML/BI = 100/1.00).

Table 2. Substitution models used for Bayesian analyses in this study.

Analyses	Number of ingroup sequences	outgroup	Substitution models used for Bayesian analyses/ Number of characters with gaps			
			ITS	LSU	<i>tef1</i>	<i>tub2</i>
<i>Aplosporella</i> 2-genes	24	<i>Alanomyces indica</i> CBS 134264	SYM+G /553	–	GTR+G /417	–
<i>Dothiorella</i> 3-genes	66	<i>Lasiodiopodia americana</i> CFCC 50065	GTR+I+G /494	–	GTR+G /322	GTR+I+G /448
<i>Phaeobotryon</i> 3-genes	36	<i>Alanphillipsia aloicola</i> CBS 138896	GTR+I /488	HKY+I /562	HKY+G/299	–

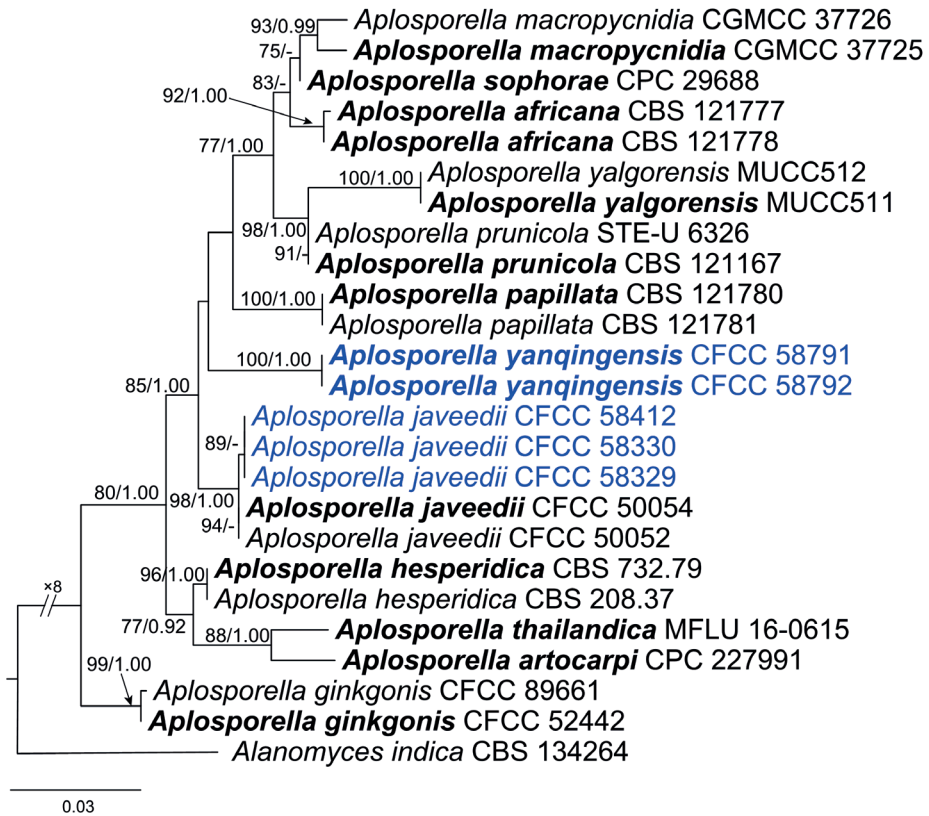


Figure 1. Phylogram of *Aplosporella* resulting from a maximum likelihood analysis based on combined ITS and *tef1* loci. Numbers above the branches indicate ML bootstrap values (ML-BS \geq 70%) and Bayesian Posterior Probabilities (BPP \geq 0.9). The tree is rooted with *Alanomyces indica* CBS 134264. Ex-type isolates are in bold. Isolates from the present study are marked in blue.

Species of *Dothiorella*

Three isolates clustered in two clades for the individual genes (ITS, *tef1- α* , and *tub2*), as well as the combined gene dataset (Fig. 2). In ML analysis based on the combined gene dataset, the matrix had 478 distinct alignment patterns. Estimated base frequencies are as follows: A = 0.203201, C = 0.315247, G = 0.248158, T = 0.233395; substitution rates: AC = 0.994643, AG = 2.280369, AT = 1.123589, CG = 0.895887, CT = 4.309165, GT = 1.000000; gamma distribution shape parameter: α = 0.210467. The isolate CFCC 58299 grouped with *Do. alpina* (ML/BI = 84/0.95), while the isolates CFCC 58549 and 58788 formed a distinct clade from the other species (ML/BI = 100/1.00).

Species of *Phaeobotryon*

Five isolates clustered into three clades for the individual genes (ITS, LSU, and *tef1- α*), as well as the combined gene dataset (Fig. 3). In ML analysis based on the combined gene dataset, the matrix had 223 distinct alignment patterns. Estimated base frequencies are as

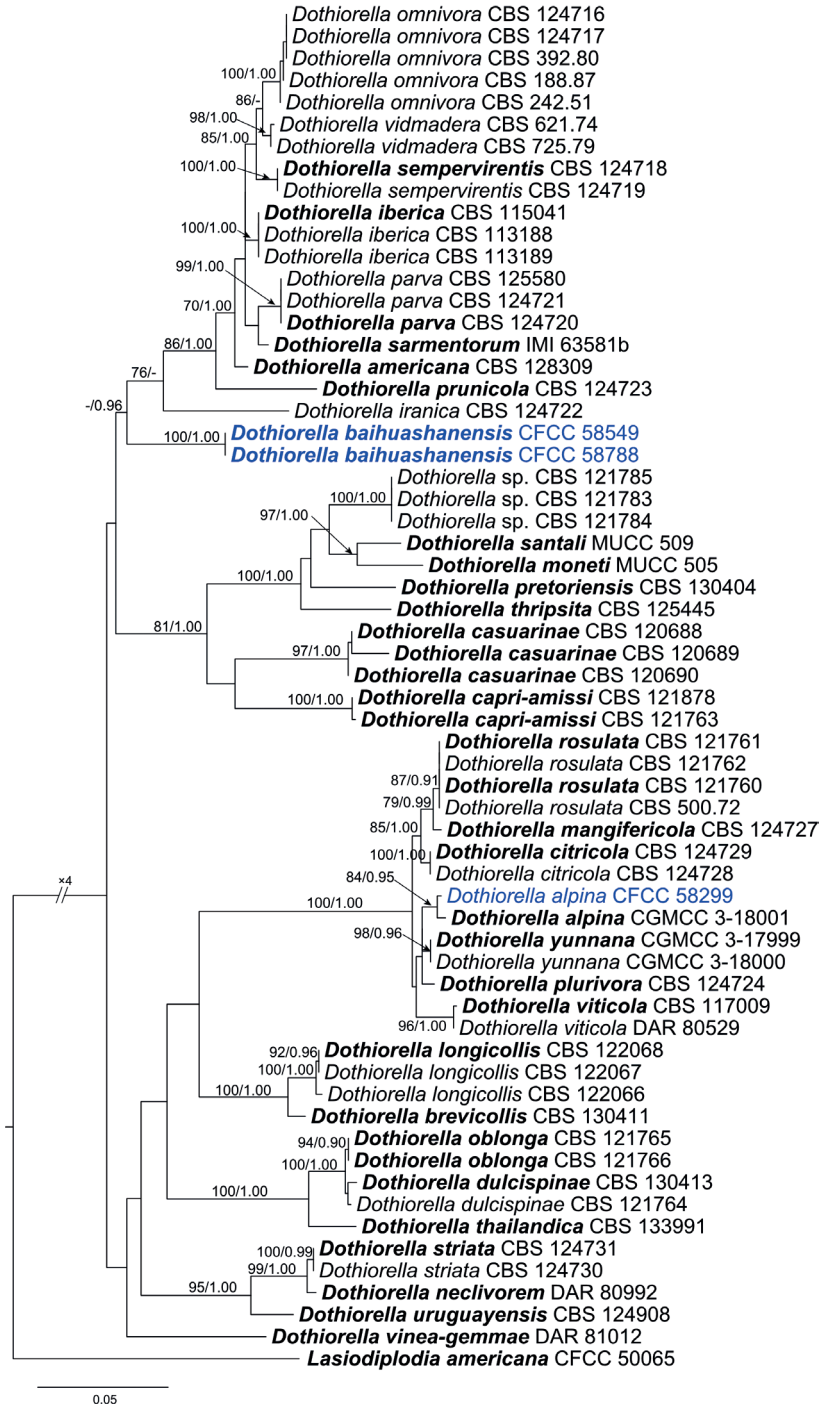


Figure 2. Phylogram of *Dothiorella* resulting from a maximum likelihood analysis based on combined ITS, *tef1* and *tub2* loci. Numbers above the branches indicate ML bootstrap values (ML-BS $\geq 70\%$) and Bayesian Posterior Probabilities (BPP ≥ 0.9). The tree is rooted with *Lasiodiplodia americana* CFCC 50065. Ex-type isolates are in bold. Isolates from the present study are marked in blue.

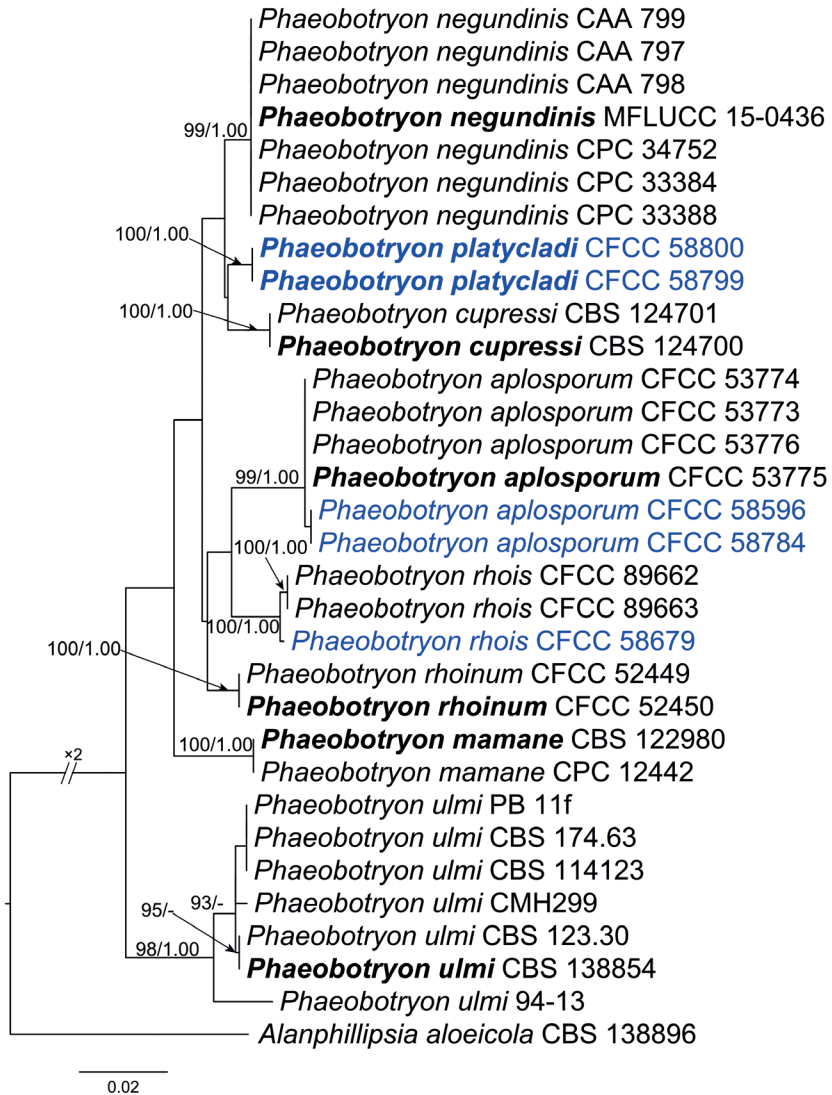


Figure 3. Phylogram of *Phaeobotryon* resulting from a maximum likelihood analysis based on combined ITS, LSU, and *tef1* loci. Numbers above the branches indicate ML bootstrap values (ML-BS \geq 70%) and Bayesian Posterior Probabilities (BPP \geq 0.9). The tree is rooted with *Alanphillipsia aloecicola* CBS 138896. Ex-type isolates are in bold. Isolates from the present study are marked in blue.

follows: A = 0.223233, C = 0.267753, G = 0.277657, T = 0.231357; substitution rates: AC = 0.862696, AG = 2.117465, AT = 0.455729, CG = 1.132740, CT = 4.957268, GT = 1.000000; gamma distribution shape parameter: α = 0.272408. The isolate CFCC 58679 grouped with *Ph. rhois* (ML/BI = 100/1.00). The isolates CFCC 58596 and 58784 formed a unique lineage distinct from, but related to *Ph. aplosporum* as their closest relatives (ML/BI = 99/1.00). The isolates CFCC 58799 and 58800 formed a clade of their own separating them from other *Phaeobotryon* lineages (ML/BI = 100/1.00).

Taxonomy

Based on DNA sequences and morphology, seven species belonging to three genera were identified. Of these, *Aplosporella javeedii*, *Dothiorella alpina*, *Phaeobotryon aplosporum*, and *Pb. rhois* are known species. The remaining three species are identified as new species (*Aplosporella yanqingensis*, *Dothiorella baihuashanensis*, and *Phaeobotryon platycladi*) and described below. Collect information and notes of all seven species were provided.

***Aplosporella javeedii* Jami, Gryzenh., Slippers & M.J. Wingf., Fungal Biol. 118(2): 174 (2013)**

Description. See Fan et al. 2015.

Materials examined. CHINA, Yunnan Province, Kunming City, Panlong District, Jinma County, Bailongsi Town, 25°3'44"N, 102°45'22"E, on dead branches of *Populus canadensis*, 11 August 2022, Lu Lin & Ziqiang Wu (BJFC CF20230101, living culture CFCC 58330). Beijing City, Mentougou District, G109 National Highway, 40°3'2"N, 115°52'58"E, on dead branches of *Populus beijingensis*, 25 August 2022, Lu Lin & Xinlei Fan (BJFC CF20230102, living culture CFCC 58329). Changping District, Liucun Town, Wangjiayuan Village, 40°10'23"N, 116°4'9"E, on dead branches of *Populus alba* var. *pyramidalis*, 22 September 2022, Lu Lin & Xinlei Fan (BJFC CF20230103, living culture CFCC 58412).

Notes. *Aplosporella javeedii* was first discovered on *Celtis africana* and *Searsia lancea* in South Africa (Jami et al. 2014). Fan et al. (2015), Zhu et al. (2018), and Pan et al. (2019) expanded the host range of *Aplosporella javeedii* to more than ten host families in China. This species has not been reported outside South Africa and China.

***Aplosporella yanqingensis* L. Lin & X.L. Fan, sp. nov.**

Mycobank No: 847680

Fig. 4

Etymology. Named after the collection site of the type specimen, Yanqing District in Beijing City.

Description. Conidiomata pycnidial, immersed to semi immersed, erumpent from bark surface, multilocular, 650–1500 µm in diam. Disc straw to greenish olivaceous, circular to ovoid, 350–650 µm in diam, with one central ostiole per disc. Ostioles inconspicuous, sometimes covered below disc by lighter entostroma, 100–300 µm in diam. Locules multiple, irregularly arranged, subdivided frequently by invaginations with common walls. Conidiophores reduced to conidiogenous cells. Conidiogenous cells hyaline, phialidic, 6.0–13.5 × 2.0–3.0 µm (av. ± S.D. = 10.7 ± 2.0 × 2.5 ± 0.2 µm). Paraphyses present, hyaline, smooth-walled, septate, unbranched, 26.5–37.5 × 2.0–3.0 µm (av. ± S.D. = 32.0 ± 3.5 × 2.4 ± 0.3 µm). Conidia aseptate, smooth, ellipsoid to subcylindrical,

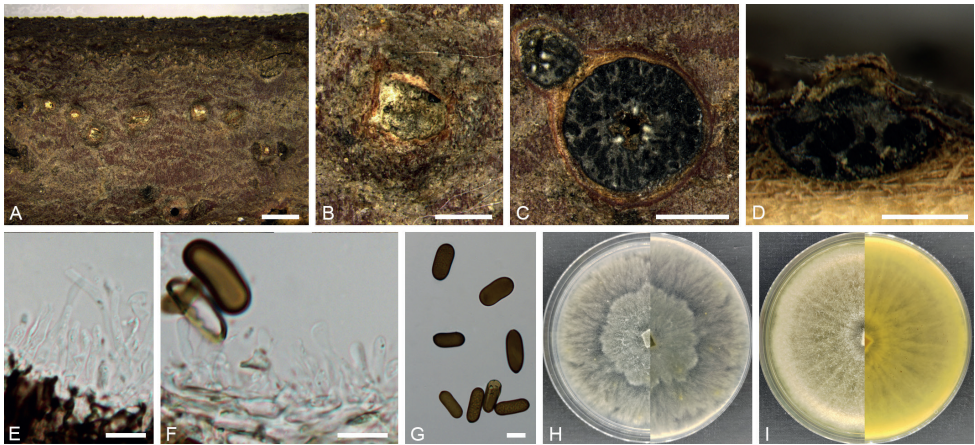


Figure 4. *Aplosporella yanqingensis* (BJFC CF20230104) **A, B** habit of conidiomata on twig **C** transverse section of conidiomata **D** longitudinal section through a conidioma **E, F** conidiogenous cells and paraphyses **G** conidia **H** colony on PDA at 14 days **I** colony on MEA at 14 days. Scale bars: 2 mm (**A**); 1 mm (**C**); 500 μm (**B, D**); 10 μm (**E–G**).

brown when mature, 16.0–21.5 \times 6.0–9.5 μm (av. \pm S.D. = 18.5 \pm 1.3 \times 7.7 \pm 0.7 μm). Sexual morph not observed.

Culture characters. Colonies on PDA spreading, white to pale grey, covering a 90 mm plate after 14 days at 25 °C. Colonies on MEA spreading, uniform with appressed aerial mycelium and crenate edge, upper white, reverse pale luteous covering a 90 mm plate after 14 days at 25 °C.

Materials examined. CHINA, Beijing City, Yanqing District, Yeyahu National Wetland Park, 40°24'55.43"N, 115°50'26.42"E, on branches of *Platyclusus orientalis*, 25 July 2022, Yukun Bai & Xinlei Fan (holotype BJFC CF20230104, ex-holotype culture CFCC 58791); 40°24'55.46"N, 115°50'26.42"E, on branches of *Platyclusus orientalis*, 25 July 2022, Yukun Bai & Xinlei Fan (paratype BJFC CF20230105, ex-paratype culture CFCC 58792).

Notes. In the multi-gene analyses, *A. yanqingensis* is distinct and forms a moderately supported lineage clade (Fig. 1). In the ITS tree, *A. yanqingensis* shows a close relationship with a clade containing *A. africana* F.J.J. Van der Walt, Slippers & G.J. Marais, *A. macropycnidia* Dou & Y. Zhang ter, *A. papillata* F.J.J. Van der Walt, Slippers & G.J. Marais, *A. prunicola* Damm & Crous, *A. sophorae* Crous & Thangavel, and *A. yalgorensis* K.M. Taylor, P.A. Barber & T.I. Burgess. However, it differs from *A. africana* by longer conidia (18.5 \times 7.7 vs. 14 \times 8.5 μm) (Slippers et al. 2014), differs from *A. macropycnidia* by shorter paraphyses (32.0 \times 2.4 vs. 38.4 \times 2.9 μm) (Dou et al. 2017), differs from *A. papillata* by larger conidiogenous cells (10.7 \times 2.5 vs. 7.4 \times 2 μm) (Slippers et al. 2014), and differs from *A. prunicola* and *A. yalgorensis* by smaller conidia (18.5 \times 7.7 vs. 20.2 \times 11 for *A. prunicola* and 19.9 \times 10.7 for *A. yalgorensis*) (Damm et al. 2007; Taylor et al. 2009). Besides, *A. yanqingensis* differs from

A. sophorae by 25/528 in ITS region. Therefore, *A. yanqingensis* is introduced herein as a novel species. This is a new record of species in *Aplosporella* occurring on the host genus *Platycladus*.

***Dothiorella alpina* (Y. Zhang ter. & Min Zhang) Phookamsak & Hyde, Asian Journal of Mycology 3(1): 168 (2020)**

= *Spencermartinsia alpina* Y. Zhang ter. & Ming Zhang, Mycosphere 7(7): 1058 (2016).

Description. See Hyde et al. 2020.

Materials examined. CHINA, Yunnan Province, Diqing Tibetan Autonomous Prefecture, Shangri-La City, Sanba County, East Ring Road, 27°36'18"N, 100°1'19"E, on dead branches of *Populus szechuanica*, 9 August 2022, Lu Lin & Min Lin (BJFC CF20230106, living culture CFCC 58299).

Notes. *Dothiorella alpina* was first introduced by Zhang et al. (2016a) as *Spencermartinsia alpina*, which has dark brown and 1-septate conidia. Hyde et al. (2020) transfer *S. alpina* to *Dothiorella* based on phylogenetic analyses of a concatenated dataset (ITS+*tefl*- α) and morphological similarity. *Dothiorella alpina* was recorded on *Cirus unshiu* in Hunan Province, China, and *Platycladus orientalis* and *Ipomoea* sp. in Yunnan Province, China. In this study, a new record of *Do. alpina* from the host *Populus szechuanica* is included.

***Dothiorella baihuashanensis* L. Lin & X.L. Fan, sp. nov.**

MycoBank No: 847681

Fig. 5

Etymology. Named after the collection site of the type specimen, Baihuashan Natural Scenic Area in Beijing City.

Description. Conidiomata pycnidial, superficial or immersed, separate, ovoid, 350–500 μm in diam, occasionally aggregated into botryose clusters. Disc black, 200–300 μm in diam. Ostioles single, central, papillate. Conidiophores reduced to conidiogenous cells. Conidiogenous cells hyaline, holoblastic, cylindrical to subcylindrical or broadly lageniform, 7.5–16.0 \times 3.5–6.5 μm (av. \pm S.D. = 11.7 \pm 2.2 \times 4.6 \pm 0.7 μm). Conidia 1-septate, hazel to blackish brown, mostly truncate at the base and constricted at the septum or with a thickening at the base of the septum, moderately thick-walled, ovoid or oblong to ellipsoidal, 22.5–35.0 \times 11.0–19.0 μm (av. \pm S.D. = 27.9 \pm 2.9 \times 14.3 \pm 2.2 μm).

Culture characters. Colonies on PDA spreading, covering a 90 mm plate after 14 days at 25 °C, upper white to pale grey, reverse buff to dark grey. Colonies on MEA spreading, covering a 90 mm plate after 14 days at 25 °C, uniform with appressed aerial mycelium and crenate edge, upper white to pale grey, reverse honey to dark grey.

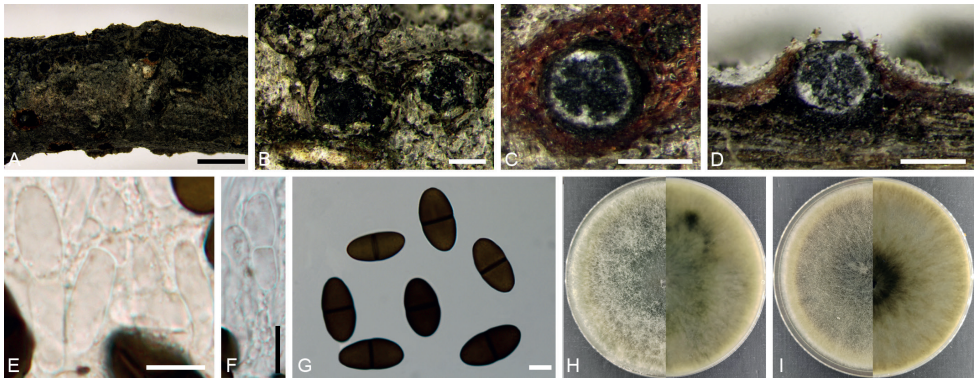


Figure 5. *Dothiorella baihuashanensis* (BJFC CF20230107) **A, B** habit of conidiomata on twig **C** transverse section of a conidioma **D** longitudinal section through a conidioma **E, F** conidiogenous cells **G** conidia **H** colony on PDA at 14 days **I** colony on MEA at 14 days. Scale bars: 1 mm (**A**); 200 μ m (**B–D**); 10 μ m (**E–G**).

Materials examined. CHINA, Beijing City, Mentougou District, Qingshui County, Baihuashan Natural Scenic Area, 39°50'18.21"N, 115°34'21.13"E, on dead branches of *Juniperus chinensis*, 23 August 2022, Lu Lin & Xinlei Fan (holotype BJFC CF20230107, ex-holotype culture CFCC 58549); 39°50'18.16"N, 115°34'21.24"E, on dead branches of *Juniperus chinensis*, 23 August 2022, Lu Lin & Xinlei Fan (paratype BJFC CF20230108, ex-paratype culture CFCC 58788).

Notes. The isolates CFCC 58549 and 58788 in this study formed a distinct lineage in the phylogenetic trees of each individual gene (ITS, *tef1- α* , and *tub2*) and the combined gene dataset (Fig. 2). They were isolated from the branches *Juniperus chinensis*. *Dothiorella iberica* was also recorded to host genus *Juniperus* (Alves et al. 2013). However, these two species are not closely related in our phylogenetic analysis.

Phaeobotryon aplosporum M. Pan & X.L. Fan, Mycol. Prog. 18(11): 1356 (2019)

Description. See Pan et al. 2019.

Materials examined. CHINA, Beijing City, Mentougou District, Qingshui County, Baihuashan Natural Scenic Area, 39°51'11"N, 115°32'37"E, on dead branches of *Juglans mandshurica*, 23 August 2022, Lu Lin & Xinlei Fan (BJFC CF20230112, living culture CFCC 58596; BJFC CF20230113, living culture CFCC 58784).

Notes. *Phaeobotryon aplosporum* was first discovered from *Rhus typhina* and *Syzygium aromaticum* (Pan et al. 2019). It can be distinguished from other species in *Phaeobotryon* by its aseptate conidia (Pan et al. 2019). In this study, the conidia formed on the specimen BJFC CF20230112 are dark brick when mature, aseptate, (16.5–20.0 \times 6.0–9.0 μ m (av. \pm S.D. = 18.3 \pm 1.1 \times 7.5 \pm 0.8 μ m), which overlap with the morphological characteristics described by Pan et al. (2019). Phylogenetically,

the isolates CFCC 58596 and 58784 were clustered in a clade with *Ph. aplosporum* with high statistical support (ML/Bi = 99/1). Therefore, the isolates CFCC 58596 and 58784 are identified as *Ph. aplosporum*. The current study extends its host range to *Juglans mandshurica*.

***Phaeobotryon platycladi* L. Lin & X.L. Fan, sp. nov.**

Mycobank No: 847682

Fig. 6

Etymology. Named after the host genus, *Platycladus*.

Description. Conidiomata pycnidial, scattered, subglobose to globose, erumpent, exuding faint yellow translucent conidial droplets from central ostioles, unilocular, 150–250 μm diam. Disc black, 80–200 μm in diam. Ostioles single, central, papillate, 21–35 μm . Conidiophores reduced to conidiogenous cells. Conidiogenous cells hyaline, smooth, thin-walled, cylindrical, holoblastic, phialidic, proliferating internally with visible periclinal thickening, 5.5–14.0 \times 2.5–4.0 μm (av. \pm S.D. = 10.2 \pm 2.5 \times 3.2 \pm 0.4 μm). Conidia initially hyaline, oval, both ends broadly rounded, aseptate, rarely becoming 1-septate, 23.0–31.0 \times 9.5–12.5 μm (av. \pm S.D. = 26.2 \pm 2.5 \times 10.8 \pm 0.8 μm).

Culture characters. Colonies on PDA spreading, upper white to buff, reverse buff to isabelline covering a 90 mm plate after 14 days at 25 $^{\circ}\text{C}$. Colonies on MEA spreading, stratiform, with appressed aerial mycelium and crenate edge, upper white to isabelline, reverse buff to hazel, covering a 90 mm plate after 14 days at 25 $^{\circ}\text{C}$.

Materials examined. CHINA, Beijing City, Haidian District, National Botanic Gardens, 39 $^{\circ}$ 59'42.41"N, 116 $^{\circ}$ 12'47.24"E, on dead branches of *Platycladus orientalis*,

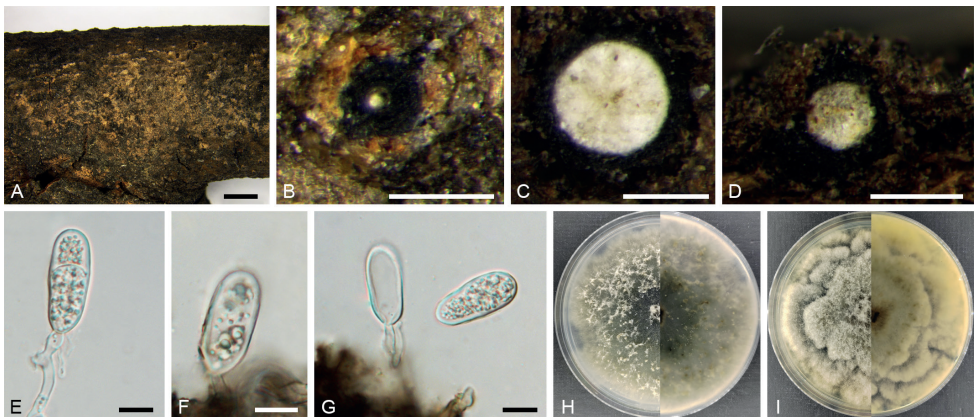


Figure 6. *Phaeobotryon platycladi* (BJFC CF20230110) **A, B** habit of conidiomata on twig **C** transverse section of a conidioma **D** longitudinal section through a conidioma **E–G** conidiogenous cells and conidia **H** colony on PDA at 14 days **I** colony on MEA at 14 days. Scale bars: 2 mm (**A**); 200 μm (**B–D**); 10 μm (**E–G**).

4 August 2022, Yukun Bai & Xinlei Fan (holotype BJFC CF20230110, ex-holotype culture CFCC 58799); 39°59'42.43"N, 116°12'47.46"E, on dead branches of *Platyclusus orientalis*, 4 August 2022, Yukun Bai & Xinlei Fan (paratype BJFC CF20230111, ex-paratype culture CFCC 58800).

Notes. *Phaeobotryon platycladi* is monophyletic with *Ph. cupressi* in the phylogenetic tree without a significant statistical support. Conidial sizes of the two species overlap, but there are differences in 6/488 in ITS region, 3/556 in LSU region, and 18/293 in *tefl*- α gene with gaps.

***Phaeobotryon rhois* C.M. Tian, X.L. Fan & K.D. Hyde, Phytotaxa 205(2): 95 (2015)**

Description. See Fan et al. 2015.

Materials examined. CHINA, Beijing City, Yanqing District, Zhangshanying County, 40°28'33"N, 115°49'58"E, on dead branches of *Populus alba* var. *pyramidalis*, 16 September 2022, Lu Lin & Chengming Tian (BJFC CF20230109, living culture CFCC 58679).

Notes. *Phaeobotryon rhois* was first discovered on *Rhus typhina* distributed in Ningxia Province, China (Fan et al. 2015). Pan et al. (2019) reported this species from *Dioscorea nipponica*, *Platyclusus orientalis* and *Rhamnus davurica* in Beijing, China. The current study extends its host range to *Populus alba* var. *pyramidalis*.

Discussion

In this study, a total of 13 isolates are identified as seven species of Botryosphaeriales, including three new species (*Aplosporella yanqingensis*, *Dothiorella baihuashanensis*, and *Phaeobotryon platycladi*) and four known species (*A. javeedii*, *Do. alpina*, *Ph. aplosporum*, and *Ph. rhois*). All three new species were isolated from coniferous trees: *A. yanqingensis* and *Ph. platycladi* from *Platyclusus orientalis* and *Do. baihuashanensis* from *Juniperus chinensis*. Furthermore, the new records of *Do. alpina* from the host species *Populus szechuanica*, *Ph. aplosporum* from *Juglans mandshurica*, and *Ph. rhois* from *Populus alba* var. *pyramidalis* are included.

The fungi of Botryosphaeriales play various ecological roles, such as saprotrophs, endophytes, or plant pathogens (Phillips et al. 2005, 2008, 2013; Luque et al. 2016). Some fungi exhibit strong pathogenicity, leading to severe diseases in different parts of various plants, such as *Botryosphaeria dothidea*, which can cause apple ring rot of stems and fruits (Zhang et al. 2016b), as well as poplar cankers (Li et al. 2019), and the dieback and leaf spot diseases of *Euonymus japonicus* (Lin et al. 2023). Sometimes their ecological roles change, such as *Diplodia sapinea*, which is both an endophytic and a plant pathogenic fungus (Slippers et al. 2013). In this article, all species were isolated from diseased plant tissues, and their pathogenicity remains to be verified.

In this study, both *Dothiorella* and *Phaeobotryon* belong to Botryosphaeriaceae. Slippers et al. (2013) mentioned that some morphological features within Botryosphaeriaceae are not always stable, such as pigment production of conidia. These features might have already existed before the diversification of the group and have undergone further changes later (Slippers et al. 2013). In this study, only aseptate conidia were observed in *Phaeobotryon platycladi*, and they may become pigmented with age. Moreover, whether septate or not seem to be an unstable characteristic throughout the genus *Phaeobotryon*. Phillips et al. (2013) mentioned that in most cases, the conidia of *Phaeobotryon* have two septa when mature. However, both the *Phaeobotryon aplosporum* observed in this study and the one described by Pan et al. (2019) have pigmented but without septa. *Phaeobotryon rhoinum* also shows pigmented and aseptate conidia (Daranagama et al. 2016). Other species of *Phaeobotryon* with pigmented and septate conidia are either saprobic or pathogenic, but *Ph. aplosporum* and *Ph. rhoinum* are both pathogenic (Rathnayaka et al. 2023). The phylogenetic state analysis of the trophic pattern, conidial colour, and separation of Botryosphaeriales conducted by Rathnayaka et al. (2023) indicate that this may correspond to nutritional mode.

Acknowledgements

This research was funded by the National Natural Science Foundation of China (32101533), National Science and Technology Fundamental Resources Investigation Program of China (2021FY100900). We are grateful to Xiaohong Liang, Jing Han (the Experimental Teaching Centre, College of Forestry, Beijing Forestry University) for providing installed scientific equipment through the whole process. Lu Lin is grateful for the assistance of Ziqiang Wu (Southwest Forestry University) and Min Lin during the specimen collection, also Yixuan Li and Aoli Jia (Beijing Forestry University) during this study. Xinlei Fan would like to acknowledge the support of strain preservation of Chungeng Piao and Minwei Guo (China Forestry Culture Collection Centre, Chinese Academy of Forestry, Beijing).

References

- Alves A, Barradas C, Phillips AJL, Correia A (2013) Diversity of Botryosphaeriaceae species associated with conifers in Portugal. *European Journal of Plant Pathology* 135(4): 791–804. <https://doi.org/10.1007/s10658-012-0122-2>
- Bezerra JDP, Crous PW, Aiello D, Gullino ML, Polizzi G, Guarnaccia V (2021) Genetic diversity and pathogenicity of Botryosphaeriaceae species associated with symptomatic citrus plants in Europe. *Plants* 10(3): e492. <https://doi.org/10.3390/plants10030492>
- Carbone I, Kohn LM (1999) A Method for designing primer sets for speciation studies in filamentous Ascomycetes. *Mycologia* 91(3): 553–556. <https://doi.org/10.1080/00275514.1999.12061051>

- Damm U, Fourie PH, Crous PW (2007) *Aplosporella prunicola*, a novel species of anamorphic Botryosphaeriaceae. *Fungal Diversity* 27: 35–43.
- Daranagama DA, Thambugala KM, Campino B, Alves A, Bulgakov TS, Phillips AJL, Liu XZ, Hyde KD (2016) *Phaeobotryon negundinis* sp. nov. (Botryosphaeriales) from Russia. *Mycosphere* 7(7): 933–941. <https://doi.org/10.5943/mycosphere/si/1b/2>
- Dou ZP, Lu M, Wu JR, He W, Zhang Y (2017) A new species and interesting records of *Aplosporella* from China. *Sydowia* 69: 1–7.
- Doyle JJ, Doyle JL (1990) Isolation of plant DNA from fresh tissue. *Focus* 12: 13–15. <https://doi.org/10.2307/2419362>
- Ekanayaka AH, Dissanayake AJ, Jayasiri SC, To-anun C, Jones EBG, Zhao Q, Hyde KD (2016) *Aplosporella thailandica*; a novel species revealing the sexual-asexual connection in Aplosporellaceae (Botryosphaeriales). *Mycosphere* 7(4): 440–447. <https://doi.org/10.5943/mycosphere/7/4/4>
- Fan XL, Hyde KD, Liu JK, Liang YM, Tian CM (2015) Multigene phylogeny and morphology reveal *Phaeobotryon rhois* sp. nov. (Botryosphaeriales, Ascomycota). *Phytotaxa* 205(2): 90–98. <https://doi.org/10.11646/phytotaxa.205.2.2>
- Glass NL, Donaldson GC (1995) Development of primer sets designed for use with the PCR to amplify conserved genes from filamentous ascomycetes. *Applied and Environmental Microbiology* 61(4): 1323–1330. <https://doi.org/10.1128/aem.61.4.1323-1330.1995>
- Guindon S, Dufayard JF, Lefort V, Anisimova M, Hordijk W, Gascuel O (2010) New algorithms and methods to estimate maximum-likelihood phylogenies: Assessing the performance of PhyML 3.0. *Systematic Biology* 59(3): 307–321. <https://doi.org/10.1093/sysbio/syq010>
- Hyde KD, de Silva NI, Jeewon R, Bhat DJ, Phookamsak R, Doilom M, Boonmee S, Jayawardena RS, Maharachchikumbura SSN, Senanayake IC, Manawasinghe IS, Liu NG, Abeywickrama PD, Chaiwan N, Karunarathna A, Pem D, Lin CG, Sysouphanthong P, Luo ZL, Wei DP, Wanasinghe DN, Norphanphoun C, Tennakoon DS, Samarakoon MC, Jayasiri SC, Jiang HB, Zeng XY, Li JF, Wijesinghe SN, Devadatha B, Goonasekara ID, Brahmanage RS, Yang EF, Aluthmuhandiram JVS, Dayarathne MC, Marasinghe DS, Li WJ, Dissanayake LS, Dong W, Huanraluek N, Lumyong S, Liu JK, Karunarathna SC, Jones EBG, Al-Sadi AM, Xu JC, Harishchandra D, Sarma VV (2020) AJOM new records and collections of fungi: 1–100. *Asian Journal of Mycology* 3(1): 22–294. <https://doi.org/10.5943/ajom/3/1/3>
- Jami F, Slippers B, Wingfield MJ, Gryzenhout M (2014) Botryosphaeriaceae species overlap on four unrelated, native South African hosts. *Fungal Biology* 118(2): 168–179. <https://doi.org/10.1016/j.funbio.2013.11.007>
- Jiang N, Voglmayr H, Xue H, Piao CG, Li Y (2022) Morphology and phylogeny of *Pestalotiopsis* (Sporocadaceae, Amphisphaeriales) from Fagaceae leaves in China. *Microbiology Spectrum* 10(6): 03272–22. <https://doi.org/10.1128/spectrum.03272-22>
- Katoh K, Standley DM (2013) MAFFT multiple sequence alignment software version 7: Improvements in performance and usability. *Molecular Biology and Evolution* 30(4): 772–780. <https://doi.org/10.1093/molbev/mst010>

- Li GQ, Li BJ, Li BQ, et al. (2019) First report of *Botryosphaeria dothidea* causing canker on *Populus tomentosa* in China. *Plant Disease* 103(4): e693. <https://doi.org/10.1094/PDIS-08-18-1451-PDN>
- Lin L, Pan M, Gao H, Tian CM, Fan XL (2023) The Potential Fungal Pathogens of *Euonymus japonicus* in Beijing, China. *Journal of Fungi* 9(2): e271. <https://doi.org/10.3390/jof9020271>
- Luque J, Gómez LD, Melgarejo P (2016) *Botryosphaeria* species associated with apple stem rot in southern Spain. *European Journal of Plant Pathology* 145(1): 205–217. <https://doi.org/10.1007/s10658-015-0836-9>
- Nouri MT, Lawrence DP, Holland LA, Doll DA, Kallsen CE, Culumber CM, Nylander JAA (2004) MrModeltest v2. Distributed by the Author; Evolutionary Biology Center, Uppsala University, Uppsala.
- O'Donnell K, Cigelnik E (1997) Two divergent intragenomic rDNA ITS2 types within a monophyletic lineage of the fungus *Fusarium* are nonorthologous. *Molecular Phylogenetics and Evolution* 7(1): 103–116. <https://doi.org/10.1006/mpev.1996.0376>
- Pan M, Zhu HY, Bezerra JD, Bonthond G, Tian CM, Fan XL (2019) Botryosphaeralean fungi causing canker and dieback of tree hosts from Mount Yudu in China. *Mycological Progress* 18: 1341–1361. <https://doi.org/10.1007/s11557-019-01532-z>
- Peng C, Shi TY, Xia GC, Tian CM (2023) A New Species of *Phaeobotryon* from Galls of *Juniperus formosana* Branches in China. *Journal of Fungal Research* 21(1–3): 31–41. <https://doi.org/10.13341/j.jfr.2023.0004> [in Chinese]
- Phillips A, Alves A, Correia A, Luque J (2005) Two new species of *Botryosphaeria* with brown, 1-septate ascospores and *Dothiorella* anamorphs. *Mycologia* 97(2): 513–529. <https://doi.org/10.1080/15572536.2006.11832826>
- Phillips AJL, Alves A, Abdollahzadeh J, Slippers B, Wingfield MJ, Groenewald JZ, Crous PW (2013) The Botryosphaeriaceae: Genera and species known from culture. *Studies in Mycology* 76: 51–167. <https://doi.org/10.3114/sim0021>
- Phillips AJL, Hyde KD, Alves A, Liu J-KJ (2019) Families in Botryosphaerales: A phylogenetic, morphological and evolutionary perspective. *Fungal Diversity* 94(1): 1–22. <https://doi.org/10.1007/s13225-018-0416-6>
- Rambaut A (2018) FigTree v.1.4.4. <http://tree.bio.ed.ac.uk/software/figtree/>
- Rannala B, Yang Z (1996) Probability distribution of molecular evolutionary trees: A new method of phylogenetic inference. *Journal of Molecular Evolution* 43(3): 304–311. <https://doi.org/10.1007/BF02338839>
- Rathnayaka AR, Chethana KT, Phillips AJ, Jones EG (2022) Two new species of Botryosphaeriaceae (Botryosphaerales) and new host/geographical records. *Phytotaxa* 564(1): 8–38. <https://doi.org/10.11646/phytotaxa.564.1.2>
- Rathnayaka AR, Chethana KWT, Phillips AJL, Liu JK, Samarakoon MC, Jone EBG, Karunaratna SC, Zhao CL (2023) Re-evaluating Botryosphaerales: Ancestral state reconstructions of selected characters and evolution of nutritional modes. *Journal of Fungi* 9(2): e184. <https://doi.org/10.3390/jof9020184>
- Rayner RW (1970) *A Mycological Colour Chart*. Commonwealth Mycological Institute, London.

- Ronquist F, Huelsenbeck JP (2003) MrBayes 3: Bayesian phylogenetic inference under mixed models. *Bioinformatics* 19(12): 1572–1574. <https://doi.org/10.1093/bioinformatics/btg180>
- Schoch CL, Shoemaker R, Seifert K, Hambleton S, Spatafora JW, Crous PW (2006) A multi-gene phylogeny of the Dothideomycetes using four nuclear loci. *Mycologia* 98(6): 1041–1052. <https://doi.org/10.1080/15572536.2006.11832632>
- Sharma R, Kulkarni G, Sonawane MS (2017) *Alanomyces*, a new genus of Aplosporellaceae based on four loci phylogeny. *Phytotaxa* 297(2): 168–175. <https://doi.org/10.11646/phytotaxa.297.2.4>
- Slippers B, Boissin E, Phillips AJL, Groenewald JZ, Lombard L, Wingfield MJ, Postma A, Burgess T, Crous PW (2013) Phylogenetic lineages in the Botryosphaerales: A systematic and evolutionary framework. *Studies in Mycology* 76(1): 31–49. <https://doi.org/10.3114/sim0020>
- Slippers B, Roux J, Wingfield MJ, Van der Walt FJJ, Jami F, Mehl JWM, Marais GJ (2014) Confronting the constraints of morphological taxonomy in the Botryosphaerales. *Persoonia* 33(1): 155–168. <https://doi.org/10.3767/003158514X684780>
- Stamatakis A (2014) RAxML version 8: A tool for phylogenetic analysis and post-analysis of large phylogenies. *Bioinformatics* 30(9): 1312–1313. <https://doi.org/10.1093/bioinformatics/btu033>
- Sun JE, Meng CR, Phillips AJL, Wang Y (2022) Two new *Botryosphaeria* (Botryosphaerales, Botryosphaeriaceae) species in China. *MycoKeys* 94: 1–16. <https://doi.org/10.3897/mycokeys.94.91340>
- Tamura K, Stecher G, Peterson D, Filipski A, Kumar S (2013) MEGA6: Molecular evolutionary genetics analysis version 6.0. *Molecular Biology and Evolution* 30(12): 2725–2729. <https://doi.org/10.1093/molbev/mst197>
- Taylor K, Barber PA, Hardy GESJ, Burgess TI (2009) Botryosphaeriaceae from tuart (*Eucalyptus gomphocephala*) woodland, including descriptions of four new species. *Mycological Research* 113(3): 337–353. <https://doi.org/10.1016/j.mycres.2008.11.010>
- Theissen F, Sydow H (1918) Vorentwürfe zu den Pseudosphaerales. *Annales Mycologici* 16: 1–34.
- Vilgalys R, Hester M (1990) Rapid genetic identification and mapping of enzymatically amplified ribosomal DNA from several *Cryptococcus* species. *Journal of Bacteriology* 172(8): 4238–4246. <https://doi.org/10.1128/jb.172.8.4238-4246.1990>
- Wang CB, Yang J, Li Y, Xue H, Piao CG, Jiang N (2023) Multi-gene phylogeny and morphology of two new *Phyllosticta* (Phyllostictaceae, Botryosphaerales) species from China. *MycoKeys* 95: 189–207. <https://doi.org/10.3897/mycokeys.95.100414>
- White TJ, Bruns T, Lee S, Taylor JW (1990) Amplification and direct sequencing of fungal ribosomal RNA genes for phylogenetics. In: Innis MA, Gelfand DH, Sninsky JJ, White TJ (Eds) *PCR protocols: a guide to methods and applications*. New York. <https://doi.org/10.1016/B978-0-12-372180-8.50042-1>
- Wijayawardene NN, Phillips AJL, Tibpromma S, Dai DQ, Selbmann L, Monteiro JS, Aptroot A, Flakus A, Rajeshkumar KC, Coleine C, Pereira DS, Fan X, Zhang L, Maharachchikumbura SSN, Souza MF, Kukwa M, Suwannarach N, Rodriguez-Flakus P, Ashtekar

- N, Dauner L, Tang LZ, Jin XC, Karunarathna SC (2021) Looking for the undiscovered asexual taxa: Case studies from lesser studied life modes and habitats. *Mycosphere* 12(1): 471–490. <https://doi.org/10.5943/mycosphere/12/1/17>
- Wyka SA, Broders KD (2016) The new family Septorioideaceae, within the Botryosphaerales and *Septorioides strobi* as a new species associated with needle defoliation of *Pinus strobus* in the United States. *Fungal Biology* 120(8): 1057–1066. <https://doi.org/10.1016/j.funbio.2016.04.005>
- Xiao XE, Wang W, Crous PW, Wang HK, Jiao C, Huang F, Pu ZX, Zhu ZR, Li HY (2021) Species of Botryosphaeriaceae associated with citrus branch diseases in China. *Persoonia* 47(1): 106–135. <https://doi.org/10.3767/persoonia.2021.47.03>
- Yang T, Groenewald JZ, Cheewangkoon R, Jami F, Abdollahzadeh J, Lombard L, Crous PW (2017) Families, genera, and species of Botryosphaerales. *Fungal Biology* 121(4): 322–346. <https://doi.org/10.1016/j.funbio.2016.11.001>
- Zhang M, He W, Wu JR, Zhang Y (2016a) Two new species of *Spencermartinsia* (Botryosphaeriaceae, Botryosphaerales) from China. *Mycosphere* 7(7): 942–949. <https://doi.org/10.5943/mycosphere/si/1b/4>
- Zhang Y, Guan X, Wang G, Yang X, Li B, Xu Y (2016b) First report of *Botryosphaeria dothidea* causing apple ring rot of stems and fruits in China. *Plant Disease* 100(4): e865. <https://doi.org/10.1094/PDIS-09-15-1094-PDN>
- Zhang W, Groenewald JZ, Lombard L, Schumacher RK, Phillips AJL, Crous PW (2021) Evaluating species in Botryosphaerales. *Persoonia* 46(1): 63–115. <https://doi.org/10.3767/persoonia.2021.46.03>
- Zhu HY, Tian CM, Fan XL (2018) Studies of botryosphaerial fungi associated with canker and dieback of tree hosts in Dongling Mountain of China. *Phytotaxa* 348(2): 63–76. <https://doi.org/10.11646/phytotaxa.348.2.1>

Supplementary material I

Strains used in the molecular analyses in this study

Author: Lu Lin

Data type: table (Excel spreadsheet)

Copyright notice: This dataset is made available under the Open Database License (<http://opendatacommons.org/licenses/odbl/1.0/>). The Open Database License (ODbL) is a license agreement intended to allow users to freely share, modify, and use this Dataset while maintaining this same freedom for others, provided that the original source and author(s) are credited.

Link: <https://doi.org/10.3897/mycokeys.97.102653.suppl1>

Three new species of *Trichoderma* (Hypocreales, Hypocreaceae) from soils in China

Rui Zhao¹, Li-Juan Mao², Chu-Long Zhang¹

1 Ministry of Agriculture Key Laboratory of Molecular Biology of Crop Pathogens and Insects, Key Laboratory of Biology of Crop Pathogens and Insects of Zhejiang Province, Institute of Biotechnology, Zhejiang University, Hangzhou 310058, China **2** Analysis Center of Agrobiological and Environmental Science, Zhejiang University, Hangzhou, Zhejiang 310058, China

Corresponding author: Chu-Long Zhang (clzhang@zju.edu.cn)

Academic editor: N. Boonyuen | Received 8 February 2023 | Accepted 17 April 2023 | Published 2 May 2023

Citation: Zhao R, Mao L-J, Zhang C-L (2023) Three new species of *Trichoderma* (Hypocreales, Hypocreaceae) from soils in China. MycoKeys 97: 21–40. <https://doi.org/10.3897/mycokeys.97.101635>

Abstract

Trichoderma spp. are diverse fungi with wide distribution. In this study, we report on three new species of *Trichoderma*, namely *T. nigricans*, *T. densissimum* and *T. paradensissimum*, collected from soils in China. Their phylogenetic position of these novel species was determined by analyzing the concatenated sequences of the second largest nuclear RNA polymerase subunit encoding gene (*rpb2*) and the translation elongation factor 1- α encoding gene (*tef1*). The results of the phylogenetic analysis showed that each new species formed a distinct clade: *T. nigricans* is a new member of the *Atroviride* Clade, and *T. densissimum* and *T. paradensissimum* belong to the *Harzianum* Clade. A detailed description of the morphology and cultural characteristics of the newly discovered *Trichoderma* species is provided, and these characteristics were compared with those of closely related species to better understand the taxonomic relationships within the *Trichoderma*.

Keywords

Hypocreales, new species, phylogenetic analysis, taxonomy, *Trichoderma*

Introduction

The genus *Trichoderma* (Ascomycota, Sordariomycetes, Hypocreales) is widely studied and applied because of their economical and ecological significance. In agriculture, they are avirulent plant symbionts used for plant protection and growth promotion

(Harman et al. 2004), and as a biological agent to control of fungal diseases (Lorito et al. 2010; Zin and Badaluddin 2020). In addition, *Trichoderma* species have been applied for the production of enzymes and bioactive compounds of industrial utility (Ahamed and Vermette 2008; Sun et al. 2016; Stracquadanio et al. 2020). *Trichoderma* species possessing stress tolerance to different environmental factors hold significant promise for addressing environmental issues such as severe contamination (Kredics et al. 2001; Tripathi et al. 2013). Meanwhile, a few of *Trichoderma* species cause disease in cultivated mushrooms or are reported as causes of serious infections in humans (Kuhls et al. 1999; Savoie and Mata 2003). Members of *Trichoderma* are widely distributed in varied ecosystems, and are frequently found on soil, decaying wood, compost, or other organic matter and as endophytes in plant tissues (Samuels 2006; Zheng et al. 2021).

Traditionally, *Trichoderma* species were identified based on their morphology and growth characteristics (Rifai 1969; Bissett 1984, 1991a, b). However, as the *Trichoderma* species richness has increased, it has been difficult to distinguish them because species in this genus are highly similar in morphology (Bissett et al. 2003; Overton et al. 2006). With the development of molecular biology, more reliable identification is provided as DNA barcoding was introduced to recognize *Trichoderma* (Druzhinina et al. 2006). The most commonly used DNA barcode loci are the internal transcribed spacer (ITS), translation elongation factor 1–alpha encoding gene (*tef1*) and the second largest nuclear RNA polymerase subunit encoding gene (*rpb2*) (Druzhinina et al. 2006; Atanasova et al. 2013; Chaverri et al. 2015; Cai and Druzhinina 2021). The combination of multi-gene (*rpb2* and *tef1*) phylogenetic analysis and phenotypic characteristics is usually applied in the species identification of *Trichoderma* (Chaverri and Samuels 2004; Zhu and Zhuang 2015a, b; Zheng et al. 2021; Cao et al. 2022). Recently, Cai and Druzhinina (2021) have developed an authoritative protocol that provides a standard for the molecular identification of *Trichoderma*. It is based on *rpb2* \geq 99% and *tef1* \geq 97%, one species can be identified. If the unique sequences do not meet the *rpb2* \geq 99% or *tef1* \geq 97%, it can be considered a new species. This protocol is advocated for the identification of *Trichoderma* species by the International Subcommittee on Taxonomy of *Trichoderma* (<https://trichoderma.info/>; accessed on 18 Oct 2022).

Fungal diversity is enormous in China (Sun et al. 2012; Lu 2019). Since the first record of *Trichoderma* from China in 1895, many new *Trichoderma* species have been ceaselessly discovered, with most of them isolated from soils, litter, mushrooms and endophytes (Zhang et al. 2005; Yu et al. 2007; Zhang et al. 2007; Li et al. 2013; Zhu and Zhuang 2015a, b; Chen and Zhuang 2016; Qin and Zhuang 2016; Chen and Zhuang 2017; Qiao et al. 2018; Gu et al. 2020; Zhang et al. 2020; Zheng et al. 2021; An et al. 2022; Cao et al. 2022). In a previous study conducted by Dou et al. (2019), a total of 485 *Trichoderma* strains were obtained from soils in three provinces of China: Shanxi, Shaanxi, Shandong. The online multilocus identification system (MIST) was employed in a previous study conducted by Dou et al. (2020) to re-identify *Trichoderma*. The present study therefore had to identify new taxa, the sequences of which do not meet the known *Trichoderma* species, based on the multi loci phylogenetic analysis and morphological features observation.

Materials and methods

Isolation of strains

In accordance with a prior study by Dou et al. (2019), a total of 485 *Trichoderma* strains were extracted from soil samples gathered from three provinces in China. Of these strains, 334 were sourced from Shandong, 107 from Shanxi, and 44 from Shaanxi. The isolation of these strains was aided by the use of a selective medium (Dou et al. 2019).

All strains of *Trichoderma* were kept in 4 °C Refrigerator and –80 °C Ultra Low Temperature Refrigerator in the Ministry of Agriculture Key Laboratory of Molecular Biology of Crop Pathogens and Insects, Institute of Biotechnology, Zhejiang University, Hangzhou, China. In addition, the holotype and ex-type culture were deposited in the China General Microbiological Culture Collection Center (CGMCC; <https://www.cgmcc.net/english/>; accessed on 16 Sep 2022).

Morphological characterizations

The morphological observation of the colonies was based on strains grown on potato dextrose agar (PDA; 10g potato extract, 20g dextrose, 13g agar, 1 L distilled water), cornmeal dextrose agar (CMD; 40g cornmeal, 20g dextrose, 15g agar, 1 L distilled water), malt extract agar (MEA; 20g malt extract, 15g agar, 1 L distilled water), and synthetic low nutrient agar (SNA; 1 g KH_2PO_4 , 1 g KNO_3 , 0.5 g MgSO_4 , 0.5 g KCl, 0.2 g glucose, 0.2 g sucrose, 15 g agar, 1 L distilled water) medium for 7 d in an incubator at 25 °C with alternating 12 h/12h light/dark cycle. Growth–rate trials were performed on 9 cm Petri dishes with CMD, PDA, MEA and SNA at 25 °C, 30 °C, and 35 °C. The Petri dishes were incubated in darkness for up to 1 week or until the colony covered the agar surface. Colony radii were measured daily, and trials were replicated three times.

Microscopic preparations were made by mounted on lactic acid, and at least 30 measurements per structure were documented and examined under a Nikon Eclipse 80i microscope (Nikon Corp.). Length (L) and width (W) of the phialides, conidia and chlamydospores were measured, respectively, and the ratio of length to width was calculated. Measurement values are expressed as (a–)b–c(–d), where (a) represents the lowest extreme value, b–c contains the minimum value of 90% of the calculated values, and (d) denotes the highest extreme value. The letter “n” indicates the total number of measurements taken (Aignon et al. 2021; Li et al. 2021).

DNA extraction, polymerase chain reaction (PCR) and sequencing

The mycelia of pure cultures were scraped directly from plates after 2–3 d growth on PDA at 25 °C and used to extract DNA, and the genomic DNA was extracted as described by Jiang et al. (2016). For the amplifications of *rpb2* and *tefl* gene fragments, two different primer pairs were used EF1/EF2 for *tefl* (O’Donnell et al. 1998) and fRPB2–7cR/

fRPB2–5F for *rpb2* (Liu et al. 1999). The polymerase chain reaction (PCR) amplifications were performed in a total reaction volume of 20 μ L, including 10 μ L of Easy Flash PCR MasterMix (Easy–Do, China), 0.8 μ L of each primer (10 μ M), 0.4 μ L genomic DNA (\sim 0.2 μ g). PCR reactions were run in a LifePro Thermal Cycler (Technology Co., Ltd. Hangzhou, China) following the PCR thermal cycle programs described by Zhu and Zhuang (2015b). PCR products were purified with the PCR product purification kit and sequencing was carried out in both directions with the same primers on an ABI 3730 XL DNA sequencer (Applied Biosystems, Foster City, CA, USA) by Sunya Biotechnology Co., Hangzhou, China. Sequences generated in this study are deposited in GenBank and the accession numbers are provided in Table 1.

Phylogenetic analyses

The phylogeny was constructed with the concatenated sequences of *rpb2* and *tef1*. The species closely related to our strain were determined by NCBI BLAST searches with *rpb2* and *tef1* sequences (Altschul et al. 1990; <https://blast.ncbi.nlm.nih.gov/Blast.cgi/>; accessed on 16 Jun 2022), and the closely related sequences were retrieved from NCBI database for subsequent phylogenetic analysis. The GenBank accession numbers of sequences retrieved are provided in Table 1. The sequences were aligned with MAFFT (Katoh and Standley 2013), and then the alignments were manually adjusted with MEGA7 (Kumar et al. 2018) and the fragments that were suitable for molecular identification were trimmed according to Cai and Druzhinina (2021). The trimmed sequences were concatenated using SequenceMatrix v.1.8 (Vaidya et al. 2011). The following phylogenetic analysis was performed in PhyloSuite platform (Zhang et al. 2020). The best–fit partition model was selected using ModelFinder (Kalyaanamoorthy et al. 2017) according to BIC criterion. Maximum likelihood (ML) phylogenies were inferred using IQ–TREE (Lam–Tung et al. 2015) under Edge–linked partition model for 5000 ultrafast (Minh et al. 2013) bootstraps, as well as the Shimodaira–Hasegawa–like approximate likelihood–ratio test (Guindon et al. 2010). Bayesian Inference phylogenies were inferred using MrBayes 3.2.6 (Ronquist et al. 2012) under partition model. The phylogenetic tree was visualized in FigTree v1.4.3. (<http://tree.bio.ed.ac.uk/software/figtree/>; accessed on 04 Oct 2016) with maximum likelihood bootstrap proportions (MLBP) greater than 70% and Bayesian inference posterior probabilities (BIPP) greater than 0.9, as shown at the nodes.

Results

Sequence analysis

The comparison of *rpb2* and *tef1* sequences between the query strain and the reference strain revealed that the similarity did not meet the $rpb2 \geq 99\%$ and $tef1 \geq 97\%$ criteria as outlined in Table 2. Additionally, the query strain exhibited unique *tef1* and *rpb2*

Table 1. Strain numbers and corresponding GenBank accession numbers of sequences used for phylogenetic analyses.

Species name	Strain number	GenBank accession numbers	
		<i>rpb2</i>	<i>tefl</i>
<i>T. afroharzianum</i>	CBS 124620 ^{ET}	FJ442691	FJ463301
<i>T. afroharzianum</i>	GJS 04–193	FJ442709	FJ463298
<i>T. anaharzianum</i>	YMF 1.00383 ^T	MH158995	MH183182
<i>T. asiaticum</i>	YMF 1.00168	MH262575	MH236492
<i>T. asiaticum</i>	YMF 1.00352 ^T	MH158994	MH183183
<i>T. atrobrunneum</i>	CBS 548.92 ^T	–	AF443942
<i>T. atrobrunneum</i>	GIS 04–67	FJ442724	FJ463360
<i>T. atrobrunneum</i>	GJS 05–101	FJ442745	FJ463392
<i>T. atroviride</i>	CBS 119499	FJ860518	FJ860611
<i>T. atroviride</i>	CBS 142.95 ^{ET}	EU341801	AY376051
<i>T. breve</i>	CGMCC 3.18398 ^T	KY687983	KY688045
<i>T. breve</i>	HMAS 248845	KY687984	KY688046
<i>T. densissimum</i>	T31818	OP357965	OP357967
<i>T. densissimum</i>	T32434 = CGMCC 3.24126^T	OP357966	OP357971
<i>T. densissimum</i>	T32465	OP357963	OP357972
<i>T. densissimum</i>	T32353	OP357964	OP357970
<i>T. guizhouense</i>	CBS 131803 ^T	JQ901400	JN215484
<i>T. guizhouense</i>	HGUP 0039	JQ901401	JX089585
<i>T. harzianum</i>	CBS 226.95 ^{ET}	AF545549	AF348101
<i>T. harzianum</i>	TRS55	KP009121	KP008803
<i>T. harzianum</i>	TRS94	KP009120	KP008802
<i>T. nigricans</i>	T32450	OP357958	OP357973
<i>T. nigricans</i>	T32794	OP357960	OP357975
<i>T. nigricans</i>	T32781 = CGMCC40314^T	OP357959	OP357974
<i>T. obovatum</i>	YMF 1.06211 ^T	MT038432	MT070144
<i>T. obovatum</i>	YMF 1.6190	MT038433	MT070143
<i>T. paradensissimum</i>	T31823 = CGMCC 3.24125^T	OP357962	OP357968
<i>T. paradensissimum</i>	T31824	OP357961	OP357969
<i>T. paratroviride</i>	CBS 136489 ^T	KJ665321	KJ665627
<i>T. paratroviride</i>	S489	KJ665322	KJ665628
<i>T. paraviride</i>	YMF 1.04628 ^T	MK775513	MK775508
<i>T. pholiotae</i>	JZBQH12 ^T	ON649972	ON649919
<i>T. pholiotae</i>	JZBQH11	ON649971	ON649918
<i>T. pyramidale</i>	CBS 135574 ^{ET}	KJ665334	KJ665699
<i>T. pyramidale</i>	T20	KX632570	KX632627
<i>T. simile</i>	YMF 1.06201 ^T	MT052184	MT070154
<i>T. simile</i>	YMF1.6180	MT052185	MT070153
<i>T. uncinatum</i>	YMF 1.04622 ^T	MK795990	MK795986
<i>T. viride</i>	TRS575	KP009081	KP008931
<i>T. viride</i>	CBS 119325 ^{ET}	EU711362	DQ672615
<i>T. zelobreve</i>	CGMCC 3.19695 ^T	MN605872	MN605883
<i>T. zelobreve</i>	CGMCC 3.19696	MN605873	MN605884
<i>T. zeloharzianum</i>	YMF 1.00268 ^{ET}	MH158996	MH183181
<i>Protocrea farinosa</i>	CBS 121551 ^T	OP357962	EU703889
<i>Protocrea pallida</i>	CBS 299.78 ^{ET}	EU703948	EU703900

Note: Newly-sequenced material is indicated in bold type. T Indicates a type culture. ET Indicates an epitype culture.

Table 2. The similarity of *rpb2* and *tefl* between the query species and related species.

Query species	Related species	Sequences similarity value(%)	
		<i>rpb2</i>	<i>tefl</i>
<i>Trichoderma nigricans</i> T32781 ^T	<i>T. atroviride</i> CBS 142.95 ^{ET}	97.91	91.29
	<i>T. obovatum</i> YMF 1.06211 ^T	98.15	86.68
	<i>T. paratroviride</i> CBS 136489 ^T	98.65	87.53
	<i>T. uncinatum</i> YMF 1.04622 ^T	98.56	94.40
<i>T. paradensissimum</i> T31818 ^T	<i>T. densissimum</i> T31823 ^T	97.54	99.20
	<i>T. asiaticum</i> YMF1.00352 ^T	96.92	98.06
	<i>T. guizhouense</i> HGUP 0038 ^T	97.05	98.29
	<i>T. pholiotae</i> JZBQH12 ^T	97.42	99.16
	<i>T. simile</i> YMF 1.06201 ^T	97.17	97.83
<i>T. densissimum</i> T31823 ^T	<i>T. paradensissimum</i> T31818 ^T	97.54	99.20
	<i>T. asiaticum</i> YMF 1.00352 ^T	97.79	98.06
	<i>T. guizhouense</i> HGUP 0038 ^T	97.17	98.29
	<i>T. pholiotae</i> JZBQH12 ^T	98.04	100
	<i>T. simile</i> YMF 1.06201 ^T	97.66	97.83

Note: T Indicates a type culture. ET Indicates an epitype culture.

sequences that do not conform to the $sp\Xi!(rpb2_{99} \cong tef1_{97})$ standard for known *Trichoderma* species, according to Cai and Druzhinina (2021). These findings suggest that these strains could potentially be classified as new species, and therefore, phylogenetic analyses were conducted on their *rpb2* and *tefl* sequences.

Multi-locus phylogeny

Multi-loci phylogenetic analyses were performed on sequences obtained from 43 strains, consisting of 30 strains from the *Harzianum* Clade, 10 strains from the *Atroviride* Clade, and 3 strains from the *Viride* Clade. The combined *rpb2* and *tefl* regions were further analyzed by the methods of ML and BI, with *Protocrea farinosa* CBS 121551 and *P. pallida* CBS 299.78 as the outgroup. The tree topology derived from the ML analysis (Fig. 1) was consistent with that obtained in a BI analysis. However, details regarding the BI analysis were not provided in the text. All strains formed a monophyletic group with higher statistical support, designated as *T. nigricans* (MLBP/BIBP = 100/1.00), *T. densissimum* (MLBP/BIBP = 100/1.00) and *T. paradensissimum* (MLBP/BIBP = 99/1.00). Of the three new species, *T. nigricans* belonged to the *Atroviride* Clade, whereas *T. densissimum* and *T. paradensissimum* were located in the *Harzianum* Clade (Fig. 1). *Trichoderma nigricans* was closely related with *T. atroviride*, and associated with *T. obovatum*, *T. uncinatum*, and *T. paratroviride*. This clade had high statistics support (MLBP/BIBP = 94/0.99). *Trichoderma densissimum* was closely related with *T. paradensissimum*, and associated with *T. pholiotae*, *T. guizhouense*, *T. asiaticum* and *T. simile*, with high support value (MLBP/BIBP = 95/1.00).

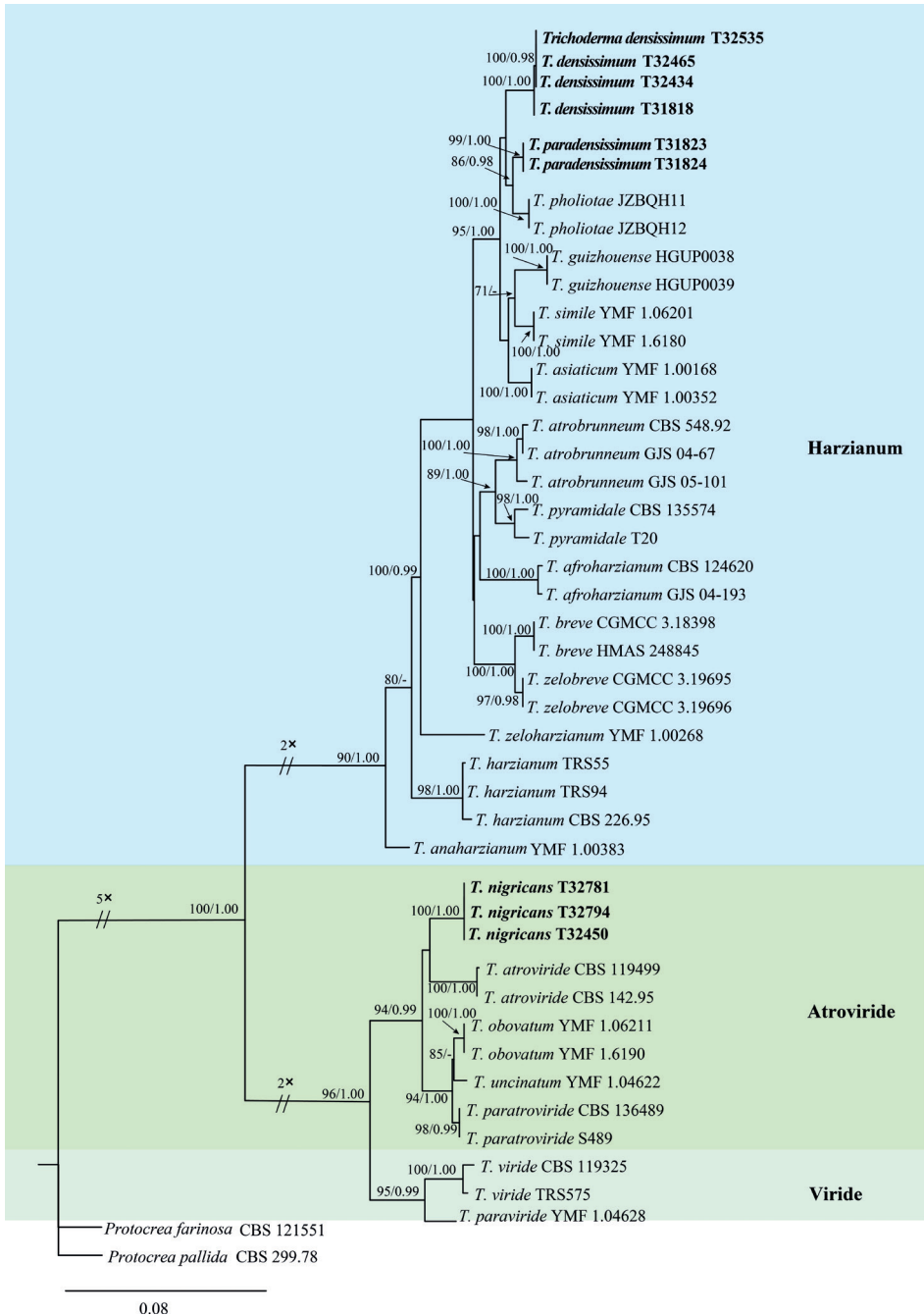


Figure 1. Phylogenetic tree generated by the maximum likelihood analysis using the concatenated sequences of *rpb2* and *tefl* loci of the genus *Trichoderma*. Maximum Likelihood Bootstrap values $\geq 70\%$ (left) and Bayesian posterior probability values ≥ 0.9 (right) are indicated at nodes (MLBP/BIBP). *Protocrea farinosa* CBS 121551 and *P. pallida* CBS 299.78 were chosen as the outgroup. Novel species proposed here are indicated in bold.

Taxonomy

Trichoderma nigricans C.L. Zhang, sp. nov.

Mycobank No: 845506

Fig. 2

Etymology. The Latin specific epithet “*nigricans*” refers to the “blackish green” color of the mass of conidia.

Diagnosis. Phylogenetically, *T. nigricans* was found to form a distinct clade and was closely related to *T. atroviride*, *T. paratroviride*, *T. obovatum*, and *T. uncinatum* (Fig. 1). In terms of growth characteristics, *T. nigricans* was observed to have a larger colony radius on CMD after 72 h, and its mycelium covered the plate at both 25 °C and 30 °C. On PDA, *T. nigricans* grew faster than *T. atroviride*, *T. paratroviride*, *T. obovatum*, and *T. uncinatum* at 25 °C, with its mycelium also covering the plate.

Type. CHINA: Shandong Province, Dezhou City, 37°21'07"N, 116°23'40"E, 5 m alt., isolated from soils of peach rhizosphere. Oct 2015, Y. Jiang T32781 (Holotype CGMCC 40314, stored in a metabolically inactive state. Ex-type culture CGMCC 40314).

Description. Optimal growth at 25 °C, slow at 35 °C on all media.

Colony radius on CMD after 72 h: mycelium covers the plate at 25 °C and 30 °C, 20–22 mm at 35 °C. Colony well-defined, hyaline, sparse aerial mycelia, indistinctly zonate, conidiation begins to develop within 72 h, white at first and turning green after 3–4 d. After 7 d, abundant dark green conidiation around the margin, radially arranged within 2–3 ill-defined concentric zones in the outer half of the colony. Abundant chlamydo spores. No diffusing pigment noted, pleasant odor apparent.

Colony radius on PDA after 72 h: mycelium covers the plate at 25 °C, 55–61 mm at 30 °C, 16 mm at 35 °C. Colony similar to CMD but growth a little slower, colony not dark green. Colony well-defined at 35 °C, abundant white thick aerial mycelia. Chlamydo spores abundant. No diffusing pigment noted, obvious pleasant odor.

Colony radius on MEA after 72 h: 58–60 mm at 25 °C, 53–55 mm at 30 °C, 11–12 mm at 35 °C. Colony also similar to CMD, but conidiation is yellow green, more abundant around the inoculation plug, uniform distribution all around. No diffusing pigment noted, odor indistinct.

Colony radius on SNA after 72 h: 5–7 mm at 25 °C, 5–6 mm at 30 °C and 35 °C. Colonies well-defined, hyaline, scant aerial mycelia. Slight conidiation dispersedly distributed around the inoculation plug, with white floccose indistinctly zonate tufts or pustules in the margin. No diffusing pigment noted, odor indistinct. Conidiophores consisting of a main axis with side branches mostly at right angles or slightly inclined upward; branches straight or curved, often only longer in basal positions, not re-branching, solitary, paired or in whorls of three. Phialides solitary or commonly in whorls of 2–3, variable in shape, either narrowly lageniform to subulate, particularly when terminal on the main axis, or stout to nearly ampulliform and distinctly swollen, sometimes ampulliform to subglobose, (4.7–)6.0–8.9(–12.1) ×

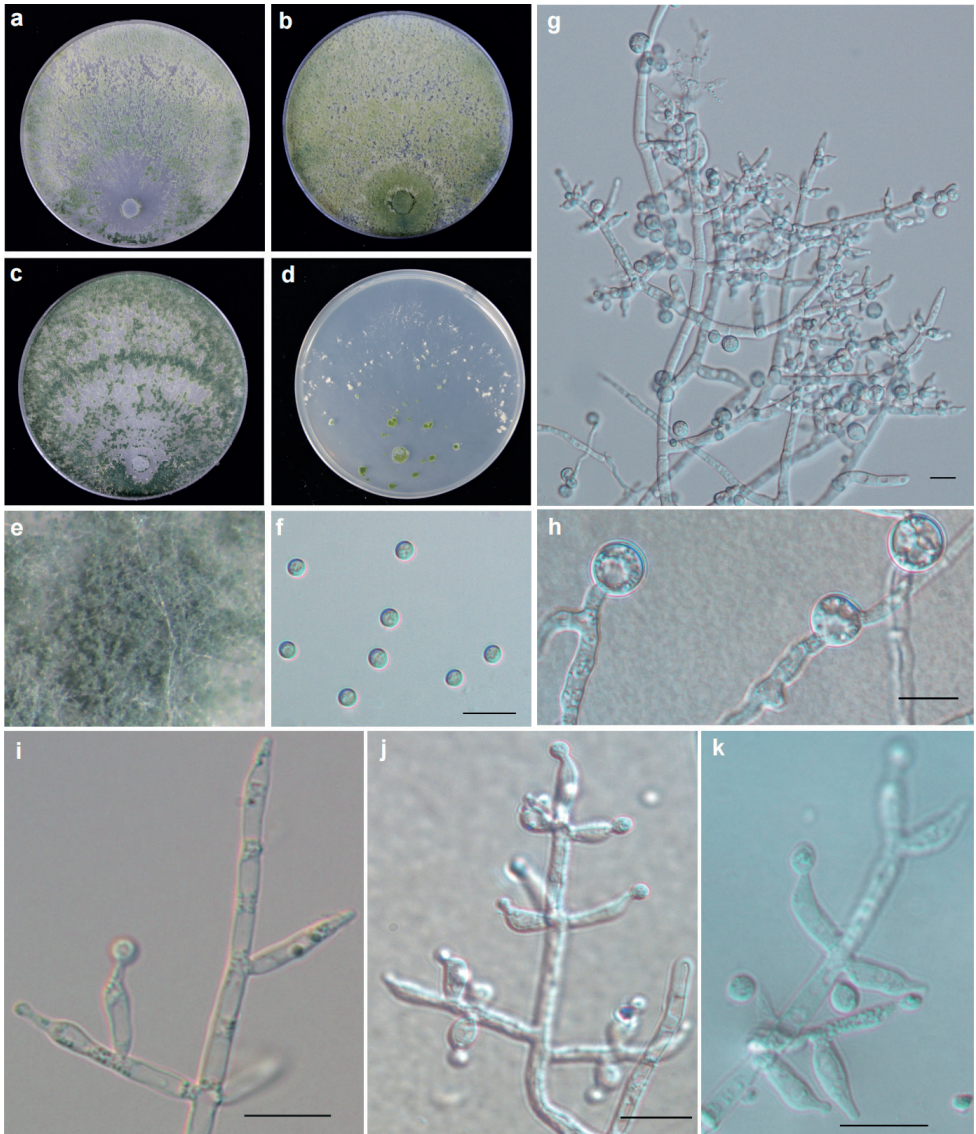


Figure 2. Cultures and anamorph of *T. nigricans* strain T32781 **a–d** cultures on different media at 25 °C with a 12 h light and 12 h darkness cycle after 7 d (**a** on PDA **b** on MEA **c** on CMD **d** on SNA) **e** Conidiation pustules on PDA after 7 d **f** conidia **g, i–k** conidiophores and phialides (**g, k** on CMD 3d **i** on PAD 3d **j** on SNA 3d), **h** chlamydo-spores. Scale bars: 10 μm (**f–k**).

(2.5–)2.9–3.4(–4.5) μm (mean = 7.7 × 3.3 μm), base (1.5–)1.6–2.6(–3.0) μm (mean = 2.1 μm); phialide length/width ratio (1.2–)1.8–2.9(–3.6) (mean = 2.4) (n = 30). Conidia subglobose to globose, green, smooth, (3.0–)3.2–3.6(–3.9) × (2.8–)3.1–3.4(–3.8) μm (mean = 3.3 × 3.4 μm) with length/width ratio of 1.0–1.1 (mean = 1.1) (n = 30). Abundant chlamydo-spores, common single, sometimes terminal and

intercalary, globose to subglobose, (7.2–)7.8–9.2(–10.1) × (6.1–)7.1–9.0(–9.7) μm (mean = 8.6 × 8.1 μm) (n = 30).

Sexual morph. Unknown.

Substrate. Soil.

Distribution. China, Shandong Provinces.

Additional material examined. CHINA: Shandong Province, Jinan City, 36°33'45"N, 116°57'05"E, 105 m alt., isolated from corn soils. Aug 2015, Y. Jiang T32450. CHINA: Shandong Province, Dezhou City, 37°21'07"N, 116°23'40"E, 5 m alt., isolated from soils of corn rhizosphere, Oct 2015, Y. Jiang, T32794.

Notes. *Trichoderma nigricans* can be distinguished from similar species based on growth. After 72 h at 25 °C, *T. nigricans* mycelium covers the plate on PDA and CMD, *T. atroviride* grows to 42.8–60.5 mm on PDA, *T. obovatum* grows to 38–41 mm on CMD, *T. uncinatum* grows to 55–62 mm on CMD, *T. paratroviride* to 49–62 mm on CMD and 54–56 mm on PDA (Samuels et al. 2002; Jaklitsch and Voglmayr 2015; Zheng et al. 2021). In addition, it can be distinguished by its chlamydospores and odor. At 35 °C the growth of *T. nigricans* is restricted, and no growth occurs in *T. paratroviride* and *T. uncinatum*. Chlamydospores are either unobserved or uncommon in *T. obovatum*, *T. uncinatum*, and *T. paratroviride*. Meanwhile, the chlamydospores of *T. atroviride* and *T. nigricans* are abundant, and the volume in *T. atroviride* is usually larger than those in *T. nigricans* [(5.2–)8.5–12.0(–16.3) vs. (7.2–)7.8–9.2(–10.1) × (6.1–)7.1–9.0(–9.7) μm]. On PDA, the odor of *T. paratroviride* is pungent; it is indistinct in *T. obovatum* and *T. uncinatum*, and pleasant in *T. atroviride* and *T. nigricans*.

***Trichoderma densissimum* C.L. Zhang, sp. nov.**

MycoBank No: 845507

Fig. 3

Etymology. The Latin specific epithet “*densissimum*” refers to the thick wall of chlamydospores of this species.

Diagnosis. It is easily distinguished from these related species by its relatively large chlamydospores (11.7–)13.3–16.4 (–19.5) × (11.5–)12.8–14.6–12.8 (–16.0) μm (mean = 14.8 × 13.6 μm) (n = 30).

Type. CHINA: Shandong Province, Weifang City, 36°38'27"N, 119°01'21"E, 80 m alt., isolated from soils of apple tree rhizosphere. Oct 2015, Y. Jiang T32434 (Holotype CGMCC 3.24126, stored in a metabolically inactive state. Ex-type culture CGMCC 3.24126).

Description. Optimum temperature for growth is 30 °C on CMD, MEA and SNA and 25 °C on PDA. Growth slow at 35 °C on PDA and SNA. Chlamydospores are common on all media.

Colony radius on CMD after 72 h: 38–45 mm at 25 °C, 55–62 mm at 30 °C, 42–43 mm at 35 °C. Colonies well-defined, white, thin, aerial hyphae sparse. Conidiation was noted after 2 d around the inoculation plug, which was white at first, turning yellow green after 3–4 d, then dark green after 5–6 d. Conidiation formed 4 obvi-

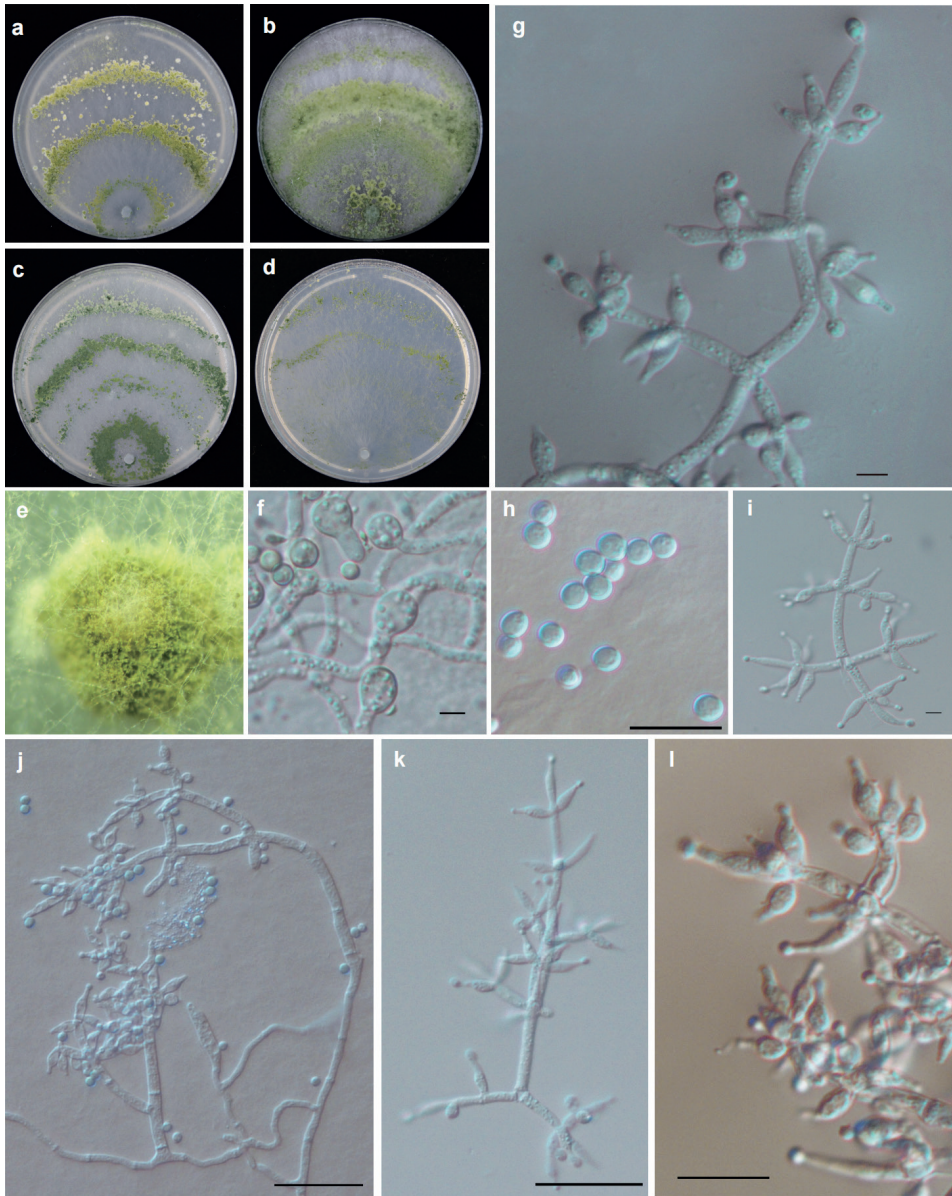


Figure 3. Cultures and anamorph of *T. densissimum* strain T32434 **a–d** cultures on different media at 25 °C with a 12 h light and 12 h darkness cycle after 7 d (**a** on PDA **b** on MEA **c** on CMD **d** on SNA) **e** conidiation pustules on PDA after 7d **g, i–l** conidiophores and phialides (**g, i–k** on CMD 3d **l** on SNA 3d) **f** chlamydospores **h** conidia. Scale bars: 10 μm (**f–l**).

ous concentric zones. No diffusing pigment noted, odor indistinct. Chlamydospores common single, sometimes terminal and intercalary, globose to subglobose, (11.7–)13.3–16.4(–19.5) \times (11.5–)12.8–14.6–12.8(–16.0) μm (mean = 14.8 \times 13.6 μm); with length/width ratio of 1.0 \times 1.3 (mean = 1.1) (n = 30).

Colony radius on PDA after 72 h: 61–66 mm at 25 °C, 60–63 mm at 30 °C, 24–31 mm at 35 °C. Colony white, regularly circular, distinctly zonate; mycelium dense and radial. Conidiation in the form on pustules, yellow–green, relatively abundant in the zonation regions. No diffusing pigment noted, odor indistinct.

Colony radius on MEA after 72 h: 62–63 mm at 25 °C, 66–67 mm at 30 °C, 44–47 mm at 35 °C. Colonies similar to that on PDA, but indistinctly zonate. No diffusing pigment noted, odor indistinct.

Colony radius on SNA after 72 h: 53 mm at 25 °C, 41–47 mm at 30 °C, 27–32 mm at 35 °C. Colony white; aerial mycelia scant and loose. Conidiation in the form of minute pustules, radial and inconspicuously zonate. No diffusing pigment noted, odor indistinct. Conidiophores pyramidal with opposing branches, the main axis with side branches is sometimes at right angles or inclined upward. The main axis and each branch commonly terminating verticillate, whorl of 3–4 phialides, sometimes in a cruciate whorl, sometimes solitary phialides. Phialides commonly ampulliform, sometimes ampulliform to subglobose (3.4–)5.7–8.0(–10.1) × (1.9–)2.5–2.9(–3.2) μm (mean = 6.2 × 2.6 μm), base (1.0–)1.4–2.1(–2.6) μm (mean = 2.2 μm); phialide length/width ratio (1.4–)2.1–3.2(–3.9)(mean = 2.6) (n = 30). Conidia subglobose to globose, green, (2.3–)2.8–3.1(–3.4) × (2.2–)2.4–2.9(–3.3) μm (mean = 2.9 × 2.7 μm), with length/width ratio of 1.0–1.4 (mean = 1.1) (n = 30).

Sexual morph. Unknown.

Substrate. Soil.

Distribution. China, Shandong and Shanxi provinces.

Additional material examined. CHINA: Shandong Province, Jinan City, 36°32'33"N, 117°01'08"E, 201 m alt., isolated from soils of wheat, Jun 2015, Y. Jiang (T31818); Shandong Province, Jining city, 34°56'21"N, 116°29'03"E, 34 m alt., isolated from soils of peach, Aug 2015, Y. Jiang T32353; Shaanxi Province, Baoji city, 34°23'25"N, 107°10'18"E, 802 m alt., isolated from soils of corn, Aug 2015, Y. Jiang T32465.

Notes. Although *T. densissimum*, *T. paradensissimum* and *T. guizhouense* share similar conidia and pyramidal conidiophores, *T. densissimum* cannot produce pigments while *T. paradensissimum* and *T. pholiotae* can produce yellowish pigment on PDA and CMD at 35 °C in the dark (Li et al. 2013; Cao et al. 2022). Characterized by producing globose to subglobose chlamydo spores, the chlamydo spores of *T. simile* are elliptic or round, unobserved in *T. guizhouense* and *T. asiaticum* (Jaklitsch and Voglmayr 2015; Zheng et al. 2021).

Trichoderma paradensissimum C.L. Zhang, sp. nov.

MycoBank No: 845508

Fig. 4

Etymology. The Latin specific epithet “*para*” means similar, and “*paradensissimum*” refers to the phylogenetic proximity and morphological similarity to *T. densissimum*.

Diagnosis. *T. paradensissimum* is characterized by the green to yellow and white pustules formed inconspicuously zonate on PDA or MEA at 25 °C of a 12-h photoperiod after 7 d.

Type. CHINA: Shanxi Province, Jincheng City, 35°26'57.9"N, 112°45'19.0"E, 929 m alt., isolated from soils of wheat rhizosphere, Jun 2015, Y. Jiang T31823 (Holotype CGMCC 3.24125, stored in a metabolically inactive state. Ex-type culture CGMCC 3.24125).

Description. Optimum temperature for growth is 30 °C on CMD, PDA and SNA and 25 °C on MEA. Chlamydo-spores were common on all media.

Colony radius on CMD after 72 h: 40–42 mm at 25 °C, 63–64 mm at 30 °C, 38–40 mm at 35 °C. Colony well-defined, white, aerial myceli loose and radial. White minute pustules were noted after 2 d around the inoculation plug, white at first, turning yellow green after 3–4 d, then dark green after 5–6 d. Around the point of inoculation, conidiation from dark green to pale green, inconspicuously zonate. Distinctive odor absent. The production of pigment was related to light, media and temperature: around the point of inoculation, it was yellowish at 35 °C in the dark.

Colony radius on PDA after 72 h: 59–65 mm at 25 °C, 64–67 mm at 30 °C, 20–24 mm at 35 °C. Colonies similar to that on MEA. Pustules were noted after 4–5 d. After 7 d, the green to yellow and white pustules were formed as inconspicuously zonate. Distinctive odor absent. The production of pigment was related to light and temperature; it was yellowish at 35 °C in the dark.

Colony radius on MEA after 72 h 58–59 mm at 25 °C, 51–53 mm at 30 °C, 34–35 mm at 35 °C. Colonies white and thick, regularly circular and radial, aerial myceli dense. A few white–yellow large pustules formed inconspicuously zonate. Diffusing pigment or distinctive odor absent.

Colony radius on SNA after 72 h 35–37 mm at 25 °C, 43–44 mm at 30 °C, 15–16 mm at 35 °C. Colony pale white; aerial myceli loose. Conidiation was minute pustules, radial and inconspicuously zonate. Around the point of inoculation, the pustules were green, but white far away from the inoculation. Diffusing pigment or distinctive odor absent. Conidiophores pyramidal; the main axis with side branches sometimes at right angles or inclined upward. The main axis and each branch commonly terminating verticillate, whorl of 3 phialides, sometimes solitary. Phialides ampulliform, (5.4–)7.4–11.0(–15.0) × (2.1–)2.7–3.1(–3.3) μm (mean = 9.4 × 2.9 μm), base (1.6–)1.8–2.3(–2.6) μm (mean = 2.0 μm); phialide length/width ratio (2.1–)2.6–3.7(–4.9) (mean = 3.2) (n = 30). Conidia subglobose to globose, green, (2.6–)2.7–3.0(–3.5) × (2.4–)2.5–2.9(–3.2) μm (mean = 2.9 × 2.7 μm), with length/width ratio of 1.0–1.2 (mean = 1.1) (n = 30). Chlamydo-spores abundant, common single, sometimes terminal and intercalary, globose to subglobose, (4.6–)5.1–6.2(–6.8) × (3.7–)4.6–5.9(–6.7) μm (mean = 5.7 × 5.4 μm); length/width ratio 1.0×1.3(mean = 1.1) (n = 30).

Sexual morph. Unknown.

Substrate. Soil.

Distribution. China, Shanxi Province.

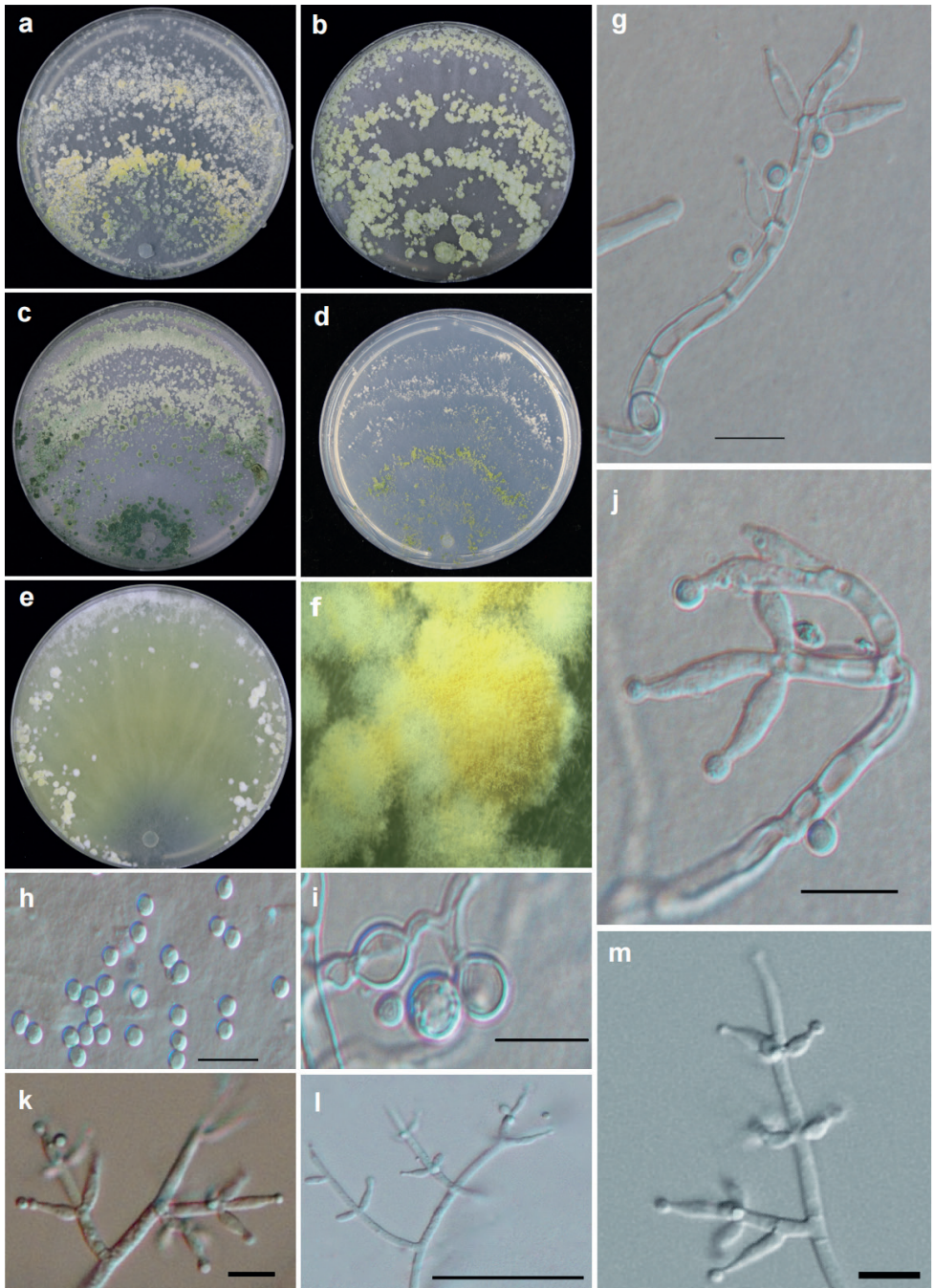


Figure 4. Cultures and anamorph of *T. paradensissimum* strain T31823 **a–d** cultures on different media at 25 °C with a 12 h light and 12 h darkness cycle after 7 d (**a** on PDA **b** on MEA **c** on CMD **d** on SNA) **e** culture on PDA at 35 °C with darkness after 7 d **f** conidiation pustules on PDA after 7 d **g, j–m** conidiophores and phialides (**g, j** on CMD 3 d **k–m** on SNA 3 d) **h** conidia **i** chlamydozoospores. Scale bars: 10 µm (**g–m**).

Additional material examined. CHINA: Shanxi Province, Jincheng City, 35°26'58.1"N, 112°45'19.4"E, 929 m alt., isolated from soil of wheat rhizosphere, Jun 2015, Y. Jiang T31824.

Notes. Similar species can be distinguished according to the pigment: *T. paradensissimum* can produce yellowish pigment on PDA and CMD at 35 °C in the dark, whereas *T. guizhouense* typically at 35 °C reverse forming a dull orange to brown pigment. However, *T. densissimum*, *T. asiaticum*, *T. simile* and *T. zelobreve* cannot produce diffusing pigment on PDA. *Trichoderma pholiotae* and *T. paradensissimum* can both produce yellow pigment on PDA, but *T. pholiotae* has a slightly fruity odor on both PDA and CMD, while *T. paradensissimum* does not have a distinctive odor (Cao et al. 2022).

Discussion

All three new species were isolated from soils. Based on morphology and phylogenetic analyses, the taxonomic positions of three new species were explored. Of these species, *T. nigricans* was grouped into the *Atroviride* Clade, while *T. densissimum* and *T. paradensissimum* were associated with the *Harzianum* Clade.

The genus *Trichoderma* contains at least eight infrageneric clades, of which the *Harzianum* clade is one of the largest (Cai and Druzhinina 2021). The *Harzianum* clade consists of more than 95 accepted species, which are morphologically heterogeneous and phylogenetically complicated (Cao et al. 2022). Two of the newly described species, *T. densissimum* and *T. paradensissimum*, belong to the *Harzianum* Clade, which are closely related to *T. pholiotae*, associated with *T. guizhouense*, *T. asiaticum*, and *T. simile*. The chlamydo-spores of the *Harzianum* Clade members are usually either rarely numerous or not observed, and this is consistent with observations for *T. guizhouense*, *T. asiaticum*, *T. breve*, *T. bannaense*, and *T. atrobrunneum*, among others. In *T. simile*, the chlamydo-spores are either elliptic or round in shape (Li et al. 2013; Chaverri et al. 2015; Jang et al. 2018; Gu et al. 2020). In contrast, the chlamydo-spores of *T. densissimum* and *T. paradensissimum* are numerous, globose to subglobose, and relatively large, especially in *T. densissimum*. Our phylogenetic analyses revealed that *T. densissimum* and *T. paradensissimum* are closely related due to the minimal genetic variation observed in their ITS and *tef1* sequences. Moreover, both species exhibit similar growth characteristics and possess numerous chlamydo-spores. However, their genetic variation in the sequences of *rpb2* (similarity < 99%) differentiate them as distinct species. In addition, *T. densissimum* exhibits green conidiation with 3–4 distinct concentric zones and no diffusing pigment, while *T. paradensissimum* exhibits inconspicuously zonate green to yellow conidiation with white pustules and yellowish pigment.

Trichoderma atroviride and *T. paratroviride* were classified to the *Viride* Clade (Jaklitsch and Voglmayr 2015). However, with the addition of *T. obovatum* and *T. uncinatum*, they were assigned to the *Atroviride* Clade by (Zheng et al. 2021). In this study, the new species *T. nigricans* was also identified as a member of the *Atroviride* Clade. The results of the phylogenetic analysis indicated a close relationship between *T. nigricans*

and *T. atroviride*. Morphologically, *T. nigricans* shares many similarities with *T. atroviride*, including the production of a strong coconut odor in PDA cultures and the presence of abundant chlamydospores. *Trichoderma nigricans* exhibits a faster growth rate on PDA in comparison to *T. atroviride*, with the former's mycelium covering a larger area of the plate and its colony radius measuring between 42.8–60.5 mm after 72 h at 25 °C. Colony radius is *T. nigricans* 16 mm vs. *T. atroviride* (0–)0.3–3.2(–8.3) mm at 35 °C (Samuels et al. 2002).

Numerous biological control agents have been derived from species in the *Atroviride* and *Harzianum* clade to effectively control soil-borne diseases (Chaverri et al. 2015), such as *T. atroviride*, *T. guizhouense*, *T. afroharzianum*, and *T. atrobrunneum* (Longa et al. 2010; Rees et al. 2022; Zhang et al. 2022; Zhao et al. 2022). The discovery of *T. nigricans*, *T. densissimum*, and *T. paradensissimum* in this study highlights the diversity of *Trichoderma* in China and provides valuable information for the development of *Trichoderma*-based biocontrol agents. Further research is necessary to explore the diversity of *Trichoderma* in China and to investigate their potential as biocontrol agents against plant diseases.

Acknowledgements

This work was supported by the Provincial Key Research and Development Plan of Zhejiang, China (2020C02027).

References

- Ahamed A, Vermette P (2008) Culture-based strategies to enhance cellulase enzyme production from *Trichoderma reesei* RUT–C30 in bioreactor culture conditions. *Biochemical Engineering Journal* 40(3): 399–407. <https://doi.org/10.1016/j.bej.2007.11.030>
- Aignon HL, Naseer A, Matheny PB, Yorou NS, Ryberg M (2021) *Mallocybe africana* (Inocybaceae, Fungi), the first species of *Mallocybe* described from Africa. *Phytotaxa* 478(1): 49–60. <https://doi.org/10.11646/phytotaxa.478.1.3>
- Altschul SF, Gish W, Miller W, Myers EW, Lipman DJ (1990) Basic local alignment search tool. *Journal of Molecular Biology* 215(3): 403–410. [https://doi.org/10.1016/S0022-2836\(05\)80360-2](https://doi.org/10.1016/S0022-2836(05)80360-2)
- An X, Cheng G, Gao H, Li X, Yang Y, Li D, Li Y (2022) phylogenetic analysis of *Trichoderma* species associated with green mold disease on mushrooms and two new pathogens on *Ganoderma sichuanense*. *Journal of Fungi* (Basel, Switzerland) 8(7): e704. <https://doi.org/10.3390/jof8070704>
- Atanasova L, Druzhinina IS, Jaklitsch WM (2013) *Trichoderma*: Biology and Applications. Two hundred *Trichoderma* species recognized on the basis of molecular phylogeny. CABI Publishing, New York, 10–42. <https://doi.org/10.1079/9781780642475.0010>
- Bissett J (1984) A revision of the genus *Trichoderma*. I. Section *Longibrachiatum* sect. nov. *Canadian Journal of Botany* 62(5): 924–931. <https://doi.org/10.1139/b84-131>

- Bissett J (1991a) A revision of the genus *Trichoderma*. II. Infrageneric classification. Canadian Journal of Botany 69(11): 2357–2372. <https://doi.org/10.1139/b91-297>
- Bissett J (1991b) A revision of the genus *Trichoderma*. III. Section Pachybasium. Canadian Journal of Botany 69(11): 2373–2417. <https://doi.org/10.1139/b91-298>
- Bissett J, Szakacs G, Nolan CA, Druzhinina I, Gradinger C, Kubicek CP (2003) New species of *Trichoderma* from Asia. Canadian Journal of Botany 81(6): 570–586. <https://doi.org/10.1139/b03-051>
- Cai F, Druzhinina IS (2021) In honor of John Bissett: Authoritative guidelines on molecular identification of *Trichoderma*. Fungal Diversity 107(1): 1–69. <https://doi.org/10.1007/s13225-020-00464-4>
- Cao Z, Qin W, Zhao J, Liu Y, Wang S, Zheng S (2022) Three new *Trichoderma* species in *Harzianum* clade associated with the contaminated substrates of edible fungi. Journal of Fungi 8(11): e1154. <https://doi.org/10.3390/jof8111154>
- Chaverri P, Samuels GJ (2004) *Hypocreal Trichoderma* (Ascomycota, Hypocreales, Hypocreaceae): Species with green ascospores. Studies in Mycology 48(48): 1–116.
- Chaverri P, Branco-Rocha F, Jaklitsch W, Gazis R, Degenkolb T, Samuels GJ (2015) Systematics of the *Trichoderma harzianum* species complex and the re-identification of commercial biocontrol strains. Mycologia 107(3): 558–590. <https://doi.org/10.3852/14-147>
- Chen K, Zhuang W (2016) *Trichoderma shennongjianum* and *Trichoderma tibetense*, two new soil-inhabiting species in the Strictipile clade. Mycoscience 57(5): 311–319. <https://doi.org/10.1016/j.myc.2016.04.005>
- Chen K, Zhuang W (2017) Discovery from a large-scaled survey of *Trichoderma* in soil of China. Scientific Reports 7(1): e9090. <https://doi.org/10.1038/s41598-017-07807-3>
- Dou K, Gao J, Zhang C, Yang H, Jiang X, Li J, Li Y, Wang W, Xian H, Li S, Liu Y, Hu J, Chen J (2019) *Trichoderma* biodiversity in major ecological systems of China. Journal of Microbiology 57(8): 668–675. <https://doi.org/10.1007/s12275-019-8357-7>
- Dou K, Lu Z, Wu Q, Ni M, Yu C, Wang M, Li Y, Wang X, Xie H, Chen J, Zhang C (2020) MIST: A multilocus identification system for *Trichoderma*. Applied and Environmental Microbiology 86(18): e01532–e20. <https://doi.org/10.1128/AEM.01532-20>
- Druzhinina IS, Kopchinskiy AG, Kubicek CP (2006) The first 100 *Trichoderma* species characterized by molecular data. Mycoscience 47(2): 55–64. <https://doi.org/10.1007/S10267-006-0279-7>
- Gu X, Wang R, Sun Q, Wu B, Sun J (2020) Four new species of *Trichoderma* in the *Harzianum* clade from northern China. MycoKeys 73: 109–132. <https://doi.org/10.3897/mycokeys.73.51424>
- Guindon S, Dufayard JF, Lefort V, Anisimova M, Hordijk W, Gascuel O (2010) New algorithms and methods to estimate maximum-likelihood phylogenies: Assessing the performance of PhyML 3.0. Systematic Biology 59(3): 307–321. <https://doi.org/10.1093/sysbio/syq010>
- Harman GE, Howell CR, Viterbo A, Chet I, Lorito M (2004) *Trichoderma* species – opportunistic, avirulent plant symbionts. Nature Reviews. Microbiology 2(1): 43–56. <https://doi.org/10.1038/nrmicro797>
- Jaklitsch WM, Voglmayr H (2015) Biodiversity of *Trichoderma* (Hypocreaceae) in Southern Europe and Macaronesia. Studies in Mycology 80(1): 1–87. <https://doi.org/10.1016/j.si-myc.2014.11.001>

- Jang S, Kwon SL, Lee H, Jang Y, Park MS, Lim YW, Kim C, Kim JJ (2018) New report of three unrecorded species in *Trichoderma harzianum* species complex in Korea. *Mycobiology* 46(3): 177–184. <https://doi.org/10.1080/12298093.2018.1497792>
- Jiang Y, Wang J, Chen J, Mao L, Feng X, Zhang C, Lin F (2016) *Trichoderma* Biodiversity of Agricultural Fields in East China Reveals a Gradient Distribution of Species. *PLoS ONE* 11(8): e160613. <https://doi.org/10.1371/journal.pone.0160613>
- Kalyaanamoorthy S, Minh BQ, Wong TKF, von Haeseler A, Jermin LS (2017) ModelFinder: Fast model selection for accurate phylogenetic estimates. *Nature Methods* 14(6): 587–589. <https://doi.org/10.1038/nmeth.4285>
- Katoh K, Standley DM (2013) MAFFT multiple sequence alignment software version 7: Improvements in performance and usability. *Molecular Biology and Evolution* 30(4): 772–780. <https://doi.org/10.1093/molbev/mst010>
- Kredics L, Antal Z, Manczinger L, Nagy E (2001) Breeding of mycoparasitic *Trichoderma* strains for heavy metal resistance. *Letters in Applied Microbiology* 33(2): 112–116. <https://doi.org/10.1046/j.1472-765x.2001.00963.x>
- Kuhls K, Lieckfeldt E, Borner T, Gueho E (1999) Molecular reidentification of human pathogenic *Trichoderma* isolates as *Trichoderma longibrachiatum* and *Trichoderma citrinoviride*. *Medical Mycology* 37(1): 25–33. <https://doi.org/10.1080/02681219980000041>
- Kumar S, Stecher G, Li M, Knyaz C, Tamura K (2018) MEGA X: Molecular evolutionary genetics analysis across computing platforms. *Molecular Biology and Evolution* 35(6): 1547–1549. <https://doi.org/10.1093/molbev/msy096>
- Lam-Tung N, Schmidt HA, Arndt VH, Quang MB (2015) IQ-TREE: A fast and effective stochastic algorithm for estimating maximum-likelihood phylogenies. *Molecular Biology and Evolution* 32(1): 268–274. <https://doi.org/10.1093/molbev/msu300>
- Li Q, Tan P, Jiang Y, Hyde KD, McKenzie EHC, Bahkali AH, Kang J, Wang Y (2013) A novel *Trichoderma* species isolated from soil in Guizhou, *T. guizhouense*. *Mycological Progress* 12(2): 167–172. <https://doi.org/10.1007/s11557-012-0821-2>
- Li G, Li S, Buyck B, Zhao S, Xie X, Shi L, Deng C, Meng Q, Sun Q, Yan J, Wang J, Li M (2021) Three new *Russula* species in sect. *Ingratae* (Russulales, Basidiomycota) from southern China. *MycoKeys* 84: 103–139. <https://doi.org/10.3897/mycokeys.84.68750>
- Liu YJ, Whelen S, Hall BD (1999) Phylogenetic relationships among ascomycetes: Evidence from an RNA polymerase II subunit. *Molecular Biology and Evolution* 16(12): 1799–1808. <https://doi.org/10.1093/oxfordjournals.molbev.a026092>
- Longa C, Savazzini F, Tosi S, Elad Y, Pertot I (2010) Evaluating the survival and environmental fate of the biocontrol agent *Trichoderma atroviride* SC1 in vineyards in northern Italy. *Journal of Applied Microbiology* 106(5): 1549–1557. <https://doi.org/10.1111/j.1365-2672.2008.04117.x>
- Lorito M, Woo SL, Harman GE, Monte E (2010) Translational research on *Trichoderma*: From ‘omics to the field. *Annual Review of Phytopathology* 48(1): 395–417. <https://doi.org/10.1146/annurev-phyto-073009-114314>
- Lu D (2019) Recording fungal diversity in Republican China: Deng Shuqun’s research in the 1930s. *Archives of Natural History* 46(1): 139–152. <https://doi.org/10.3366/anh.2019.0562>

- Minh BQ, Nguyen M, Haeseler AV (2013) Ultrafast approximation for phylogenetic bootstrap. *Molecular Biology and Evolution* 30(5): 1188–1195. <https://doi.org/10.1093/molbev/mst024>
- O'Donnell K, Kistler HC, Cigelnik E, Ploetz RC (1998) Multiple evolutionary origins of the fungus causing Panama disease of banana: Concordant evidence from nuclear and mitochondrial gene genealogies. *Proceedings of the National Academy of Sciences of the United States of America* 95(5): 2044–2049. <https://doi.org/10.1073/pnas.95.5.2044>
- Overton BE, Stewart EL, Geiser DM (2006) Taxonomy and phylogenetic relationships of nine species of *Hypocrea* with anamorphs assignable to *Trichoderma* section *Hypocreanum*. *Studies in Mycology* 56: 39–65. <https://doi.org/10.3114/sim.2006.56.02>
- Qiao M, Du X, Zhang Z, Xu J, Yu Z (2018) Three new species of soil-inhabiting *Trichoderma* from southwest China. *MycKeys* 44: 63–80. <https://doi.org/10.3897/mycokeys.44.30295>
- Qin W, Zhuang W (2016) Seven wood-inhabiting new species of the genus *Trichoderma* (Fungi, Ascomycota) in *Viride* clade. *Sci Rep–Uk* 6(1): 27074. <https://doi.org/10.1038/srep27074>
- Rees HJ, Drakulic J, Cromey MG, Bailey AM, Foster GD (2022) Endophytic *Trichoderma* spp. can protect strawberry and privet plants from infection by the fungus *Armillaria mellea*. *PLoS ONE* 17(8): e271622. <https://doi.org/10.1371/journal.pone.0271622>
- Rifai MA (1969) A revision of the genus *Trichoderma*. Commonwealth Mycological Institute, London, 56 pp.
- Ronquist F, Teslenko M, Paul V, Ayres DL, Darling A, Höhna S, Larget B, Liu L, Suchard MA, Huelsenbeck JP (2012) MrBayes 3.2: Efficient bayesian phylogenetic inference and model choice across a large model space. *Systematic Biology* 61(3): 539–542. <https://doi.org/10.1093/sysbio/sys029>
- Samuels GJ (2006) *Trichoderma*: Systematics, the sexual state, and ecology. *Phytopathology* 96(2): 195–206. <https://doi.org/10.1094/PHYTO-96-0195>
- Samuels GJ, Dodd SL, Gams W, Castlebury LA, Petrini O (2002) *Trichoderma* species associated with the green mold epidemic of commercially grown *Agaricus bisporus*. *Mycologia* 94(1): 146–170. <https://doi.org/10.1080/15572536.2003.11833257>
- Savoie JM, Mata G (2003) *Trichoderma harzianum* metabolites pre-adapt mushrooms to *Trichoderma aggressivum* antagonism. *Mycologia* 95(2): 191–199. <https://doi.org/10.1080/15572536.2004.11833104>
- Stracquandano C, Quiles JM, Meca G, Cacciola S (2020) Antifungal Activity of Bioactive Metabolites Produced by *Trichoderma asperellum* and *Trichoderma atroviride* in Liquid Medium. *Journal of Fungi* 6(4): e263. <https://doi.org/10.3390/jof6040263>
- Sun R, Liu Z, Fu K, Fan L, Chen J (2012) *Trichoderma* biodiversity in China. *Journal of Applied Genetics* 53(3): 343–354. <https://doi.org/10.1007/s13353-012-0093-1>
- Sun J, Pei Y, Li E, Li W, Hyde KD, Yin WB, Liu X (2016) A new species of *Trichoderma* hypoxylon harbours abundant secondary metabolites. *Scientific Reports* 6(1): e37369. <https://doi.org/10.1038/srep37369>
- Tripathi P, Singh PC, Mishra A, Chauhan PS, Dwivedi S, Bais RT, Tripathi RD (2013) *Trichoderma*: A potential bioremediator for environmental clean up. *Clean Technologies and Environmental Policy* 15(4): 541–550. <https://doi.org/10.1007/s10098-012-0553-7>

- Vaidya G, Lohman DJ, Meier R (2011) SequenceMatrix: Concatenation software for the fast assembly of multi-gene datasets with character set and codon information. *Cladistics* 27(2): 171–180. <https://doi.org/10.1111/j.1096-0031.2010.00329.x>
- Yu Z, Qiao M, Zhang Y, Zhang K (2007) Two new species of *Trichoderma* from Yunnan, China. *Antonie van Leeuwenhoek* 92(1): 101–108. <https://doi.org/10.1007/s10482-006-9140-4>
- Zhang CL, Druzhinina IS, Kubicek CP, Xu T (2005) *Trichoderma* biodiversity in China: Evidence for a North to South distribution of species in East Asia. *FEMS Microbiology Letters* 251(2): 251–257. <https://doi.org/10.1016/j.femsle.2005.08.034>
- Zhang CL, Liu SP, Lin FC, Kubicek CP, Druzhinina IS (2007) *Trichoderma taxi* sp nov., an endophytic fungus from Chinese yew *Taxus mairei*. *FEMS Microbiology Letters* 270(1): 90–96. <https://doi.org/10.1111/j.1574-6968.2007.00659.x>
- Zhang D, Gao F, Jakovli I, Zou H, Wang GT (2020) PhyloSuite: An integrated and scalable desktop platform for streamlined molecular sequence data management and evolutionary phylogenetics studies. *Molecular Ecology Resources* 20(1): 348–355. <https://doi.org/10.1111/1755-0998.13096>
- Zhang G, Yang H, Zhang X, Zhou F, Wu X, Xie X, Zhao X, Zhou H (2022) Five new species of *Trichoderma* from moist soils in China. *MycKeys* 87: 133–157. <https://doi.org/10.3897/mycokeys.87.76085>
- Zhao Y, Chen X, Cheng J, Xie J, Lin Y, Jiang D, Fu Y, Chen T (2022) Application of *Trichoderma* Hz36 and Hk37 as Biocontrol Agents against Clubroot Caused by *Plasmodiophora brassicae*. *Journal of Fungi* 8(8): e777. <https://doi.org/10.3390/jof8080777>
- Zheng H, Qiao M, Lv Y, Du X, Zhang K, Yu Z (2021) New Species of *Trichoderma* Isolated as Endophytes and Saprobes from Southwest China. *Journal of Fungi* 7(6): e467. <https://doi.org/10.3390/jof7060467>
- Zhu ZX, Zhuang WY (2015a) Three new species of *Trichoderma* with hyaline ascospores from China. *Mycologia* 107(2): 328–345. <https://doi.org/10.3852/14-141>
- Zhu ZX, Zhuang WY (2015b) *Trichoderma* (*Hypocrea*) species with green ascospores from China. *Persoonia* 34(1): 113–129. <https://doi.org/10.3767/003158515X686732>
- Zin NA, Badaluddin NA (2020) Biological functions of *Trichoderma* spp. for agriculture applications. *Annals of Agricultural Science* 65(2): 168–178. <https://doi.org/10.1016/j.aas.2020.09.003>

Soil-borne Ophiostomatales species (Sordariomycetes, Ascomycota) in beech, oak, pine, and spruce stands in Poland with descriptions of *Sporothrix roztoczensis* sp. nov., *S. silvicola* sp. nov., and *S. tumida* sp. nov.

Piotr Bilański¹, Robert Jankowiak¹, Halvor Solheim², Paweł Fortuna¹, Łukasz Chyrzyński¹, Paulina Warzecha¹, Stephen Joshua Taerum³

1 Department of Forest Ecosystems Protection, University of Agriculture in Krakow, Al. 29 Listopada 46, 31-425 Krakow, Poland **2** Norwegian Institute of Bioeconomy Research, P.O. Box 115, 1431, Ås, Norway **3** The Connecticut Agricultural Experiment Station, Department of Plant Pathology and Ecology, Jenkins-Waggoner Laboratory, 123 Huntington Street P.O. Box 1106, New Haven, CT 06504-1106, USA

Corresponding author: Robert Jankowiak (r.jankowiak@urk.edu.pl)

Academic editor: M. Ruskiewicz-Michalska | Received 10 November 2022 | Accepted 19 April 2023 | Published 16 May 2023

Citation: Bilański P, Jankowiak R, Solheim H, Fortuna P, Chyrzyński Ł, Warzecha P, Taerum SJ (2023) Soil-borne Ophiostomatales species (Sordariomycetes, Ascomycota) in beech, oak, pine, and spruce stands in Poland with descriptions of *Sporothrix roztoczensis* sp. nov., *S. silvicola* sp. nov., and *S. tumida* sp. nov.. MycoKeys 97: 41–69. <https://doi.org/10.3897/mycokeys.97.97416>

Abstract

Ophiostomatales (Ascomycota) contains many species, most of which are associated with bark beetles. Some members of this order are plant or animal pathogens, while others colonize soil, different plant tissues, or even carpophores of some Basidiomycota. However, little is known about soil-inhabiting Ophiostomatales fungi. A survey of these fungi associated with soil under beech, oak, pine, and spruce stands in Poland yielded 623 isolates, representing 10 species: *Heinzbutinia grandicarpa*, *Leptographium procerum*, *L. radiaticola*, *Ophiostoma piliferum*, *O. quercus*, *Sporothrix brunneoviolacea*, *S. dentifunda*, *S. eucastaneae*, and two newly described taxa, namely *Sporothrix roztoczensis* sp. nov. and *S. silvicola* sp. nov. In addition, isolates collected from fallen shoots of *Pinus sylvestris* that were pruned by *Tomicus* sp. are described as *Sporothrix tumida* sp. nov. The new taxa were morphologically characterized and phylogenetically analyzed based on multi-loci sequence data (ITS, β -tubulin, calmodulin, and translation elongation factor 1- α genes). The Ophiostomatales species were especially abundant in soil under pine and oak stands. *Leptographium procerum*, *S. silvicola*, and *S. roztoczensis* were the most frequently isolated species from soil under pine stands, while *S. brunneoviolacea* was the most abundant in soil under oak stands. The results highlight that forest soil in Poland has a wide diversity of Ophiostomatales taxa, but further studies are required to uncover the molecular diversity and phylogenetic relationships of these fungi, as well as their roles in soil fungal communities.

Keywords

3 new taxa, ophiostomatalean fungi, phylogenetics, *Pinus sylvestris*, soil-inhabiting fungi, *Sporothrix*, taxonomy

Introduction

Ophiostomatales (Sordariomycetidae, Ascomycota) contains a single family, the Ophiostomataceae, which includes 16 well-defined genera together with many taxa of uncertain phylogenetic position. *Leptographium*, *Ophiostoma*, and *Sporothrix* represent the genera with the largest numbers of taxa, which are grouped into species complexes based on morphology and phylogenetic relationships. These fungi are characterized by the presence of globose ascomata with short to very long necks and ascospores that vary in size and shape, mostly allantoid, bacilliform, and cylindrical with sheaths. The asexual morphs exhibit five conidiophore types: hyalorhinocladia-like, leptographium-like, pesotum-like, raffaelea-like, and sporothrix-like. The species in this order are best known as wood-inhabiting fungi that live in association with various arthropods, but many species can also occupy other habitats such as soil, carpophores, plant infructescences or animal tissues (de Beer and Wingfield 2013; de Beer et al. 2013a, b, 2016, 2022).

Little is known about the diversity of Ophiostomatales species in different soil ecosystems, although some *Sporothrix* spp. have been reported in soil worldwide. The currently known soil-inhabiting species include *S. aurorae* (X.D. Zhou & M.J. Wingf.) Z.W. de Beer, T.A. Duong & M.J. Wingf., *S. bragantina* (Pfenning & Oberw.) Z.W. de Beer, T.A. Duong & M.J. Wingf., *S. brasiliensis* Marimon, Gené, Cano & Guarro, *S. brunneoviolacea* Madrid, Gené, Cano & Guarro, *S. chilensis* A.M. Rodrigues, Choppa, G.F. Fernandes, de Hoog & Z.P. de Camargo, *S. dimorphospora* (Roxon & S.C. Jong) Madrid, Gené, Cano & Guarro, *S. globosa* Marimon, Cano, Gené, Deanna A. Sutton, H. Kawas. & Guarro, *S. guttiliformis* de Hoog, *S. humicola* de Mey., Z.W. de Beer & M.J. Wingf., *S. inflata* de Hoog, ‘*S. inflata* 2’, *S. luriei* (Ajello & Kaplan) Marimon, Gené, Cano & Guarro, *S. mexicana* Marimon, Gené, Cano & Guarro, *S. narcissi* (Limber) Z.W. de Beer, T.A. Duong & M.J. Wingf., *S. pallida* (Tubaki) Matsush., *S. schenckii* Hektoen & C.F. Perkins, *S. stenoceras* (Robak) Z.W. de Beer, T.A. Duong & M.J. Wingf., and *S. stylites* de Mey., Z.W. de Beer & M.J. Wingf. (de Beer et al. 2003, 2016). Among them, *S. brunneoviolacea*, *S. dimorphospora* (Madrid et al. 2010), *S. inflata*, ‘*S. inflata* 2’ (de Hoog 1974; de Beer et al. 2016), *S. pallida*, *S. schenckii* (de Meyer et al. 2008; de Beer et al. 2016), and *S. stenoceras* (Novotný and Šrůtka 2004) have been reported from European soils. Some of these soil-borne species, namely *S. brasiliensis*, *S. chilensis*, *S. globosa*, *S. luriei*, and *S. schenckii*, are agents of human and animal sporotrichosis (López-Romero et al. 2011; Zhang et al. 2015; Rodrigues et al. 2017; Ramírez-Soto et al. 2018).

Members of the Ophiostomatales are typically tree- or wood-infecting fungi, and are commonly associated with bark- and wood-dwelling beetles and their associated

mites (de Beer et al. 2022). The association between these fungi and subcortical insects has been extensively investigated in Poland (e.g. Jankowiak and Kolařík 2010; Jankowiak and Bilański 2013a, b, c; Jankowiak et al. 2017, 2019a). Polish and South African studies have demonstrated that wounded hardwoods provide habitat for a large diversity of Ophiostomatales species (Musvuugwa et al. 2016; Jankowiak et al. 2019b). The findings from studies in Poland also provided the first evidence that European nitidulid beetles act as effective vectors of *Ophiostoma* spp. and *Sporothrix* spp. (Jankowiak et al. 2019b). The Polish surveys led to the discovery and description of many Ophiostomatales species (e.g. Linnakoski et al. 2016; Aas et al. 2018; Jankowiak et al. 2018a, 2019c, 2020, 2021; Strzałka et al. 2020; Ostafińska et al. 2021).

Previous studies of soil-borne fungi belonging to the Ophiostomatales were limited to *Sporothrix* species (e.g. de Meyer et al. 2008; Madrid et al. 2010) and even this genus remains largely unstudied. The aim of this study was to explore the diversity of Ophiostomatales members associated with soil under forest trees in Poland from a taxonomic perspective and to describe potential resultant new species. Fungi were baited with branch fragments that were buried in soil under beech, oak, pine, and spruce forests. We also describe a *Sporothrix* species that was isolated from fallen shoots of *Pinus sylvestris* L. mentioned in a previously published study (Jankowiak and Kolařík 2011).

Materials and methods

Study area

Wood samples were collected from four forest districts located in southern Poland (Józefów, Krzeszowice, Siewierz, and Węgierska Górką) between 2015–2019. In each district, 10 stands dominated by *Fagus sylvatica* L. (Krzeszowice, Małopolskie Province), *Picea abies* (L.) H. Karst. (Węgierska Górką, Śląskie Province), *P. sylvestris* (Józefów, Lubelskie Province), and *Quercus robur* L. (Siewierz, Śląskie Province) were selected, making a total of 40 stands (10 stands for each tree species). The stands were managed and between 35 to 135 years of age.

All sampled stands have temperate climates. Węgierska Górką is located in the lower montane belt of the Western Carpathians (607–896 m a.s.l.) with an average annual temperature and precipitation of 6.5 °C and approximately 950 mm, respectively. The other forest stands are in the Highlands of Poland (217–347 m a.s.l.) with average annual temperature and precipitation of 7–8 °C and approximately 600–800 mm, respectively. Tree-stratum vegetation in Józefów is dominated by *P. sylvestris*, but also consists of *Abies alba* Mill., *Alnus glutinosa* (L.) Gaertn., *Betula pendula* Roth, *P. abies*, and *Q. robur*. In Krzeszowice, *F. sylvatica* is the dominant tree species, but other species are also present, such as *Carpinus betulus* L., *P. sylvestris*, and *Q. robur*. Siewierz stands are dominated by *Q. robur*, but also include *Acer pseudoplatanus* L., *A. glutinosa*, *B. pendula*, *C. betulus*, *Larix decidua* Mill., *P. abies*, and *P. sylvestris*. Finally, vegetation in Węgierska Górką is dominated by *P. abies*, but also contains *A. alba* and *F. sylvatica*.

Soil samples for laboratory analyses were collected from each stand (10 samples per stand, for a total of 400 samples). The samples were collected from the humus A mineral horizon (10 cm deep) after the upper organic O horizon was removed. Freshly collected soil samples were dried and then sieved through a 2 mm mesh sieve. The particle size distribution was analyzed using a laser diffraction method (Analysette 22, Fritsch, Idar-Oberstein, Germany). The pH of soil samples in H₂O and KCl was determined by a potentiometric method (Ostrowska et al. 1991). All stands were characterized by high soil acidity, with the pH ranging from 3.81 to 6.10 (in H₂O) and 2.91 to 5.67 (in KCl). After air-drying, soil samples were sifted through a sieve with a mesh diameter of 2 mm. The particle size distribution was determined using laser diffraction (Analysette 22, Fritsch, Idar-Oberstein, Germany). Soil textures were sandy in 27 stands and silty in the remaining 13 stands.

Isolation of fungi

Fungi were isolated using branches (25 cm × 5 cm × 5 cm) of *F. sylvatica*, *P. abies*, *P. sylvestris*, and *Q. robur* that were cut along the axes. Healthy branches were taken from trees that represented the dominant species in each stand; for example, in stands dominated by *F. sylvatica*, only its branches were used. Each branch was autoclaved in a sterile plastic bag and was stored for 1–2 days at a temperature of 5 °C. They were then removed from the bags and immediately placed in the soil. Ten sterilized branches were placed in each stand. Branches were buried in the humus mineral A horizon after the organic O horizon was removed, at random locations in the stands (Suppl. material 1: fig. S1). There is no information about the occurrence of Ophiostomatales species in specific soil levels. We have used the humus mineral horizon (A) because this level is characterized by high thermal and humidity stability (Ekici et al. 2014; Neto et al. 2017). Due to potential fungal infection from roots, the branches were placed 2 m away from tree roots. The branches were buried after the main flight period of the root-feeding bark beetles to avoid colonization by insects carrying other Ophiostomatales species (Jankowiak and Bilański 2013a) and were retrieved two months after they were initially buried. After removal, the branches were placed in separate sterile bags and moved to the laboratory of Robert Jankowiak at the University of Agriculture in Krakow, Poland (Suppl. material 1: fig. S2). A total of 400 samples were collected during the study from every stand type (100 from beech stands, 100 from oak, 100 from pine, and 100 from spruce). No signs of insect presence (adults, larvae, bites, wood holes, galleries) were visible on any branch.

The branches were washed under tap water and dried on blotting paper and covered with cotton wool saturated with 96% ethanol for 15 seconds to sterilize the wooden surfaces. A sterile wood chisel was then used to remove the surface of the wood up to a depth of 2 mm. From each block, six small fragments of discolored wood (4 × 4 mm) were taken with a sterile chisel and placed in Petri dishes containing 2% malt extract agar (MEA; Biocorp Polska Sp. z o.o., Warszawa, 20 g Biocorp malt extract, 20 g Biocorp agar, and 1000 mL sterile water) amended with cycloheximide (200 mg/L, Aldrich-Sigma, St. Louis, Co. LLC.) and tetracycline (50 mg/L, Aldrich-Sigma, St.

Louis, Co. LLC). Based on the preliminary morphological investigation, emerging cultures resembling members of the Ophiostomatales were purified by transferring small pieces of mycelium or spore masses from individual colonies to fresh 2% MEA. Cultures were incubated at room temperature in the dark at 22 °C. After two weeks of incubation, the purified fungal cultures were grouped into morphotypes. Depending on the number of isolates that belonged to the same morphotype, 1–12 isolates per morphotype were chosen for molecular identification (Table 1). In the end, the isolates were categorized into ten morphotypes.

The collection details for the *Sporothrix* species isolated from fallen shoots of *P. sylvestris* (Table 1) are described in a study by Jankowiak and Kolařík (2011). The cultures are maintained in the culture collection of the Department of Forest Ecosystems Protection, University of Agriculture in Krakow, Poland. The ex-type isolates and representative isolates of the new species described were deposited in the culture collection (CBS) of the Westerdijk Fungal Biodiversity Institute, Utrecht, The Netherlands and in the culture collection (CMW) of the Forestry and Agricultural Biotechnology Institute (FABI) at the University of Pretoria, South Africa. Dried cultures were deposited as holotype specimens in the Mycological Herbarium (O) of the Natural History Museum at the University of Oslo, Norway.

Microscopy and growth studies

Morphological characters were examined for selected isolates including the type specimens. Cultures were grown on 2% Malt Extract Agar (MEA) made up of 20 g Bacto malt extract and 20 g Bacto agar powder (Becton Dickinson and Company, Franklin Lakes, USA) in 1 L of deionized water. In attempts to induce ascomata formation, autoclaved twigs of host trees were placed at the centres of agar plates containing 2% MEA. To promote the production of ascomata, single conidial isolates were crossed following the technique described by Grobbelaar et al. (2009). These cultures were incubated at 25 °C and monitored regularly for the appearance of developing structures.

Samples of fungal tissues were placed in 80% lactic acid on glass slides, and developing structures were observed using a Nikon Eclipse 50i microscope (Nikon Corporation, Tokyo, Japan) with an Invenio 5S digital camera (DeltaPix, Maalov, Denmark) to capture photographic images. Color designations were based on the color charts of Kornerup and Wanscher (1978). For each taxonomically relevant structure, fifty measurements were made, when possible, using the Coolview 1.6.0 software (Precop-tic, Warsaw, Poland). Averages, ranges, and standard deviations were presented in the format '(min–)(mean–SD)–(mean+SD)(–max)'

Growth characteristics of the novel species were determined by analyzing the radial growth for two isolates per species. Agar disks (5 mm in diameter) were cut from the actively growing margins of fungal colonies and these disks were placed at the centres of plates containing 2% MEA. Four replicate plates for each isolate of the three putative new species were incubated in the dark. The isolates were grown at 5, 10, 15, 20, 25, 30 and 35 °C. The radial growth was determined 14 days after inoculation, and growth rates were calculated as mm/day.

Table 1. Isolates from this study used in the phylogenetic analyses.

Taxon no.	Fungal species	Isolate no ^a			Source	Site	GenBank accessions ^b				
		CBS	CMW	KFL			ITS	LSU	TUB2	TBE1	CAL
1	<i>Heinzhuberia grandicarpa</i>			KFL2,3PFDb	Wood buried in soil of <i>Quercus robur</i> stand	Siewierz	OP594819			OP588965	OP589005
				KFL42So	Wood buried in soil of <i>Pinus sylvestris</i> stand	Łóżeńfów				OP588956	
2	<i>Leptoglyphium procerum</i>			KFL51So	Wood buried in soil of <i>Pinus sylvestris</i> stand	Łóżeńfów				OP588957	
				KFL59So	Wood buried in soil of <i>Pinus sylvestris</i> stand	Łóżeńfów		OP594816		OP588958	OP589002
				KFL62So	Wood buried in soil of <i>Pinus sylvestris</i> stand	Łóżeńfów		OP594817		OP588959	OP589003
				KFL68So	Wood buried in soil of <i>Pinus sylvestris</i> stand	Łóżeńfów		OP594818		OP588960	OP589004
				KFL70So	Wood buried in soil of <i>Pinus sylvestris</i> stand	Łóżeńfów				OP588961	
				KFL77So	Wood buried in soil of <i>Pinus sylvestris</i> stand	Łóżeńfów				OP588962	
3	<i>Leptoglyphium radiaticola</i>			KFL94So	Wood buried in soil of <i>Pinus sylvestris</i> stand	Łóżeńfów				OP588963	
				KFL104So	Wood buried in soil of <i>Pinus sylvestris</i> stand	Łóżeńfów				OP588964	
				KFL6So	Wood buried in soil of <i>Pinus sylvestris</i> stand	Łóżeńfów		OP594813		OP588952	OP588998
				KFL15So	Wood buried in soil of <i>Pinus sylvestris</i> stand	Łóżeńfów				OP588953	OP588999
				KFL16So	Wood buried in soil of <i>Pinus sylvestris</i> stand	Łóżeńfów		OP594814		OP588954	OP589000
				KFL65So	Wood buried in soil of <i>Pinus sylvestris</i> stand	Łóżeńfów		OP594815		OP588955	OP589001
4	<i>Ophiostoma ptiliferum</i>			KFL65aob	Wood buried in soil of <i>Pinus sylvestris</i> stand	Łóżeńfów	OP594820		OP588966	OP589006	
				KFL11So	Wood buried in soil of <i>Pinus sylvestris</i> stand	Łóżeńfów			OP588967	OP589007	
				KFL5Db	Wood buried in soil of <i>Quercus robur</i> stand	Siewierz	OP594822		OP588968	OP589008	
5	<i>Ophiostoma quercus</i>			KFL10Db	Wood buried in soil of <i>Quercus robur</i> stand	Siewierz	OP594823		OP588969		
				KFL55Db	Wood buried in soil of <i>Quercus robur</i> stand	Siewierz	OP594824		OP588970		
				KFL64PFDb	Wood buried in soil of <i>Quercus robur</i> stand	Siewierz	OP594825		OP588971	OP589009	
6	<i>Sporothrix brunneoviolacea</i>			KFL16PFDb	Wood buried in soil of <i>Quercus robur</i> stand	Siewierz	OP594826		OP588972	OP589010	
				KFL32PFaDb	Wood buried in soil of <i>Quercus robur</i> stand	Siewierz	OP594827		OP588973	OP589037	
				KFL41PFDb	Wood buried in soil of <i>Quercus robur</i> stand	Siewierz	OP594828		OP588974	OP589038	
				KFL19PFaDb	Wood buried in soil of <i>Quercus robur</i> stand	Siewierz	OP594829		OP588975	OP589013	
				KFL65PFDb	Wood buried in soil of <i>Quercus robur</i> stand	Siewierz	OP594830		OP588976	OP589040	
				KFL19PFbDb	Wood buried in soil of <i>Quercus robur</i> stand	Siewierz	OP594831		OP588977	OP589015	
7	<i>Sporothrix dentifunda</i>			KFL20PFDb	Wood buried in soil of <i>Quercus robur</i> stand	Siewierz	OP594832		OP588978	OP589016	
				KFL89PFDb	Wood buried in soil of <i>Quercus robur</i> stand	Siewierz	OP594833		OP588979	OP589043	
				KFL21PFaDb	Wood buried in soil of <i>Quercus robur</i> stand	Siewierz	OP594834		OP588980	OP589044	
				KFL21PFbDb	Wood buried in soil of <i>Quercus robur</i> stand	Siewierz	OP594835		OP588981	OP589045	
				KFL28PFDb	Wood buried in soil of <i>Quercus robur</i> stand	Siewierz	OP594836		OP588982	OP589020	
				KFL37PFDb	Wood buried in soil of <i>Quercus robur</i> stand	Siewierz	OP594837		OP588983	OP589020	

Taxon no.	Fungal species	Isolate no ^a			Source	Site	GenBank accessions ^b			
		CBS	CMW	KFL			ITS	LSU	TUB2	TEF1
8	<i>Sporothrix euastaneae</i>			KFL54PEDb	Wood buried in soil of <i>Quercus robur</i> stand	Siewierz	OP594838	OP588984	OP589021	OP589046
9	<i>Sporothrix metzozensis</i> sp. nov.	147973	57307	KFL36So KFL96So ^T	Wood buried in soil of <i>Pinus sylvestris</i> stand	Józefów	OP594846	OP588992	OP589029	OP589054
		147972	57306	KFL78So ^C	Wood buried in soil of <i>Pinus sylvestris</i> stand	Józefów	OP594847	OQ449632	OP589030	OP589055
		147974	57308	KFL89So	Wood buried in soil of <i>Pinus sylvestris</i> stand	Józefów	OP594848	OQ449633	OP589031	OP589056
10	<i>Sporothrix silvicola</i> sp. nov.			KFL85PEDb	Wood buried in soil of <i>Quercus robur</i> stand	Józefów	OP594849	OP588995	OP589032	OP589057
		149238		KFL3So	Wood buried in soil of <i>Pinus sylvestris</i> stand	Siewierz	OP594839	OP588985	OP589022	OP589047
		149241		KFL5So KFL48So ^T	Wood buried in soil of <i>Pinus sylvestris</i> stand	Józefów	OP594840	OP588986	OP589023	OP589048
		149239		KFL38So	Wood buried in soil of <i>Pinus sylvestris</i> stand	Józefów	OP594841	OP588987	OP589024	OP589049
		149240		KFL116So ^C	Wood buried in soil of <i>Pinus sylvestris</i> stand	Józefów	OP594842	OQ449630	OP589025	OP589050
		149242		KFL36Sw	Wood buried in soil of <i>Pinus sylvestris</i> stand	Józefów	OP594843	OP588988	OP589026	OP589051
11	<i>Sporothrix tumida</i> sp. nov.	147970	57304	KFL53RJ ^{TD}	Wood buried in soil of <i>Picea abies</i> stand	Józefów	OP594844	OQ449631	OP589027	OP589052
		147971	57305	KFL85RJ ^{TD}	Shoots of Scots pine pruned by <i>Tomiscus</i> sp.	Andrychów	OP594845	OP588991	OP589028	OP589053
					Shoots of Scots pine pruned by <i>Tomiscus</i> sp.	Mielec	OP594850	OQ449634	OP589033	OP589058
					Shoots of Scots pine pruned by <i>Tomiscus</i> sp.	Mielec	OP594851	OQ449635	OP589034	OP589059

^a CBS = Westerdijk Fungal Biodiversity Institute, Utrecht, The Netherlands; CMW = Culture Collection of the Forestry and Agricultural Biotechnology Institute (FABI), University of Pretoria, Pretoria, South Africa; KFL = Culture collection of the Department of Forest Ecosystems Protection; University of Agriculture in Krakow, Poland.

^b ITS = internal transcribed spacer region of the nuclear ribosomal DNA gene; LSU = internal transcribed spacer region 2 and the 28S large subunit of the nrDNA gene; TUB2 = β -tubulin; TEF1 = Translation elongation factor 1-alpha; CAL = calmodulin.

^c additional specimen examined.

^d Isolates collected during previous surveys in Poland and identified as *Sporothrix* sp. 1 (Jankowiak and Kolarik 2011).

^T denotes ex-type cultures.

PCR, sequencing, and phylogenetic analyses

DNA was extracted using the Genomic Mini AX Plant Kit (A&A Biotechnology, Gdynia, Poland) according to the manufacturer's protocol. For fungi that resided in the genus *Leptographium*, the nuclear large subunit (LSU) region was amplified using the primers LR0R and LR5 (Vilgalys and Hester 1990), the β -tubulin (*TUB2*) gene was amplified using the primers Bt2a and Bt2b (Glass and Donaldson 1995), and the elongation factor 1- α (*TEF1*) gene was amplified using the primers EF2F (Marincowitz et al. 2015) and EF2R (Jacobs et al. 2004). For all other fungi, the internal transcribed spacer regions 1 and 2 (ITS), including the 5.8S region, were amplified using the primers ITS1F and ITS4 (White et al. 1990; Gardes and Bruns 1993), the *TUB2* gene was amplified using the primers Bt2a and Bt2b (Glass and Donaldson 1995), and the *TEF1* gene was amplified using the primers F-728F (Carbone and Kohn 1999) and EF2 (O'Donnell et al. 1998). In addition, the calmodulin (*CAL*) gene was amplified with the primer pairs CL1 and CL2a (O'Donnell et al. 2000) or CL3F and CL3R (de Beer et al. 2016) for fungi that reside in the genus *Sporothrix*. For new *Sporothrix* species, LSU region was amplified using the primers LR0R and LR5 (Vilgalys and Hester 1990). PCR and sequencing were conducted following the protocols described by Jankowiak et al. (2019c). All sequences obtained in this study were deposited in GenBank. The obtained ITS/LSU sequences were compared with sequences in NCBI GenBank for preliminary identifications and were used to determine generic placement in the Ophiostomatales. For *Leptographium* and *Ophiostoma* spp. the *TUB2* and *TEF1* datasets were analyzed separately for each species complex. For *Sporothrix* spp., the *CAL*, *TUB2* and *TEF1* datasets were analyzed across the entire genus.

Phylogenetic trees were generated independently for each gene. Resulting trees were visually compared for topological incongruences. Genes showing no topological incongruence for *Sporothrix* spp. were combined and analyzed as a concatenated dataset. Sequence alignments were performed using the online version of MAFFT v7 (Katoh and Standley 2013). The ITS, LSU, *TUB2*, *CAL*, and *TEF1* datasets were aligned using the E-INS-i strategy with a 200PAM/k=2 scoring matrix, a gap opening penalty of 1.53 and an offset value of 0.00. The alignments were checked manually with BioEdit v.2.7.5 (Hall 1999). Phylogenetic trees were inferred for each of the datasets using three different methods: Maximum likelihood (ML), Maximum Parsimony (MP), and Bayesian inference (BI). For ML and BI analyses, the best-fit substitution models for each aligned dataset were established using the corrected Akaike Information Criterion (AIC) in jModelTest 2.1.10 (Guindon and Gascuel 2003; Darriba et al. 2012). ML analyses were carried out with PhyML 3.0 (Guindon et al. 2010), utilizing the Montpellier online server (<http://www.atgc-montpellier.fr/phyml/>). Node support values and the overall reliability of the ML tree topology were assessed using 1000 bootstrap pseudoreplicates.

MP analyses were performed using PAUP* 4.0b10 (Swofford 2003). Gaps were treated as a fifth state. Confidence levels for the nodes within the inferred tree topolo-

gies were determined using 1000 bootstrap replicates. Tree bisection and reconnection (TBR) were selected as the branch swapping option. The tree length (TL), Consistency Index (CI), Retention Index (RI), Homoplasy Index (HI), and Rescaled Consistency Index (RC) were recorded for each analyzed dataset after the trees were generated.

BI analyses using Markov Chain Monte Carlo (MCMC) methods were carried out with MrBayes v3.1.2 (Ronquist and Huelsenbeck 2003). Four MCMC chains were run for 10 million generations applying the best-fit model for each dataset. Trees were sampled every 100 generations, resulting in 100,000 trees. Tracer v1.4.1 (Rambaut and Drummond 2007) was used to determine the burn-in value for each dataset. The remaining trees were used to generate a 50% majority rule consensus tree, which allowed for calculating posterior probability values for the nodes. All alignments and trees were deposited into TreeBASE (Reviewer access URL: <http://purl.org/phylo/treebase/phyloids/study/TB2:S29855?x-access-code=62dd9f4ad30f131a52104b44860daf9e&format=html>).

Results

Collections of fungi

In total, 623 Ophiostomatales isolates were obtained from 2400 wooden samples (six pieces from each of 400 branches; Table 2). Five hundred and forty-one isolates were collected from pine, 79 isolates were collected from oak, and three isolates were collected from Norway spruce. No isolates were obtained from the beech wooden fragments (Table 2).

Based on morphological observations, the fungal isolates obtained from this study were arranged into 10 species. Five fungal species were isolated from pine while six species were isolated from oak fragments. Only one species (designated as taxon 10; Table 2) was isolated from pine, oak, and spruce samples. The most frequently isolated fungi were taxon 2 and taxon 10 represented by 263 and 174 isolates, respectively. The third most abundant fungus was named as taxon 9, which was isolated 66 times. In addition, 53 isolates of taxon 6 were gathered from buried oak branches (Table 2).

DNA sequence data and phylogenetic analysis

Based on analysis of ITS and LSU sequence data, of the 623 isolates collected in this study, 305, 298, 17 and 3 isolates resided in *Sporothrix* (Fig. 1), *Leptographium* (Suppl. material 2: fig. S3), *Ophiostoma* and *Heinzbutinia* (Suppl. material 2: fig. S4), respectively. Most of the isolates belonging to *Leptographium* grouped in the *L. procerum* species complex, while most of the isolates belonging to *Sporothrix* nested in the *S. inflata* species complex. Phylogenetic analyses of these datasets separated the isolates into 11 distinct taxa, eight of which were previously described species and three represented novel species.

Table 2. Number of isolates of Ophiostomatales fungi obtained from “wood traps” buried in the soil of 40 stands in this study.

Taxon no.	Fungus species	Forest stands dominated by			
		<i>Quercus robur</i>	<i>Pinus sylvestris</i>	<i>Picea abies</i>	<i>Fagus sylvatica</i>
1	<i>Heinzbutinia grandicarpa</i>	3			
2	<i>Leptographium procerum</i>		263		
3	<i>Leptographium radiaticola</i>		35		
4	<i>Ophiostoma piliferum</i>		7		
5	<i>Ophiostoma quercus</i>	10			
6	<i>Sporothrix brunneoviolacea</i>	53			
7	<i>Sporothrix dentifunda</i>	11			
8	<i>Sporothrix eucastaneae</i>	1			
9	<i>Sporothrix roztozczensis</i> sp. nov.		66		
10	<i>Sporothrix silvicola</i> sp. nov.	1	170	3	
	Total no. of isolates	79	541	3	
	Total no. of species	6	6	1	
	Number of examined fragments	600	600	600	600

In the genus *Heinzbutinia*, analyses of *TUB2* sequences data (Suppl. material 2: fig. S5) showed that taxon 1 belonged to *Heinzbutinia grandicarpa* (Kowalski & Butin) Z.W. de Beer & M. Procter. In *Leptographium* genus, taxon 2 was represented by nine isolates grouping in the *L. procerum* species complex (Suppl. material 2: fig. S3) and *TUB2* and *TEF1* sequence analyses confirmed this taxon was conspecific with *L. procerum* (W.B. Kendr.) M.J. Wingf. (Suppl. material 2: figs S6, S7). Taxon 3 was represented by four isolates that grouped in the *L. galeiforme* species complex (Suppl. material 2: fig. S3) and *TUB2* and *TEF1* sequence analyses confirmed that these isolates represented *L. radiaticola* (J.J. Kim, Seifert & G.H. Kim) M. Procter & Z.W. de Beer (Suppl. material 2: figs S8, S9).

In the genus *Ophiostoma* taxon 4 was represented by two isolates that did not group in any species complex (Suppl. material 2: fig. S4). Analyses of *TUB2* sequence data (sSuppl. material 2: fig. S5) showed that this taxon belongs to *O. piliferum* (Fr.) Syd. & P. Syd. Taxon 5 was represented by four isolates in the *O. ulmi* species complex (Suppl. material 2: fig. S4), while *TUB2* sequences grouped this taxon with *O. quercus* (Georgev.) Nannf. (Suppl. material 2: fig. S5).

In the genus *Sporothrix*, the four isolates of taxon 7 resided in the *S. inflata* species complex and grouped with the ex-type isolate of *S. dentifunda* (Aghayeva & M.J. Wingf.) Z.W. de Beer, T.A. Duong & M.J. Wingf. based on the ITS, *TUB2*, *CAL*, and *TEF1* phylogenies (Figs 1–4). Taxa 9 and 10 also belonged to the *S. inflata* species complex (Fig. 1) as defined by de Beer et al. (2022) and were represented by four and seven isolates, respectively. Based on the *TUB2* phylogeny, taxon 9 was close to *S. dimorphospora* and ‘*S. inflata* 2’ and formed a distinct and well-supported clade, while taxon 10 formed a distinct and well-supported clade which included isolates of ‘*S. inflata* 2’ (Fig. 2). Based on the *CAL* phylogeny, taxa 9 and 10 formed two distinct and well-supported clades which were close to, but distinct from *S. dimorphospora* (Fig. 3). Based on the *TEF1* sequence data (Fig. 4), both taxa formed distinct and well-supported clades, and thus represented novel species. This was supported by the combined analyses of the ITS, *TUB2* and *CAL* datasets (Fig. 5). Taxon 8 was represented

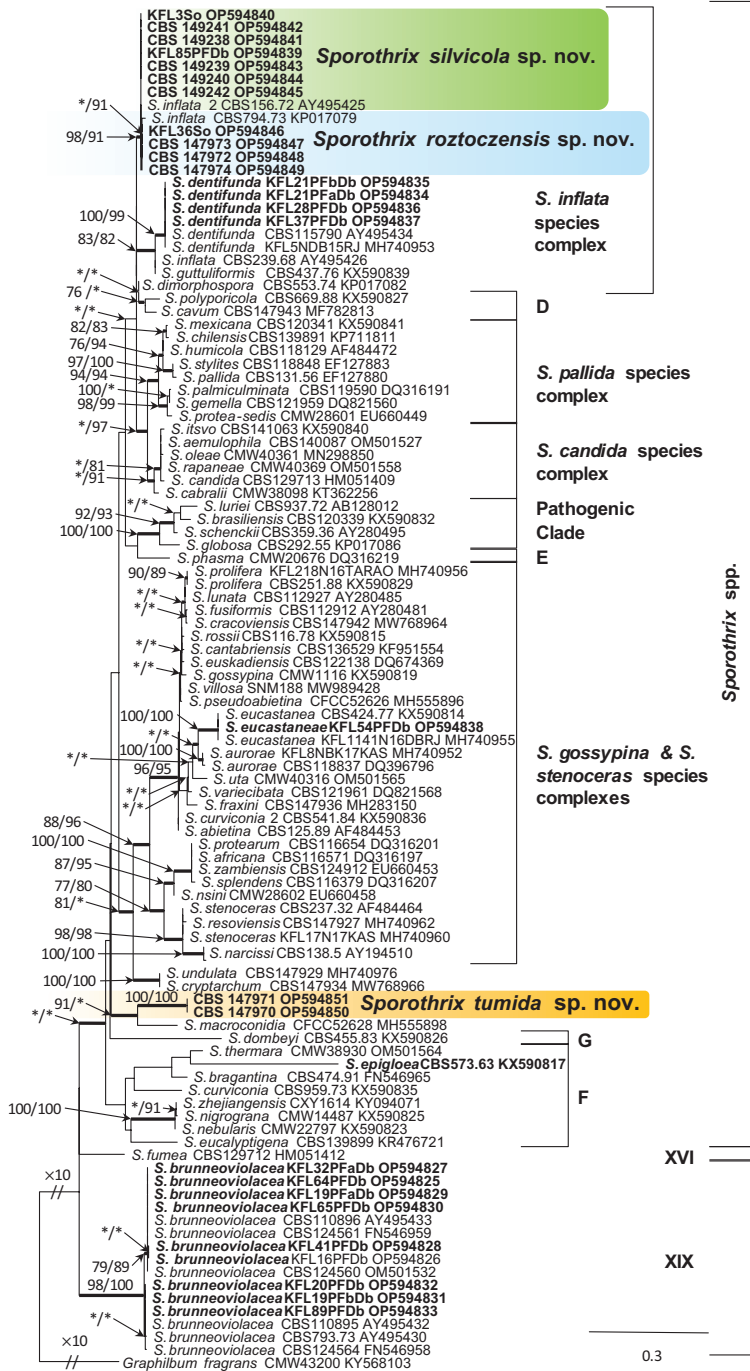


Figure 1. Phylogram from Maximum Likelihood (ML) analyses of ITS data for *Sporothrix* spp. Sequences obtained in this study are in bold. Bootstrap values ($\geq 75\%$) for ML and Maximum Parsimony (MP) analyses are presented at the nodes as follows: ML/MP. Bold branches indicate posterior probabilities values ≥ 0.95 obtained from Bayesian Inference (BI) analyses. * Bootstrap values $< 75\%$. The tree is drawn to scale (see bar) with branch lengths measured in the number of substitutions per site. *Graphilbum fragrans* represents the outgroup.

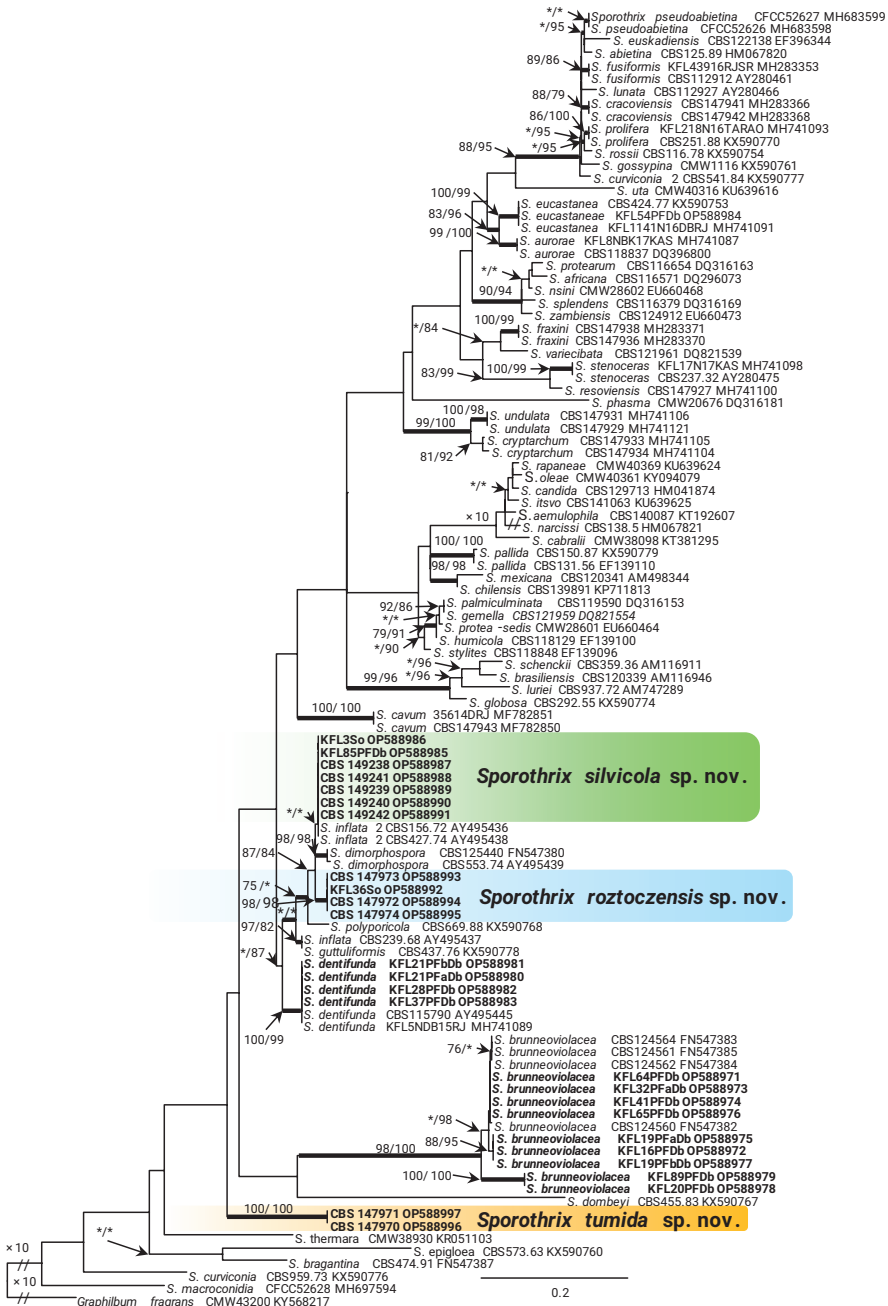


Figure 2. Phylogram from Maximum Likelihood (ML) analyses of *TUB2* data for *Sporothrix* spp. Sequences obtained in this study are in bold. Bootstrap values (if $\geq 75\%$) for ML and Maximum Parsimony (MP) analyses are presented at the nodes as follows: ML/MP. Bold branches indicate posterior probabilities values ≥ 0.95 obtained from Bayesian Inference (BI) analyses. * Bootstrap values $< 75\%$. The tree is drawn to scale (see bar) with branch lengths measured in the number of substitutions per site. *Graphilbum fragrans* represents the outgroup.

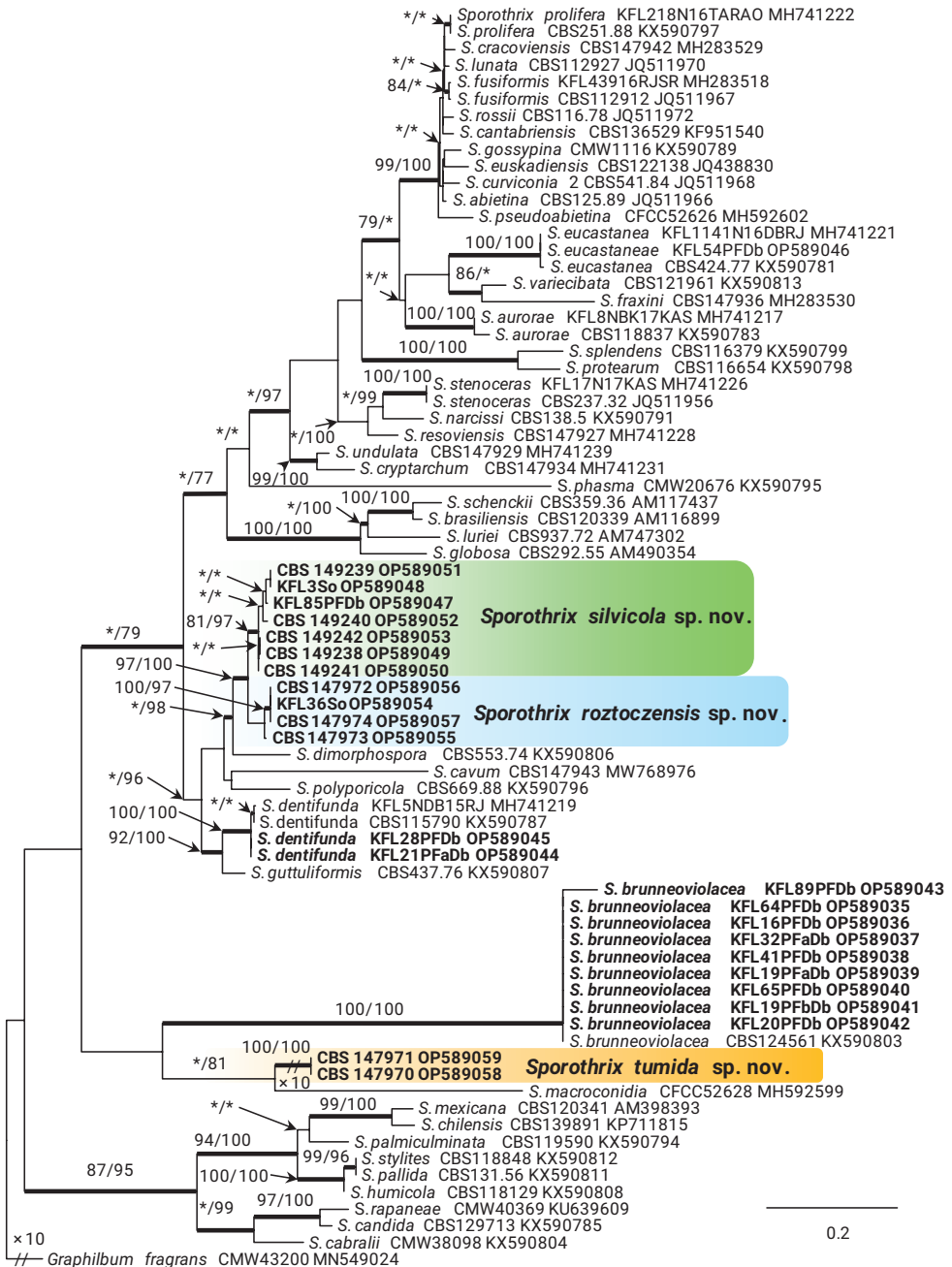


Figure 3. Phylogram from Maximum Likelihood (ML) analyses of *CAL* data for *Sporothrix* spp. Sequences obtained in this study are in bold. Bootstrap values (if $\geq 75\%$) for ML and Maximum Parsimony (MP) analyses are presented at the nodes as follows: ML/MP. Bold branches indicate posterior probabilities values ≥ 0.95 obtained from Bayesian Inference (BI) analyses. * Bootstrap values < 75%. The tree is drawn to scale (see bar) with branch lengths measured in the number of substitutions per site. *Graphilbum fragrans* represents the outgroup.

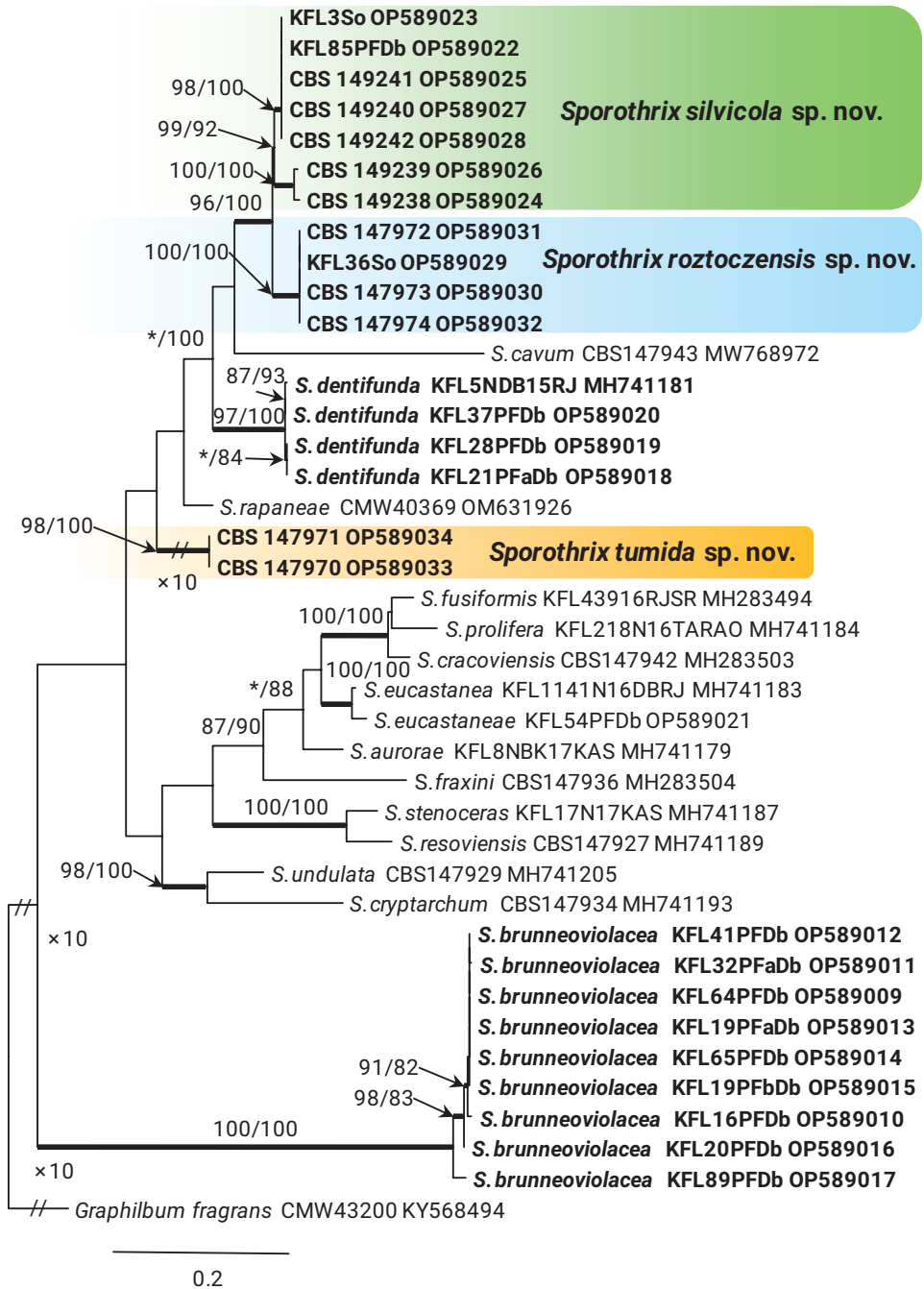


Figure 4. Phylogram from Maximum Likelihood (ML) analyses of *TEF1* data for the *Sporothrix* spp. Sequences obtained in this study are in bold. Bootstrap values (if $\geq 75\%$) for ML and Maximum Parsimony (MP) analyses are presented at the nodes as follows: ML/MP. Bold branches indicate posterior probabilities values ≥ 0.95 obtained from Bayesian Inference (BI) analyses. * Bootstrap values $< 75\%$. The tree is drawn to scale (see bar) with branch lengths measured in the number of substitutions per site. *Graphilbum fragrans* represents the outgroup.

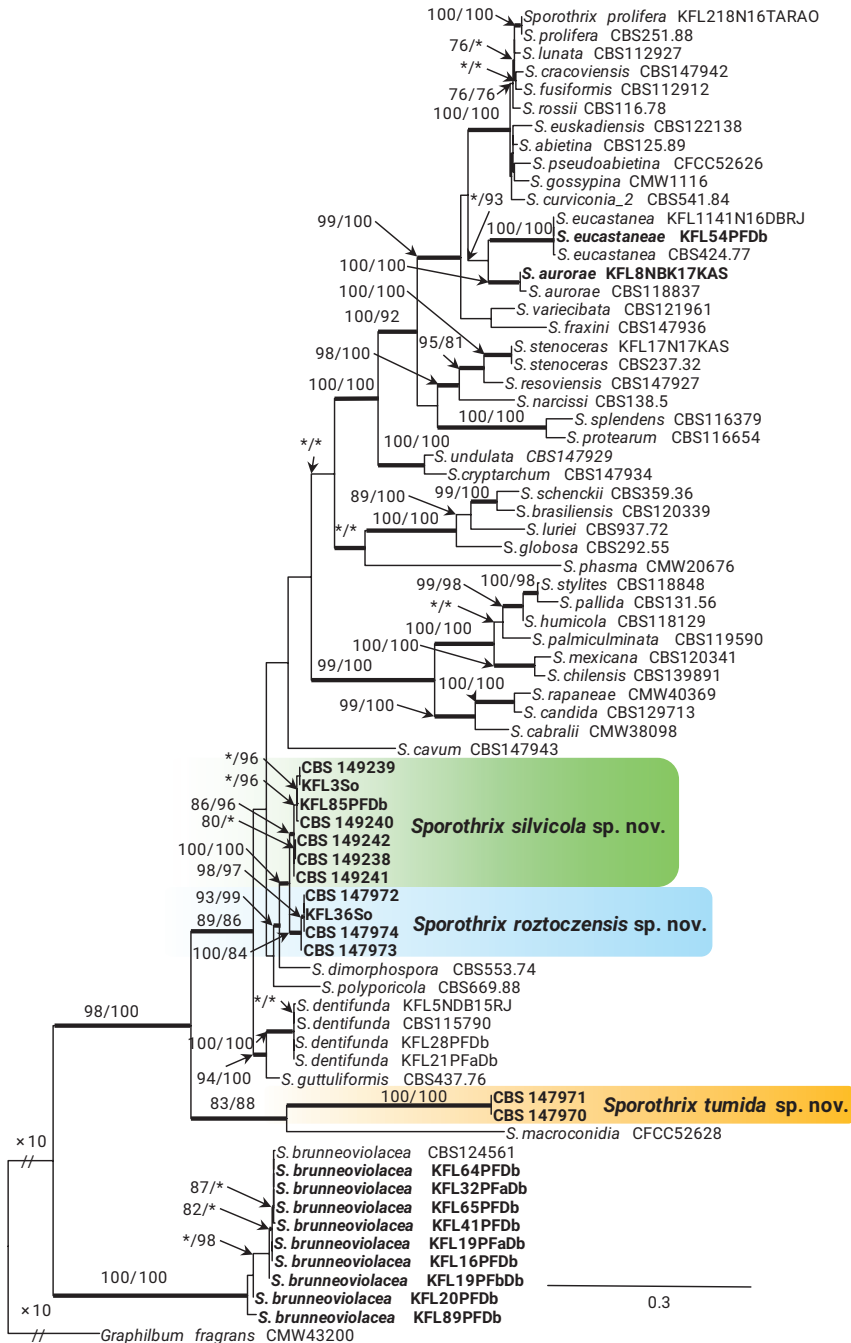


Figure 5. Phylogram from Maximum Likelihood (ML) analyses of the combined datasets of ITS+BT+CAL for *Sporothrix* spp. Sequences obtained in this study are in bold. Bootstrap values (if $\geq 75\%$) for ML and Maximum Parsimony (MP) analyses are presented at the nodes as follows: ML/MP. Bold branches indicate posterior probabilities values ≥ 0.95 obtained from Bayesian Inference (BI) analyses. * Bootstrap values $< 75\%$. The tree is drawn to scale (see bar) with branch lengths measured in the number of substitutions per site. *Graphilbum fragrans* represents the outgroup.

by one isolate and grouped in the *S. gossypina* & *S. stenoceras* species complexes (Fig. 1). *TUB2*, *CAL*, and *TEF1* phylogenies (Figs 2–4) showed that this taxon is *S. eucastaneae* (R.W. Davidson) Z.W. de Beer, T.A. Duong & M.J. Wingf. Taxon 11 was represented by two isolates collected from fallen pine shoots and did not group in any species complex (Fig. 1). The combined analyses of the ITS, *TUB2*, and *CAL* datasets (Fig. 5) showed that this taxon formed a distinct and well-supported clade which was closest to, but clearly distinct from *S. macroconidia* H.M. Wang, Q. Lu & Zhen Zhang, and thus represented a novel species.

Taxon 6 was represented by nine isolates grouped separately from *Sporothrix* and belonged to lineage XIX (Fig. 1) as defined by de Beer et al. (2022). Analyses of *TUB2* and *CAL* sequences data (Figs 2, 3) showed that this taxon is *Sporothrix brunneoviolacea*.

Taxonomy

Sporothrix roztoczensis R. Jankowiak & P. Bilański, sp. nov.

Mycobank No: 845660

Fig. 6

Etymology. Referring to the highland (from Polish: Roztocze) located in eastern Poland where this fungus was collected.

Diagnosis. *Sporothrix roztoczensis* differs from the phylogenetically closely related species *S. dimorphospora* and *S. silvicola* with respect to its conidia dimensions.

Type. POLAND, Lubelskie Province, Józefów, from wood buried in soil under 58-year-old managed *Pinus sylvestris* forest, July 2015, Ł. Chyrczyński (O-F-259436 *holotype*, culture ex-type CBS 147973).

Description. Sexual morph not observed. Asexual structures produced on sterilized Scots pine twigs placed on the surface of malt agar in Petri dishes. **Conidiophores** hyaline, one-celled, micronematous, simple or branched, either borne on vegetative hyphae or on upright hyphae. **Conidiogenous cells** blastic, cylindrical, terminal, lateral or intercalary, straight or curved, constricted at the base and tapering towards the apex, (2.3–)6.6–32.8(–50.5) μm long, (0.6–)1.1–1.6(–2) μm wide at the base, apical part forming conidia by sympodial proliferation on swollen a cluster of conidium-bearing denticles, (0.9–)1.6–3.3(–5) μm long and (1–)1.9–3.9(–6.2) μm wide, denticles very seldom arise below the swollen cluster. **Conidia** of two types: 1) abundant in cultures, hyaline, unicellular, smooth, ellipsoid, guttuliform, pointed at the base, sometimes curved (2.5–)3.2–5.1(–7) \times (1.4–)1.6–2.1(–2.5) μm , formed directly on denticles; 2) abundant in cultures, subhyaline to lightly pigmented, unicellular, globose to subglobose, sometimes pointed at the base, (2.5–)2.9–3.6(–4.1) μm in diameter, formed singly, on lateral or intercalary conidiogenous cells or denticles directly emerging from vegetative hyphae.

Culture characteristics. Colonies with optimal growth at 20 °C on 2% MEA reaching an average of 31.3 mm (\pm 3.98 mm) after 14 days, with a radial growth rate

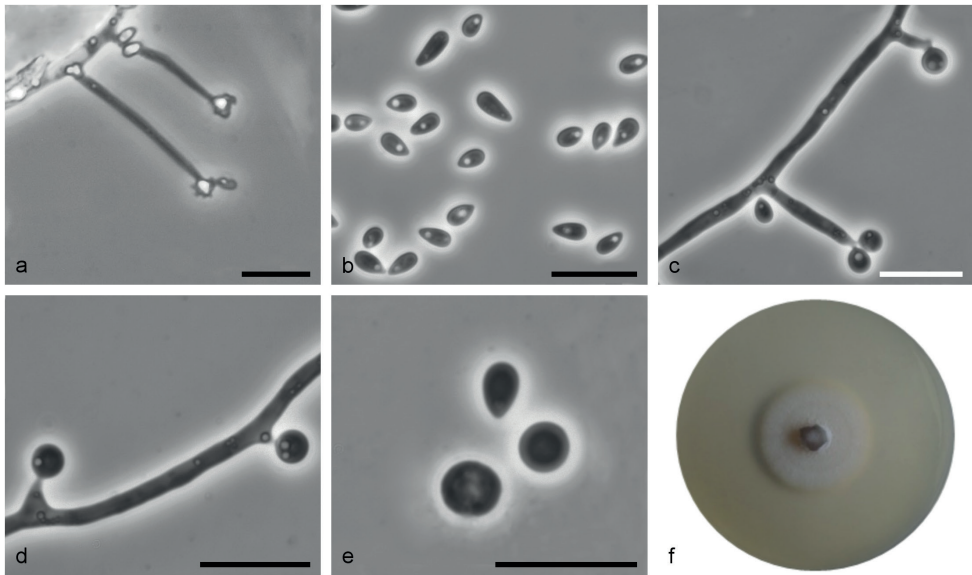


Figure 6. *Sporothrix roztozczensis* sp. nov. (CBS 147973) **a** conidiogenous cell with an inflated cluster of denticles at the apex **b** conidia **c** globose conidia arising on conidiophore **d** globose conidia arising on denticles formed directly from hyphae **e** globose conidia **f** fourteen-day-old culture on MEA. Scale bars: 10 μ m.

of 0.87 (\pm 0.14) mm/d, growth somewhat slower at 15 °C (26.3 mm diameter), no growth at 30 and 35 °C; white gray, floccose, flat, growing in a circular pattern with entire margins.

Distribution. Known only from the type location (Poland).

Additional specimen examined. POLAND, Lubelskie Province, Józefów, from wood buried in soil under 88-year-old managed *Pinus sylvestris* forest, July 2015, *Ł. Chyrzyński* (O-F-259435, culture CBS 147972).

Notes. This species is phylogenetically distinct from the other *Sporothrix* species based on the *TUB2*, *CAL*, and *TEF1* sequences. *Sporothrix roztozczensis* is closely related to *S. dimorphospora*, and *S. silvicola* sp. nov. *Sporothrix silvicola* has larger sympodial conidia (3.2–10.4 \times 1.4–3.6 μ m) compared with *S. dimorphospora* (3–8 \times 1.5–3 μ m, Madrid et al. 2010) and *S. roztozczensis* (2.5–7 \times 1.4–2.5 μ m). In addition, denticles in *S. silvicola* arise abundantly below the swollen cluster compared with other species, where denticles are limited to the apical cluster. Also the shape of pigmented conidia differed. In *S. roztozczensis* they are globose or subglobose while more obovoid in *S. dimorphospora* and *S. silvicola*. Conidia of *S. roztozczensis* are smaller (2.5–4.1 μ m in diam.) compared to *S. dimorphospora* (3–5 \times 3.5 μ m) and *S. silvicola* (2.6–4.8 \times 1.4–3.9 μ m). In addition, *S. roztozczensis* rarely produced intercalary conidiogenous cells, which are commonly found in culture of *S. silvicola*.

***Sporothrix silvicola* R. Jankowiak & P. Bilański, sp. nov.**

MycoBank No: 845658

Fig. 7

Etymology. Referring to the Latin *silva* (forest) and *-cola* (inhabiting), with reference to its woody habitat.

Diagnosis. *Sporothrix silvicola* differs from the phylogenetically closely related species *S. dimorphospora* and *S. roztoczensis* with respect to its conidia dimensions.

Type. POLAND, Lubelskie Province, Józefów, from wood buried in soil under 43-year-old managed *Pinus sylvestris* forest, July 2015, *L. Chyrzyński*, (O-F-259451 **holotype**, culture ex-type CBS 149241).

Description. Sexual morph not observed. Asexual structures produced on sterilized Scots pine twigs placed on the surface of malt agar in Petri dishes. **Conidiophores** hyaline, one-celled, micronematous, simple, either borne on vegetative hyphae or on upright hyphae. **Conidiogenous cells** blastic, cylindrical, terminal, lateral or intercalary, straight or curved, constricted at the base and tapering towards the apex, (2.2–)11.6–35.6(–60.5) μm long, (0.7–)1–1.5(–1.8) μm wide at the base, apical part forming conidia by sympodial proliferation on swollen cluster of conidium-bearing denticles, (1.4–)2.6–4.4(–5.5) μm long and (1.5–)2.1–3.4(–4.1) μm wide, denticles often arise below the swollen cluster. **Conidia** of two types: 1) abundant in cultures hyaline, unicellular, smooth, guttuliform, ellipsoid, pointed at the base, sometimes curved (3.2–)3.6–6.4(–10.4) \times (1.4–)1.6–2.5(–3.6) μm , formed directly on denticles; 2) abundant in cultures, subhyaline to lightly pigmented, unicellular, smooth, subglobose to broadly ellipsoidal, sometimes pointed at the base, (2.6–)3.1–4.1(–4.8) μm \times (1.4–)2.1–3.4(–3.9) μm diam., formed singly, on lateral or intercalary conidiogenous cells or denticles directly emerging from vegetative hyphae.

Culture characteristics. Colonies with optimal growth at 20 °C on 2% MEA reaching an average of 32 mm (\pm 1.86 mm) after 14 days, with radial growth rate 0.89 (\pm 0.07) mm/d, growth somewhat slower at 15 °C (26.6 mm diameter), no growth at 30 and 35 °C; dark grey to olivaceous with white margins, floccose, lanose with abundant white aerial hyphae, flat, growing in a circular pattern with entire margins.

Distribution. Known only from the type location (Poland).

Additional specimen examined. POLAND, Lubelskie Province, Józefów, from wood buried in soil under 93-year-old managed *Pinus sylvestris* forest, July 2015, *L. Chyrzyński* (O-F-259450, culture CBS 149240).

Notes. This species is phylogenetically distinct from the other *Sporothrix* species based on the *TUB2*, *TEF1*, and *CAL* sequences. The morphological differences between *S. dimorphospora* and *S. roztoczensis* are described in the section treating *S. roztoczensis*. *Sporothrix silvicola* had identical ITS and *TUB2* sequences as two isolates of '*S. inflata* 2' (CBS 156.72, CBS 427.74) obtained from greenhouse soil and isolated from *Lilium* sp. in the Netherlands (Aghayeva et al. 2005; de Beer et al. 2016).

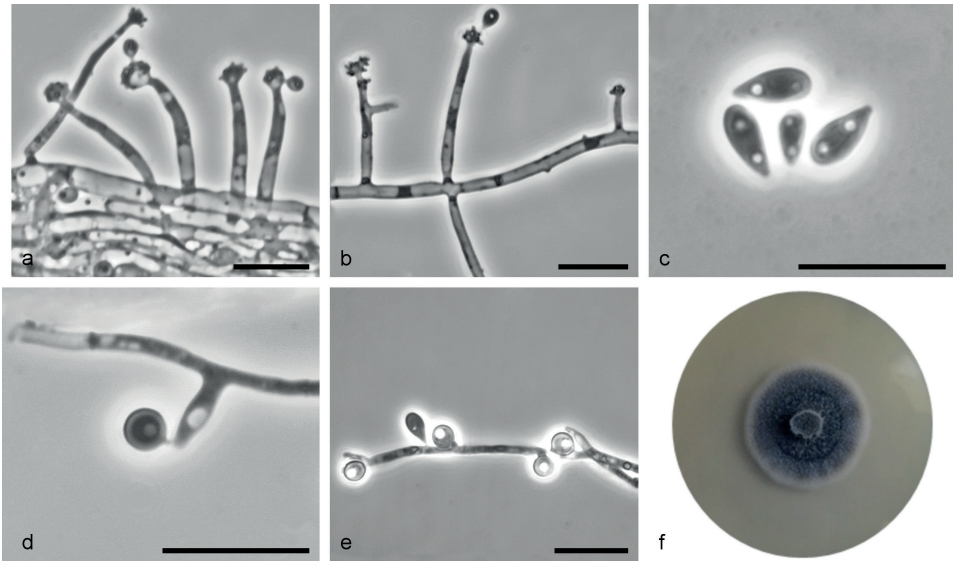


Figure 7. *Sporothrix silvicola* sp. nov. (CBS 149241) **a, b** conidiogenous cell with an inflated cluster of denticles at the apex **c** conidia **d** globose conidia arising on conidiophore **e** globose conidia arising on denticles formed directly from hyphae **f** fourteen-day-old culture on MEA. Scale bars: 10 μ m.

***Sporothrix tumida* R. Jankowiak & P. Bilański, sp. nov.**

Mycobank No: 845661

Fig. 8

Etymology. Referring to the Latin *tumeo* (swollen) to reflect the characteristically inflated hyphae and conidiogenous cells.

Diagnosis. *Sporothrix tumida* differs from the phylogenetically closely related *S. macroconidia* in respect of dimensions of its conidia.

Type. POLAND, Podkarpackie Province, Mielec, from fallen shoots of *Pinus sylvestris* pruned by *Tomicus* sp., October 2007, P. Bilański, (O-F-259433 **holotype**, culture ex-type CBS 147970).

Description. Sexual morph not observed. Asexual structures produced on sterilized Scots pine twigs placed on the surface of malt agar in Petri dishes. **Conidiophores** hyaline, one- or two-celled, micronematous, simple or slightly branched, either borne on vegetative hyphae or on upright hyphae, often inflated. **Conidiogenous cells** blastic, cylindrical, terminal, straight, constricted at the base and strong tapering towards the apex, (7.8–)12–25.4(–34.7) μ m long, (1.3–)1.6–2.6(–3.5) μ m wide at the base, apical part forming conidia by sympodial proliferation on swollen a cluster of conidium-bearing faintly developed denticles, (1–)1.2–2.5(–3.3) μ m long and (1.1–)1.4–2.9(–4.7) μ m wide, denticles sometimes arise directly from hypha. **Conidia** abundant in cultures hyaline, unicellular, smooth, guttuliform, ellipsoid, sometimes curved, slightly pointed at the base (3.4–)4.2–6.6(–8.7) \times (1.3–)1.9–3.1(–3.9) μ m.

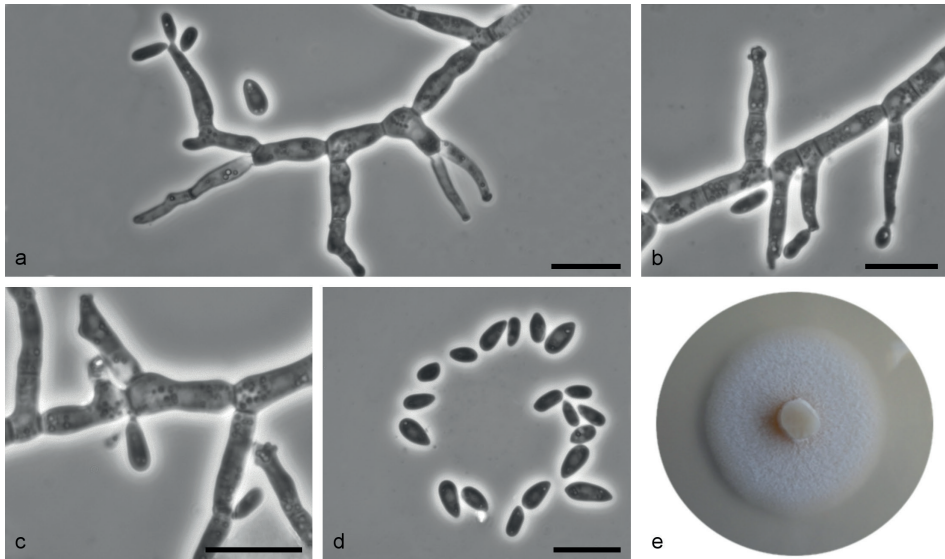


Figure 8. *Sporothrix tumida* sp. nov. (CBS 147970) **a, b** conidiogenous cell with an inflated cluster of denticles at the apex **c** denticles arising directly from hyphae **d** conidia **e** fourteen-day-old culture on MEA. Scale bars: 10 μ m.

Culture characteristics. Colonies with optimal growth at 25 °C on 2% MEA reaching an average of 36.3 mm (\pm 0.62 mm) after 14 days, with radial growth rate 1.05 (\pm 0.02) mm/d, growth somewhat slower at 30 °C (29.6 mm diameter); white, flat, floccose, growing in a circular pattern with entire margins.

Host tree. *Pinus sylvestris*.

Insect vector. *Tomicus* spp.

Distribution. Known only from the type location (Poland).

Additional specimen examined. POLAND, Podkarpackie Province, Mielec, from fallen shoots of Scots pine pruned by *Tomicus* sp., October 2007, *R. Jankowiak*, (O-F-259434, culture CBS 147971).

Notes. This species is phylogenetically distinct from the other *Sporothrix* species based on the ITS, *TUB2*, and *CAL* sequences. *Sporothrix tumida* grouped most closely with *S. macroconidia* (ITS, *CAL*) from which it can also be distinguished by dimensions of conidia (3.4–8.7 \times 1.3–3.9 μ m vs. 3.6–9.9 \times 2.5–9.9 μ m, Wang et al. 2019).

Discussion

This study reported 10 members of the Ophiostomatales associated with soil under European beech, pedunculate oak, Scots pine, and Norway spruce stands in Poland. Two of these species are newly described here (*Sporothrix roztoczensis* and *S. silvicola*) and were the most abundant species in the forest soil. This demonstrates that there is

a rich and poorly studied diversity of species of the Ophiostomatales associated with soil in European forests.

Our results revealed a greater than expected diversity of Ophiostomatales fungi in soil, while confirming that the methods used here (autoclaved branches buried in the soil) are useful for the detection of soil-borne fungi from this order. To date, *Sporothrix* is the main Ophiostomatales genus to be found in soil samples (e.g., de Hoog 1974; de Meyer et al. 2008; Madrid et al. 2010; de Beer et al. 2016; Rodrigues et al. 2017; Ramírez-Soto et al. 2018). *Leptographium* species have also been isolated from soil, although these are found primarily in tree roots (Eckhardt 2003). For example, *Leptographium wagneri* (W.B. Kendr.) M.J. Wingf., a causative agent of black stain root disease of conifers in the western United States and Canada, can be transmitted between diseased and healthy roots through continuous xylem in root grafts (Landis and Helburg 1976), by short-distance growth through soil (Goheen and Cobb 1978) and by insect vectors (Harrington and Cobb 1988).

The dominant tree species in the stands strongly affected fungal species richness and taxonomic diversity. Most of the fungi were isolated from the pine and oak stands, while only three isolates were obtained from the spruce stands, and no fungi were isolated from the beech stands. *Sporothrix silvicola* was the only fungal species found in pine-, oak- and spruce-dominated stands, although it was highly abundant only in pine stands. *Leptographium procerum* and, to a lesser extent, *L. radiaticola* and *S. roztoczensis*, were also abundant in pine stands. In contrast, wood buried in oak stands was mostly colonized by *S. brunneoviolacea* and less frequently by *S. dentifunda* and *O. quercus*.

This research demonstrated that *Sporothrix* species can be soil-borne, validating previous studies in South Africa (de Meyer et al. 2008), Spain and USA (Madrid et al. 2010). Five of the species collected in this study belong to *Sporothrix*, including the two newly described species. *Sporothrix brunneoviolacea* (Madrid et al. 2010) and '*S. inflata* 2' (de Hoog 1974; de Beer et al. 2016) were previously reported in soil from Europe, and this study shows that *S. dentifunda* and *S. eucastaneae* also occur in forest soil. The identified *Sporothrix* species showed different affinities to tree hosts, as *S. brunneoviolacea*, *S. dentifunda*, and *S. eucastaneae* were found in oak stands while *S. silvicola* and *S. roztoczensis* were reported in pine stands. This is in congruence with previous reports: *Sporothrix brunneoviolacea* was already isolated from meadow soil in Germany, from soil under mixed stands in Spain, and from the roots of *Quercus* spp. in Austria (Halmschlager and Kowalski 2003; Madrid et al. 2010). Similarly, *S. dentifunda* has been isolated from the wood of *Quercus* sp. in Poland and Hungary (Aghayeva et al. 2005), as well as from wounds on *Q. robur* in Poland (Jankowiak et al. 2019b). *Sporothrix eucastaneae* has also been previously isolated from oak stands in Poland, where this fungus was associated with oak-infesting bark beetles (Jankowiak et al. 2019a) and wounded oaks (Jankowiak et al. 2019b).

The *Sporothrix* species from pine stands, *S. silvicola* and *S. roztoczensis*, are newly described sister species that reside in the *S. inflata* species complex (de Beer et al. 2022). Although both species inhabited the same environment, they can be distinguished based on phylogenetic analyses and morphological characteristics, such as

differences in conidia dimensions and shapes. Both species produced two different conidial types, which is a characteristic that has been found in other *Sporothrix* species, including *Sporothrix dimorphospora* and *S. brunneoviolacea* (Madrid et al. 2010), *S. brasiliensis*, *S. globosa*, and *S. mexicana* (Marimon et al. 2007), as well as *S. cryptarchum* R. Jankowiak & A. Ostafińska and *S. undulata* R. Jankowiak & A. Ostafińska (Ostafińska et al. 2021). In Poland, *S. silvicola* named as '*S. inflata* 2' was also sporadically found in association with *Scolytus intricatus* (Ratzeburg) on *Q. robur* (Jankowiak et al. 2019a) and wounded *Tilia cordata* Mill. (Jankowiak et al. 2019b), suggesting that the fungus may not be limited to conifer-dominated habitats. More surveys should be conducted to determine the range of the fungus, and to test their affinities to pine forests.

Our results also demonstrated that some *Leptographium* species are soil-borne, supporting the findings of Eckhardt (2003) that *L. procerum* is a soil-borne fungus. This species was previously isolated from roots of dying and dead young Scots pines (Jankowiak et al. 2012) and was often found to be carried by root-feeding bark beetles and weevils in Poland (Jankowiak and Bilański 2013a, b, c). A high abundance of this species in soil and pine roots suggests that *L. procerum* may be capable of infecting roots via soil. According to previous studies, *L. procerum* can spread over short distances via root-to-root contact between infected and uninfected host trees, as well as through soil as short term survival in the soil around infected trees has been observed (Lackner and Alexander 1984; Alexander et al. 1988; Jacobs and Wingfield 2001; Eckhardt et al. 2004). In our opinion, the presence of *L. radiaticola* in the soil of pine stands suggests that other *Leptographium* species may be similarly transmitted. Possible transmission through soil has been also observed for *L. wagneri* (Goheen and Cobb 1978). In addition, *L. costaricense* G. Weber, Spaaij & M.J. Wingf. (Weber et al. 1996) and *L. reconditum* Jooste (Jooste 1978) were found in the rhizospheres of *Talauma sambuensis* Pittier and *Triticum*, respectively.

Although *O. piliferum* was rarely isolated in this study, we confirmed that it is soil-borne. Its presence was unsurprising because this species is commonly found staining pine wood in Poland (Jankowiak et al. 2018b, 2021). In addition, *O. piliferum* was also found in soil from sites exposed to different wood preservative types (Kirker et al. 2017). Finally, *O. quercus* was also reported in soil in this study. This globally widespread species (Taerum et al. 2018) is a common wood-infecting fungus associated with many species of bark and wood boring beetles in Poland (Jankowiak et al. 2019a, b), and may be more commonly found in soil with additional surveys.

Sporothrix tumida was collected from fallen shoots of Scots pine that were pruned by *Tomiscus* species in Poland (Jankowiak and Kolařík 2011). The species is the most closely related to *S. macroconidia*, which was recently described from *Tomiscus yunnanensis* Kirkendall & Faccoli and *T. brevipilosus* Eggers on *Pinus yunnanensis* Franch. and *P. kesiya* Royle ex Gordon in south-western China (Wang et al. 2019). The new species identified in this study can be easily distinguished from *S. macroconidia* by phylogenetic analysis and morphological characteristics.

Our work has led to the discovery of three novel *Sporothrix* species, bringing the total number of *Sporothrix* species in Poland to 20. The present study has shown that forest soil under pine and oak stands in Poland is remarkably rich in Ophiostomatales species. Our

surveys were conducted in 35–135 year old managed stands, showing that even recently managed forests can house undescribed fungal species. Additional species of these fungi will most likely emerge when more extensive surveys are conducted in other parts of Europe as forest soil fungi are influenced by a variety of biotic and abiotic factors, including climate, soil physicochemical properties, forest age, tree compositions and management type (e.g. Baldrian et al. 2012; Tedersoo et al. 2014; Goldmann et al. 2015; Urbanová et al. 2015). Therefore, future research should focus on identifying soil-borne Ophiostomatales species in forests with different tree compositions and soil characteristics.

Acknowledgements

We wish to thank Professor Ewa Błońska (University of Agriculture in Krakow, Poland) for performing the soil analyses. We thank two anonymous reviewers for their constructive comments and suggestions. We kindly thank Beata Strzałka for her help in fieldwork and fungal isolations.

This work was supported by the Ministry of Science and Higher Education of the Republic of Poland (SUB/040013–D019).

References

- Aas T, Solheim H, Jankowiak R, Bilański P, Hausner G (2018) Four new *Ophiostoma* species associated with hardwood-infesting bark beetles in Norway and Poland. *Fungal Biology* 122(12): 1142–1158. <https://doi.org/10.1016/j.funbio.2018.08.001>
- Aghayeva DN, Wingfield MJ, Kirisits T, Wingfield BD (2005) *Ophiostoma dentifundum* sp. nov. from oak in Europe, characterized using molecular phylogenetic data and morphology. *Mycological Research* 109(10): 1127–1136. <https://doi.org/10.1017/S0953756205003710>
- Alexander SA, Horner WE, Lewis KJ (1988) *Leptographium procerum* as a pathogen of pines. In: Harrington TC, Cobb Jr FW (Eds) *Leptographium* Root Diseases on Conifers. American Phytopathological Society Press, St Paul, Minnesota, 97–112.
- Baldrian P, Kolařík M, Štursová M, Kopecký J, Valášková V, Větrovský T, Žifčáková L, Šnajdr J, Rídl J, Vlček Č, Voříšková J (2012) Active and total microbial communities in forest soil are largely different and highly stratified during decomposition. *The ISME Journal* 6(2): 248–258. <https://doi.org/10.1038/ismej.2011.95>
- Carbone I, Kohn LM (1999) A method for designing primer sets for speciation studies in filamentous ascomycetes. *Mycologia* 91(3): 553–556. <https://doi.org/10.1080/00275514.1999.12061051>
- Darriba D, Taboada GL, Doallo R, Posada D (2012) jModelTest 2: More models, new heuristics and parallel computing. *Nature Methods* 9(8): 772. <https://doi.org/10.1038/nmeth.2109>
- de Beer ZW, Wingfield MJ (2013) Emerging lineages in the Ophiostomatales. In: Seifert KA, De Beer ZW, Wingfield MJ (Eds) *The Ophiostomatoid Fungi: Expanding Frontiers*. Centraalbureau voor Schimmelcultures (CBS), Utrecht, The Netherlands, CBS Biodiversity Series 12: 21–46.

- de Beer ZW, Harrington TC, Vismer HF, Vingfield BD, Wingfield MJ (2003) Phylogeny of the *Ophiostoma stenoceras*–*Sporothrix schenckii* complex. *Mycologia* 95(3): 434–441. <https://doi.org/10.1080/15572536.2004.11833088>
- de Beer ZW, Seifert KA, Wingfield MJ (2013a) The ophiostomatoid fungi: their dual position in the Sordariomycetes. In: Seifert KA, De Beer ZW, Wingfield MJ (Eds) *The Ophiostomatoid Fungi: Expanding Frontiers*. Centraalbureau voor Schimmelcultures (CBS), Utrecht, The Netherlands, CBS Biodiversity Series 12: 1–19.
- de Beer ZW, Seifert KA, Wingfield MJ (2013b) A nomenclator for ophiostomatoid genera and species in the Ophiostomatales and Microascales. In: Seifert KA, De Beer ZW, Wingfield MJ (Eds) *The Ophiostomatoid Fungi: Expanding Frontiers*. Centraalbureau voor Schimmelcultures (CBS), Utrecht, The Netherlands, CBS Biodiversity Series 12: 245–322.
- de Beer ZW, Duong TA, Wingfield MJ (2016) The divorce of *Sporothrix* and *Ophiostoma*: Solution to a problematic relationship. *Studies in Mycology* 83(1): 165–191. <https://doi.org/10.1016/j.simyco.2016.07.001>
- de Beer W, Procter M, Wingfield MJ, Marincowitz S, Duong TA (2022) Generic boundaries in the Ophiostomatales reconsidered and revised. *Studies in Mycology* 101(1): 57–120. <https://doi.org/10.3114/sim.2022.101.02>
- de Hoog GS (1974) The genera *Blastobotrys*, *Sporothrix*, *Calcarisporium* and *Calcarisporiella* gen. nov. *Studies in Mycology* 7: 1–84.
- de Meyer EM, de Beer ZW, Summerbell RC, Moharram AM, de Hoog GS, Vismer HF, Wingfield MJ (2008) Taxonomy and phylogeny of new wood- and soil-inhabiting *Sporothrix* species in the *Ophiostoma stenoceras*–*Sporothrix schenckii* complex. *Mycologia* 100(4): 647–661. <https://doi.org/10.3852/07-157R>
- Eckhardt LG (2003) *Biology and Ecology of Leptographium species and their vectors as components of loblolly Pine Decline*. PhD Thesis, Louisiana State University, Baton-Rouge, USA.
- Eckhardt LG, Jones JP, Klepzig KD (2004) Pathogenicity of *Leptographium* species associated with loblolly pine decline. *Plant Disease* 55(11): 1174–1178. <https://doi.org/10.1094/PDIS.2004.88.11.1174>
- Ekici A, Chadburn S, Chaudhary N, Hajdu LH, Marmy A, Peng S, Boike J, Burke E, Friend AD, Hauck C, Krinner G, Lange M, Miller PA, Beer C (2014) Site-level model inter-comparison of high latitude and high altitude soil thermal dynamics in tundra and barren landscapes. *The Cryosphere Discussion* 8: 4959–5013. <https://doi.org/10.5194/tcd-8-4959-2014>
- Gardes M, Bruns TD (1993) ITS primers with enhanced specificity for basidiomycetes: Application to the identification of mycorrhizae and rusts. *Molecular Ecology* 2(2): 113–118. <https://doi.org/10.1111/j.1365-294X.1993.tb00005.x>
- Glass NL, Donaldson GC (1995) Development of primer sets designed for use with the PCR to amplify conserved genes from filamentous ascomycetes. *Applied and Environmental Microbiology* 61(4): 1323–1330. <https://doi.org/10.1128/aem.61.4.1323-1330.1995>
- Goheen DJ, Cobb FW (1978) Occurrence of *Verticicladiella wageneri* and its perfect state, *Ceratocystis wageneri* sp. nov., in insect galleries. *Phytopathology* 68(8): 1192–1195. <https://doi.org/10.1094/Phyto-68-1192>

- Goldmann K, Schöning I, Buscot F, Wubet T (2015) Forest management type influences diversity and community composition of soil fungi across temperate forest ecosystems. *Frontiers in Microbiology* 6: e1300. <https://doi.org/10.3389/fmicb.2015.01300>
- Grobbelaar JW, Aghayeva DN, De Beer ZW, Bloomer P, Wingfield MJ, Wingfield BD (2009) Delimitation of *Ophiostoma quercus* and its synonyms using multiple gene phylogenies. *Mycological Progress* 8(3): 221–236. <https://doi.org/10.1007/s11557-009-0594-4>
- Guindon S, Gascuel O (2003) A simple, fast and accurate method to estimate large phylogenies by maximum-likelihood. *Systematic Biology* 52(5): 696–704. <https://doi.org/10.1080/10635150390235520>
- Guindon S, Dufayard JF, Lefort V, Anisimova M, Hordijk W, Gascuel O (2010) New algorithms and methods to estimate maximum-likelihood phylogenies: Assessing the performance of PhyML 3.0. *Systematic Biology* 59(3): 307–321. <https://doi.org/10.1093/sysbio/syq010>
- Hall TA (1999) BioEdit: a user-friendly biological sequence alignment editor and analysis program for Windows 95/98/NT. *Nucleic Acids Symposium* 41: 95–98.
- Halmeschlager E, Kowalski T (2003) *Sporothrix inflata*, a root-inhabiting fungus of *Quercus robur* and *Q. petraea*. *Mycological Progress* 2(4): 259–266. <https://doi.org/10.1007/s11557-006-0063-2>
- Harrington TC, Cobb FW (1988) *Leptographium* Root Diseases on Conifers. APS Press, St. Paul, 147 pp.
- Jacobs K, Wingfield MJ (2001) *Leptographium* Species: Tree Pathogens, Insect Associates, and Agents of Blue-Stain. APS Press, St. Paul, 207 pp.
- Jacobs K, Bergdahl DR, Wingfield MJ, Halik S, Seifert KA, Bright DE, Wingfield BD (2004) *Leptographium wingfieldii* introduced into North America and found associated with exotic *Tomicus piniperda* and native bark beetles. *Mycological Research* 108(4): 411–418. <https://doi.org/10.1017/S0953756204009748>
- Jankowiak R, Bilański P (2013a) Ophiostomatoid fungi associated with root-feeding bark beetles in Poland. *Forest Pathology* 43(5): 422–428. <https://doi.org/10.1111/efp.12049>
- Jankowiak R, Bilański P (2013b) Association of the pine-infesting *Pissodes* species with ophiostomatoid fungi in Poland. *European Journal of Forest Research* 132(3): 523–534. <https://doi.org/10.1007/s10342-013-0693-2>
- Jankowiak R, Bilański P (2013c) Diversity of ophiostomatoid fungi associated with the large pine weevil, *Hyllobius abietis*, and infested Scots pine seedlings in Poland. *Annals of Forest Science* 70(4): 391–402. <https://doi.org/10.1007/s13595-013-0266-z>
- Jankowiak R, Kolařík M (2010) Diversity and pathogenicity of ophiostomatoid fungi associated with *Tetropium* species colonizing *Picea abies* in Poland. *Folia Microbiologica* 55(2): 145–154. <https://doi.org/10.1007/s12223-010-0022-9>
- Jankowiak R, Kolařík M (2011) Ophiostomatoid fungi isolated from fallen shoots of Scots pine pruned by *Tomicus* species in Poland. *Acta Mycologica* 46(2): 201–210. <https://doi.org/10.5586/am.2011.013>
- Jankowiak R, Bilański P, Kolařík M, Wasiuta D (2012) Root-colonizing ophiostomatoid fungi associated with dying and dead young Scots pine in Poland. *Forest Pathology* 42(6): 492–500. <https://doi.org/10.1111/j.1439-0329.2012.00783.x>

- Jankowiak R, Strzałka B, Bilański P, Kacprzyk M, Lukášová K, Linnakoski R, Matwiejczuk S, Misztela M, Rossa R (2017) Diversity of Ophiostomatales species associated with conifer-infesting beetles in the Western Carpathians. *European Journal of Forest Research* 136(5–6): 939–956. <https://doi.org/10.1007/s10342-017-1081-0>
- Jankowiak R, Ostafińska A, Aas T, Solheim H, Bilański P, Linnakoski R, Hausner G (2018a) Three new *Leptographium* spp. (Ophiostomatales) infecting hardwood trees in Norway and Poland. *Antonie van Leeuwenhoek* 111(12): 2323–2347. <https://doi.org/10.1007/s10482-018-1123-8>
- Jankowiak R, Bilański P, Chyrzyński P, Strzałka B (2018b) Identification of sapstain fungi from Scots pine pallets and assessment of their staining ability. *European Journal of Plant Pathology* 150(2): 307–322. <https://doi.org/10.1007/s10658-017-1279-5>
- Jankowiak R, Strzałka B, Bilański P, Kacprzyk M, Wieczorek P, Linnakoski R (2019a) Ophiostomatoid fungi associated with hardwood-infesting bark and ambrosia beetles in Poland: Taxonomic diversity and vector specificity. *Fungal Ecology* 39: 152–167. <https://doi.org/10.1016/j.funeco.2019.02.001>
- Jankowiak R, Bilański P, Ostafińska A, Linnakoski R (2019b) Ophiostomatales associated with wounds on hardwood trees in Poland. *Plant Pathology* 68(7): 1407–1424. <https://doi.org/10.1111/ppa.13061>
- Jankowiak R, Bilański P, Strzałka B, Linnakoski R, Bosak A, Hausner G (2019c) Four new *Ophiostoma* species associated with conifer- and hardwood-infesting bark and ambrosia beetles from Czech Republic and Poland. *Antonie van Leeuwenhoek* 112(10): 1501–15021. <https://doi.org/10.1007/s10482-019-01277-5>
- Jankowiak R, Solheim H, Bilański P, Marincowitz S, Wingfield MJ (2020) Seven new species of *Graphilbum* from conifers in Norway, Poland, and Russia. *Mycologia* 112(6): 1240–1262. <https://doi.org/10.1080/00275514.2020.1778375>
- Jankowiak R, Szewczyk G, Bilański P, Jazłowiecka D, Harabin B, Linnakoski R (2021) Blue-stain fungi isolated from freshly felled Scots pine logs in Poland, including *Leptographium sosnaicola* sp. nov. *Forest Pathology* 51(2): e12672. <https://doi.org/10.1111/efp.12672>
- Jooste WJ (1978) *Leptographium reconditum* sp. nov. and observations on conidiogenesis in *Verticicladiella*. *Transactions of the British Mycological Society* 70(1): 152–155. [https://doi.org/10.1016/S0007-1536\(78\)80189-2](https://doi.org/10.1016/S0007-1536(78)80189-2)
- Katoh K, Standley DM (2013) MAFFT multiple sequence alignment software version 7, improvements in performance and usability. *Molecular Biology and Evolution* 30(4): 772–780. <https://doi.org/10.1093/molbev/mst010>
- Kirker GT, Bishell AB, Jusino MA, Palmer JM, Hickey WJ, Lindner DL (2017) Amplicon-Based Sequencing of Soil Fungi from Wood Preservative Test Sites. *Frontiers in Microbiology* 8: e1997. <https://doi.org/10.3389/fmicb.2017.01997>
- Kornerup A, Wanscher JH (1978) *Methuen Handbook of Colour* (3rd edn). Eyre Methuen, London, 252 pp.
- Lackner AL, Alexander SA (1984) Incidence and development of *Verticicladiella procera* in Virginia Christmas tree plantations. *Plant Disease* 68(3): 210–212. <https://doi.org/10.1094/PD-69-210>
- Landis TD, Helburg LB (1976) Black stain root disease of pinyon pine in Colorado. *The Plant Disease Reporter* 60: 713–717.

- Linnakoski R, Jankowiak R, Villari C, Kirisits T, Solheim H, de Beer ZW, Wingfield MJ (2016) The *Ophiostoma clavatum* species complex: A newly defined group in the Ophiostomatales including three novel taxa. *Antonie van Leeuwenhoek* 109(7): 987–1018. <https://doi.org/10.1007/s10482-016-0700-y>
- López-Romero E, Reyes-Montes MdR, Pérez-Torres A, Ruiz-Baca E, Villagómez-Castro JC, Mora-Montes HM, Flores-Carreón A, Toriello C (2011) *Sporothrix schenckii* complex and sporotrichosis, an emerging health problem. *Future Microbiology* 6(1): 85–102. <https://doi.org/10.2217/fmb.10.157>
- Madrid H, Gene J, Cano J, Silvera C, Guarro J (2010) *Sporothrix brunneoviolacea* and *Sporothrix dimorphospora*, two new members of the *Ophiostoma stenoceras*–*Sporothrix schenckii* complex. *Mycologia* 102(5): 1193–1203. <https://doi.org/10.3852/09-320>
- Marimon R, Cano J, Gene J, Sutton DA, Kawasaki M, Guarro J (2007) *Sporothrix brasiliensis*, *S. globosa*, and *S. mexicana*, three new *Sporothrix* species of clinical interest. *Journal of Clinical Microbiology* 45(10): 3198–3206. <https://doi.org/10.1128/JCM.00808-07>
- Marincowitz S, Duong TA, de Beer ZW, Wingfield MJ (2015) *Cornuvesica*: A little known mycophilic genus with a unique biology and unexpected new species. *Fungal Biology* 119(7): 615–630. <https://doi.org/10.1016/j.funbio.2015.03.007>
- Musvuugwa T, de Beer ZW, Duong TA, Dreyer LL, Oberlander K, Roets F (2016) Wounds on *Rapanea melanophloeos* provide habitat for a large diversity of Ophiostomatales including four new species. *Antonie van Leeuwenhoek* 109(6): 877–894. <https://doi.org/10.1007/s10482-016-0687-4>
- Neto JOM, Mello CR, da Silva AM, de Mello JM, Viola MR, Yanagi SNM (2017) Temporal stability of soil moisture under effect of three spacings in a eucalyptus stand. *Acta Scientiarum. Agronomy* 39(3): 393–399. <https://doi.org/10.4025/actasciagron.v39i3.32656>
- Novotný D, Šrůtka P (2004) *Ophiostoma stenoceras* and *O. grandicarpum* (Ophiostomatales), first records in the Czech Republic. *Czech Mycology* 56(1–2): 19–32. <https://doi.org/10.33585/cmy.56102>
- O'Donnell K, Kistler HC, Cigelnik E, Ploetz RC (1998) Multiple evolutionary origins of the fungus causing Panama disease of banana: Concordant evidence from nuclear and mitochondrial gene genealogies. *Proceedings of the National Academy of Sciences of the United States of America* 95(5): 2044–2049. <https://doi.org/10.1073/pnas.95.5.2044>
- O'Donnell K, Nirenberg H, Aoki T, Cigelnik E (2000) A multigene phylogeny of the *Gibberella fujikuroi* species complex: Detection of additional phylogenetically distinct species. *Mycoscience* 41(1): 61–78. <https://doi.org/10.1007/BF02464387>
- Ostafińska A, Jankowiak R, Bilański P, Solheim H, Wingfield MJ (2021) Six new species of *Sporothrix* from hardwood trees in Poland. *MycKeys* 82: 1–32. <https://doi.org/10.3897/mycokeys.82.66603>
- Ostrowska A, Gawliński S, Szczubiałka Z (1991) *Methods of Analysis and Assessment of Soil and Plant Properties*. Institute of Environmental Protection, Warszawa.
- Rambaut A, Drummond AJ (2007) Tracer v1.4. <http://beast.bio.ed.ac.uk/Tracer>
- Ramírez-Soto MC, Aguilar-Ancori EG, Tirado-Sánchez A, Bonifaz A (2018) Ecological Determinants of Sporotrichosis Etiological Agents. *Journal of Fungi* 4(3): 1–95. <https://doi.org/10.3390/jof4030095>

- Rodrigues AM, Fernandes GF, Camargo ZP (2017) Sporotrichosis. In: Bayry J (Ed.) *Emerging and Re-emerging Infectious Diseases of Livestock*. Springer International Publishing AG, Cham, Switzerland, 391–424. https://doi.org/10.1007/978-3-319-47426-7_19
- Ronquist F, Huelsenbeck JP (2003) MrBayes 3: Bayesian phylogenetic inference under mixed models. *Bioinformatics* 19(12): 1572–1574. <https://doi.org/10.1093/bioinformatics/btg180>
- Strzałka B, Jankowiak R, Bilański P, Patel N, Hausner G, Linnakoski R, Solheim H (2020) Two new species of Ophiostomatales (Sordariomycetes) associated with the bark beetle *Dryocoetes alni* from Poland. *MycoKeys* 68: 23–48. <https://doi.org/10.3897/mycokeys.68.50035>
- Swofford DL (2003) PAUP* 4.0: phylogenetic analysis using parsimony (*and other methods). Sinauer Associates, Sunderland.
- Taerum SJ, de Beer ZW, Marincowitz S, Jankowiak R, Wingfield MJ (2018) *Ophiostoma quercus*: An unusually diverse and globally widespread tree-infecting fungus. *Fungal Biology* 122(9): 900–910. <https://doi.org/10.1016/j.funbio.2018.05.005>
- Tedersoo L, Bahram M, Põlme S, Kõljalg U, Yorou NS, Wijesundera R, Ruiz LV, Vasco-Palacios AM, Thu PQ, Suija A, Smith ME, Sharp C, Saluveer E, Saitta A, Rosas M, Riit T, Ratkowsky D, Pritsch K, Põldmaa K, Piepenbring M, Phosri C, Peterson M, Parts K, Pärtel K, Otsing E, Nouhra E, Njouonkou AL, Nilsson RH, Morgado LN, Mayor J, May TW, Majuakim L, Lodge DJ, Lee SS, Larsson K-H, Kohout P, Hosaka K, Hiiesalu I, Henkel TW, Harend H, Guo L, Greslebin A, Grelet G, Geml J, Gates G, Dunstan W, Dunk C, Drenkhan R, Dearnaley J, De Kesel A, Dang T, Chen X, Buegger F, Brearley FQ, Bonito G, Anslan S, Abell S, Abarenkov K (2014) Global diversity and geography of soil fungi. *Science* 346(6213): e6213. <https://doi.org/10.1126/science.1256688>
- Urbanová M, Šnajdr J, Baldrian P (2015) Composition of fungal and bacterial communities in forest litter and soil is largely determined by dominant trees. *Soil Biology & Biochemistry* 84: 53–64. <https://doi.org/10.1016/j.soilbio.2015.02.011>
- Vilgalys R, Hester M (1990) Rapid genetic identification and mapping of enzymatically amplified ribosomal DNA from several *Cryptococcus* species. *Journal of Bacteriology* 172(8): 4238–4246. <https://doi.org/10.1128/jb.172.8.4238-4246.1990>
- Wang HM, Wang Z, Liu F, Wu CX, Zhang SF, Kong XB, Decock C, Lu Q, Zhang Z (2019) Differential patterns of ophiostomatoid fungal communities associated with three sympatric *Tomicus* species infesting pines in south-western China, with a description of four new species. *MycoKeys* 50: 93–133. <https://doi.org/10.3897/mycokeys.50.32653>
- Weber G, Spaaij F, Wingfield MJ (1996) *Leptographium costaricense* sp. nov., a new species from roots of *Talauma sambuensis* from Costa Rica. *Mycological Research* 100(6): 732–736. [https://doi.org/10.1016/S0953-7562\(96\)80206-1](https://doi.org/10.1016/S0953-7562(96)80206-1)
- White TJ, Bruns T, Lee S, Taylor J (1990) Amplification and direct sequencing of fungal ribosomal RNA genes for phylogenetics. In: Innis MA, Gelfand DH, Sninsky JJ, White TJ (Eds) *PCR Protocols: a Guide to Methods and Applications*. Academic Press, San Diego, 315–322. <https://doi.org/10.1016/B978-0-12-372180-8.50042-1>
- Zhang Y, Hagen F, Stielow B, Rodrigues AM, Samerpitak K, Zhou X, Feng P, Yang L, Chen M, Deng S, Li S, Liao W, Li R, Li F, Meis JF, Guarro J, Teixeira M, Al-Zahrani HS, Pires

de Camargo Z, Zhang L, de Hoog GS (2015) Phylogeography and evolutionary patterns in *Sporothrix* spanning more than 14 000 human and animal case reports. *Persoonia* 35(1): 1–20. <https://doi.org/10.3767/003158515X687416>

Supplementary material 1

***Pinus sylvestris* branches used to bait Ophiostomatales species from soil in this study**

Authors: Piotr Bilański, Robert Jankowiak, Halvor Solheim, Paweł Fortuna, Łukasz Chyrzyński, Paulina Warzecha, Stephen Joshua Taerum

Data type: figures (word document)

Explanation note: An example of a *Pinus sylvestris* branch used to bait Ophiostomatales from soil. *Pinus sylvestris* branches after removal from soil.

Copyright notice: This dataset is made available under the Open Database License (<http://opendatacommons.org/licenses/odbl/1.0/>). The Open Database License (ODbL) is a license agreement intended to allow users to freely share, modify, and use this Dataset while maintaining this same freedom for others, provided that the original source and author(s) are credited.

Link: <https://doi.org/10.3897/mycokeys.97.97416.suppl1>

Supplementary material 2

Phylograms from Maximum Likelihood analyses

Authors: Piotr Bilański, Robert Jankowiak, Halvor Solheim, Paweł Fortuna, Łukasz Chyrzyński, Paulina Warzecha, Stephen Joshua Taerum

Data type: figures (word document)

Explanation note: Phylogram from Maximum Likelihood (ML) analyses of LSU data for *Leptographium* spp. Phylogram from Maximum Likelihood (ML) analyses of ITS data for *Ophiostoma* spp. Phylogram from Maximum Likelihood (ML) analyses of *TUB2* data for the *Ophiostoma ulmi* species complex. Phylogram from Maximum Likelihood (ML) analyses of *TUB2* data for the *Leptographium procerum* species complex. Phylogram from Maximum Likelihood (ML) analyses of *TEF1* data for the *Leptographium procerum* species complex. Phylogram from Maximum Likelihood (ML) analyses of *TUB2* data for the *Leptographium galeiforme* species complex. Phylogram from Maximum Likelihood (ML) analyses of *TEF1* data for the *Leptographium galeiforme* species complex.

Copyright notice: This dataset is made available under the Open Database License (<http://opendatacommons.org/licenses/odbl/1.0/>). The Open Database License (ODbL) is a license agreement intended to allow users to freely share, modify, and use this Dataset while maintaining this same freedom for others, provided that the original source and author(s) are credited.

Link: <https://doi.org/10.3897/mycokeys.97.97416.suppl2>

Botryosphaeralean fungi associated with woody oil plants cultivated in Sichuan Province, China

Wen-Li Li¹, Rui-Ru Liang¹, Asha J. Dissanayake¹, Jian-Kui Liu¹

¹ School of Life Science and Technology, Center for Informational Biology, Electronic Science and Technology University, Chengdu 611731, China

Corresponding author: Jian-Kui Liu (liujiankui@uestc.edu.cn)

Academic editor: Nalin Wijayawardene | Received 7 March 2023 | Accepted 1 May 2023 | Published 23 May 2023

Citation: Li W-L, Liang R-R, Dissanayake AJ, Liu J-K (2023) Botryosphaeralean fungi associated with woody oil plants cultivated in Sichuan Province, China. MycoKeys 97: 71–116. <https://doi.org/10.3897/mycokeys.97.103118>

Abstract

Woody oil plants are important economic trees which are widely cultivated and distributed throughout China. Surveys conducted during 2020 and 2021 on several woody oil plantations from five regions of Sichuan Province, China, revealed a high diversity of Botryosphaeralean fungi. The identification of 50 botryosphaeriaceous isolates was carried out based on both morphology and multi-gene phylogenetic analysis of internal transcribed spacer region (ITS), translation elongation factor 1-alpha gene (*tef1*) and β -tubulin gene (*tub2*). This allowed the identification of twelve previously known Botryosphaerales species: *Aplosporella prunicola*, *A. ginkgonis*, *Barriopsis tectonae*, *Botryosphaeria dothidea*, *Bo. fabricerciana*, *Diplodia mutila*, *Di. seriata*, *Dothiorella sarmentorum*, *Neofusicoccum parvum*, *Sardiniella guizhouensis*, *Sphaeropsis citrigena*, and *Sp. guizhouensis*, and four novel species belonging to the genera *Diplodia* and *Dothiorella*, viz. *Di. acerigena*, *Di. pistaciicola*, *Do. camelliae* and *Do. zanthoxyli*. The dominant species isolated across the surveyed regions were *Botryosphaeria dothidea*, *Sardiniella guizhouensis* and *Diplodia mutila*, representing 20%, 14% and 12% of the total isolates, respectively. In addition, most isolates were obtained from *Pistacia chinensis* (14 isolates), followed by *Camellia oleifera* (10 isolates). The present study enhances the understanding of Botryosphaerales species diversity on woody oil plants in Sichuan Province, China.

Keywords

Botryosphaerales, diversity, new species, phylogeny, taxonomy

Introduction

Botryosphaeriaceae is a diverse group of fungi that includes endophytes, saprobes and plant pathogens (Phillips et al. 2013). They have broad host ranges, and are widely distributed in tropical and temperate regions (Batista et al. 2021). Botryosphaeriaceae was introduced by Theissen and Sydow (1918) to accommodate three genera *Botryosphaeria*, *Dibotryon* and *Phaeobotryon*. Botryosphaeriales was proposed to include the single family, Botryosphaeriaceae, based on multi-gene phylogeny (Schoch et al. 2006). Up to date, six families and 32 genera are accepted in Botryosphaeriales, while Botryosphaeriaceae is known to be the largest monophyletic family, including 22 genera and more than 200 species (<https://botryosphaeriales.org/>, accessed on 15th April 2023).

The members of Botryosphaeriaceae have been taxonomically characterized based on both sexual and asexual morphs. The production of large, ovoid to oblong, typically hyaline, aseptate ascospores, which may become brown and septate with age, as well as bitunicate asci within unilocular or multilocular botryose ascomata known as pseudothecia is typical to the sexual state (Sivanesan 1984; Phillips et al. 2005). The asexual states of Botryosphaeriaceae exhibit a wide range of conidial morphologies; for example, its conidia can be thin-walled and hyaline, or thick-walled and pigmented, aseptate or 1–2-septate (Phillips et al. 2005). Additionally, the spermatial states were also frequently observed in Botryosphaeriaceae species, which produced unicellular, hyaline, allantoid to rod-shaped spermatia on culture. Botryosphaeriaceae species are significantly different from other fungi in that the color of its aerial hyphae, changing from gray to black with age on 2% potato dextrose agar (PDA), which can be used for the rapid determination of botryosphaeriaceous fungi.

The geographic distribution and host range of botryosphaeriaceous taxa are diverse. Seven genera in Botryosphaeriaceae: *Botryosphaeria*, *Diplodia*, *Dothiorella*, *Lasiodiplodia*, *Neodeightonia*, *Neofusicoccum* and *Phaeobotryon* are common and frequently reported from various geographical regions (Batista et al. 2021), while *Botryobambusa*, *Oblongocollomyces*, *Sakireeta* and *Sardiniella* appear to be limited to a single region or country (Liu et al. 2012; Crous et al. 2015; Linaldeddu et al. 2016; Yang et al. 2017; Dissanayake et al. 2021). Many Botryosphaeriaceae species have wide host ranges (e. g. *Botryosphaeria dothidea*, *Diplodia mutila*, *Dothiorella sarmentorum*, *Lasiodiplodia theobromae* and *Neofusicoccum parvum*), while other species have narrower host ranges (e. g. *Diplodia olivarum* was reported on olive, oleaster, carob, grapevine, almond et al.) (Lazzizera et al. 2008; Granata et al. 2011; Linaldeddu et al. 2015; Olmo et al. 2016) or even in very specific hosts (e. g. *Eutiarosporella darliae* was only reported on infected wheat and wheat-stubble) (Thynne et al. 2015; Farr and Rossman 2021). Different species of Botryosphaeriaceae exhibit different environmental adaptations and host preferences (Braunsdorf et al. 2016). Botryosphaeriaceous taxa

with narrow host ranges or limited geographic distribution will be more susceptible to climatic effects (Slippers et al. 2017; Li et al. 2020).

Woody oil plants are economically important as they are used for the production of cooking and industrial oil. Recently, many Botryosphaeriaceae species have been frequently reported on woody oil plants. *Diplodia olivarum* was first reported from rotting olive drupes in Italy (Lazzizzera et al. 2008) and later it was reported as associated with declining *Prunus dulcis* trees in Spain (Gramaje et al. 2012). *Diplodia insularis* was isolated from branch canker of *Pistacia lentiscus* in Italy (Linaldeddu et al. 2015). *Dothiorella gregaria* was isolated from the stems with asymptomatic of *Zanthoxylum bungeanum* in China (Li et al. 2016b). *Botryosphaeria dothidea*, *Diplodia mutila*, *Di. seriata*, *Dothiorella iberica*, *Do. omnivora*, *Do. sarmentorum*, *Lasiodiplodia citricola*, *L. pseudotheobromae*, *L. theobromae*, *Neofusicoccum mediterraneum*, *N. nonquaesitum*, *N. parvum*, *N. ribis*, *N. vitifusiforme*, and *Neoscytalidium dimidiatum* have been reported as pathogens of *English walnut* (*Juglans regia* L.) in California (Chen et al. 2014), Chile (Jimenez Luna et al. 2022), China (Li et al. 2016a; Zhang et al. 2017), Iran (Abdollahzadeh et al. 2013; Panahandeh et al. 2019), South Africa (Cloete et al. 2011), Spain (Gramaje et al. 2012) and USA (Chen et al. 2014). However, very little is known about the Botryosphaeriales species occurring on native woody oil plants in China. Hence, the aim of this study was to gain a more comprehensive understanding of the diversity of Botryosphaeriaceae species associated with common woody oil plants grown in Sichuan Province, China.

Materials and methods

Isolates and morphology

The isolates in this study were collected from the woody oil tree plantations in Sichuan Province during the period of 2020 and 2021. The hosts include *Acer truncatum*, *Camellia oleifera*, *Idesia polycarpa*, *Olea europaea*, *Paeonia suffruticosa*, *Pistacia chinensis*, *Vernicia fordii* and *Zanthoxylum bungeanum*. The samples were collected from decayed stems, branches and twigs of woody oil trees. Mature fruiting bodies were selected for fungal isolation and for morphological observations under stereo microscope Motic SMZ 168 series. Measurements were made with Tarosoft Image Frame Work program v. 0.9.7 (Liu et al. 2010). Thirty conidia/ascospores were measured per isolate, and 10–30 measurements were taken of other morphological structures. At least 20 conidia/ascospores were used to calculate the average length/width ratio (L/W). Single spore isolation was conducted in accordance with the methods described in Chomnunti et al. (2014). Germinated spores were individually placed on PDA plates and grown at 25 °C in daylight.

Herbarium specimens were stored in the herbarium of Cryptogams Kunming Institute of Botany, Academia Sinica (KUN-HKAS) and duplicated at Herbarium, University of Electronic Science and Technology (**HUEST**), Chengdu, China. Living cultures were deposited at China General Microbiological Culture Collection Centre (**CGMCC**), Beijing, China and duplicated at the University of Electronic Science and Technology Culture Collection (**UESTCC**), Chengdu, China. MycoBank numbers were registered as outlined in MycoBank (<http://www.MycoBank.org>. Accessed on 11th November 2022).

DNA extraction, PCR amplification and sequencing

The total genomic DNA was extracted from 7day-old isolates grown on 2% PDA median at 25 °C, using the EZ gene™ fungal gDNA kit (GD2416), following the manufacturer's instructions and protocols. Partial gene sequences were determined for the internal transcribed spacer 1 and 2 including the intervening 5.8S nrDNA gene (ITS), the nuclear ribosomal 28S large subunit (LSU), the translation elongation factor 1- α gene (*tef1*), and the β -tubulin gene (*tub2*). The primers used for amplification are ITS5/ITS4 for ITS (White et al. 1990), LR0R/LR5 for LSU (Vilgalys and Hester 1990), EF1-728F/EF1-986R for *tef1* (Carbone and Kohn 1999) and Bt2a/Bt2b for *tub2* (Glass and Donaldson 1995). Polymerase chain reaction (PCR) amplification conditions were followed as of Dissanayake et al. (2021). PCR products were sent for sequencing at Beijing Tsingke Biological Engineering Technology and Services Co. Ltd. (Beijing, P.R. China). All newly generated sequences are deposited in GenBank, and the obtained accession numbers are listed in Table 1.

Phylogenetic analyses

Sequence data for phylogenetic analyses were obtained from GenBank and from recent publications regarding Botryosphaeriaceae fungi (Dissanayake et al. 2021; Xiao et al. 2021; Zhang et al. 2021; Rathnayaka et al. 2022) (See Suppl. material 1). The single gene alignments were performed using MAFFT v.7.429 online service (<https://mafft.cbrc.jp/alignment/server/>, accessed on 15 October 2022) (Katoh et al. 2019) and ambiguous regions were excluded using TrimAI with the option “-automated1”, which trimmed sequences based on similarity statistics (Capella-Gutiérrez et al. 2009). Multi-gene sequences were concatenated by Sequence matrix software (Vaidya et al. 2011). Multi-gene phylogenetic analyses were obtained from maximum likelihood (ML) and Bayesian inference (BI) analyses following Dissanayake et al. (2020).

ML analyses was performed using RAxML (Stamatakis 2006). The tree search included 1,000 non-parametric bootstrap replicates and the best scoring tree was selected from suboptimal trees under the GTRGAMMA substitution model. Maximum

Table 1. All newly generated sequences in this study. Ex-type strains are indicated with *. N/A: Not available.

Taxon	Stain Number	GenBank Accession Number			
		ITS	<i>tefl</i>	<i>tub2</i>	
<i>Aplosporella ginkgonis</i>	UESTCC 22.0091	OQ190504	OQ241438	N/A	
<i>Aplosporella prunicola</i>	UESTCC 22.0090	OQ190505	N/A	N/A	
<i>Barriopsis tectonae</i>	UESTCC 22.0092	OQ190506	OQ241439	N/A	
<i>Botryosphaeria dothidea</i>	UESTCC 22.0111	OQ190507	OQ241440	N/A	
	UESTCC 22.0109	N/A	OQ241441	N/A	
	UESTCC 22.0112	OQ190508	OQ241442	N/A	
	UESTCC 22.0113	OQ190509	OQ241443	N/A	
	UESTCC 22.0108	OQ190510	OQ241444	N/A	
	UESTCC 22.0116	OQ190511	OQ241445	N/A	
	UESTCC 22.0114	OQ190512	OQ241446	N/A	
	UESTCC 22.0115	OQ190513	OQ241447	N/A	
	UESTCC 22.0110	OQ190514	OQ241448	N/A	
	UESTCC 22.0107	OQ190515	OQ241449	N/A	
	<i>Botryosphaeria fabicerciana</i>	UESTCC 22.0117	OQ190516	OQ241450	N/A
		UESTCC 22.0118	OQ190517	OQ241451	N/A
	<i>Diplodia acerigena*</i>	CGMCC 3.24157	OQ190518	OQ241452	N/A
	<i>Diplodia acerigena</i>	UESTCC 22.0074	OQ190519	OQ241453	OQ338163
UESTCC 22.0075		OQ190520	OQ241454	OQ338164	
<i>Diplodia mutila</i>	UESTCC 22.0064	OQ190521	OQ241455	OQ338165	
	UESTCC 22.0065	OQ190522	OQ241456	OQ338166	
	UESTCC 22.0069	OQ190523	OQ241457	OQ338167	
	UESTCC 22.0068	OQ190524	OQ241458	OQ338168	
	UESTCC 22.0067	OQ190525	OQ241459	OQ338169	
	UESTCC 22.0063	OQ190526	OQ241460	OQ338170	
	CGMCC 3.24156	OQ190527	OQ241461	OQ338171	
<i>Diplodia pistaciicola*</i>	UESTCC 22.0071	OQ190528	OQ241462	OQ275062	
<i>Diplodia seriata</i>	UESTCC 22.0072	OQ190529	OQ241463	N/A	
<i>Dothiorella camelliae</i>	UESTCC 22.0080	OQ190530	N/A	OQ275063	
<i>Dothiorella camelliae*</i>	CGMCC 3.24158	OQ190531	OQ241464	OQ275064	
<i>Dothiorella camelliae</i>	UESTCC 22.0079	OQ190532	OQ241465	OQ275065	
	UESTCC 22.0078	OQ190533	OQ241466	OQ275066	
<i>Dothiorella sarmentorum</i>	UESTCC 22.0076	OQ190534	N/A	OQ275067	
	UESTCC 22.0077	OQ190535	OQ241467	OQ275068	
<i>Dothiorella zanthoxyli*</i>	CGMCC 3.24159	OQ190536	OQ241468	OQ275069	
<i>Dothiorella zanthoxyli</i>	UESTCC 22.0083	OQ190537	OQ241469	OQ275070	
	UESTCC 22.0084	OQ190538	OQ241470	OQ275071	
<i>Neofusicoccum parvum</i>	UESTCC 22.0096	OQ190539	OQ241471	N/A	
	UESTCC 22.0094	OQ190540	N/A	N/A	
	UESTCC 22.0093	OQ190541	N/A	N/A	
	UESTCC 22.0095	OQ190542	N/A	N/A	
<i>Sardiniella guizhouensis</i>	UESTCC 22.0100	OQ190543	OQ241472	N/A	
	UESTCC 22.0101	OQ190544	OQ241473	N/A	
	UESTCC 22.0099	OQ190545	OQ241474	N/A	
	UESTCC 22.0097	OQ190546	OQ241475	N/A	
	UESTCC 22.0098	OQ190547	OQ241476	N/A	
	UESTCC 22.0102	OQ190548	OQ241477	N/A	
<i>Sphaeropsis citrigena</i>	UESTCC 22.0103	OQ190549	OQ241478	N/A	
	UESTCC 22.0106	OQ190550	OQ241479	N/A	
	UESTCC 22.0105	OQ190551	OQ241480	N/A	
	<i>Sphaeropsis guizhouensis</i>	UESTCC 22.0104	OQ190552	OQ241481	N/A

likelihood bootstrap values equal or greater than 75% are marked near each node of the phylogenetic tree.

Bayesian analyses was performed in MrBayes 3.2.6 (Ronquist et al. 2012). The program MrModeltest 2.2 (Nylander 2004) was used to determine the best nucleotide substitution model for each data partition. The Markov Chain Monte Carlo (MCMC) sampling approach was used to calculate the posterior probabilities (PP) (Rannala and Yang 1996). Bayesian analyses of four simultaneous Markov chains were run for 10,000,000 generations with trees sampled every 1,000th generations. The first 20% of trees, representing the burn-in phase of the analyses, were discarded, and the remaining trees were used for calculating posterior probabilities (PP) in the majority rule consensus tree. PP values equal or greater than 0.95 are marked near each node.

Trees were visualized with FigTree v1.4.0 (Rambaut 2006), and the layout was edited using Adobe Illustrator CS6 software (Adobe Systems, USA).

Results

Phylogenetic analyses

A concatenated dataset of ITS and *tef1* was used to determine the phylogenetic position of Aplosporellaceae and Botryosphaeriaceae isolates obtained in this study. Combined sequences of ITS and *tef1* were used for the analyses of *Botryosphaeria*, while ITS, *tef1* and *tub2* were used for the analyses of *Diplodia* and *Dothiorella* isolates. All details of the alignments are provided in Table 2.

In an overview phylogenetic tree (Fig. 1), sixteen newly obtained isolates were nested with four genera of Botryosphaeriaceae, representing seven known species viz. *Barriopsis tectonae*, *Neofusicoccum parvum*, *Sardiniella guizhouensis*, *Sphaeropsis guizhouensis* and *Sp. citrigena*. Two isolates were clustered with the genus *Aplosporella* (Aplosporellaceae), and were identified as *A. ginkgonis* and *A. prunicola*.

Three individual phylogenetic trees were constructed for the genera *Botryosphaeria*, *Diplodia* and *Dothiorella*. Twelve isolates belonged to the genus *Botryosphaeria* and ten of them were nested with *Bo. dothidea*, while the remaining two isolates clustered with *Bo. fabicerciana* (Fig. 2). Another twelve isolates were treated in *Diplodia* and seven isolates were clustered with two known species of *Diplodia* (*Di. mutila* and *Di. seriata*, Fig. 3). The other five isolates did not cluster with any previously known *Diplodia* species, thus, two novel species were preliminarily identified based on phylogenetic evidence. Eight isolates were nested within *Dothiorella* and six isolates of them were occupied in the basal position of the *Dothiorella* tree and formed two well-supported subclades, representing two new species. The other two isolates were nested within the *Do. sarmentorum* isolates (Fig. 4).

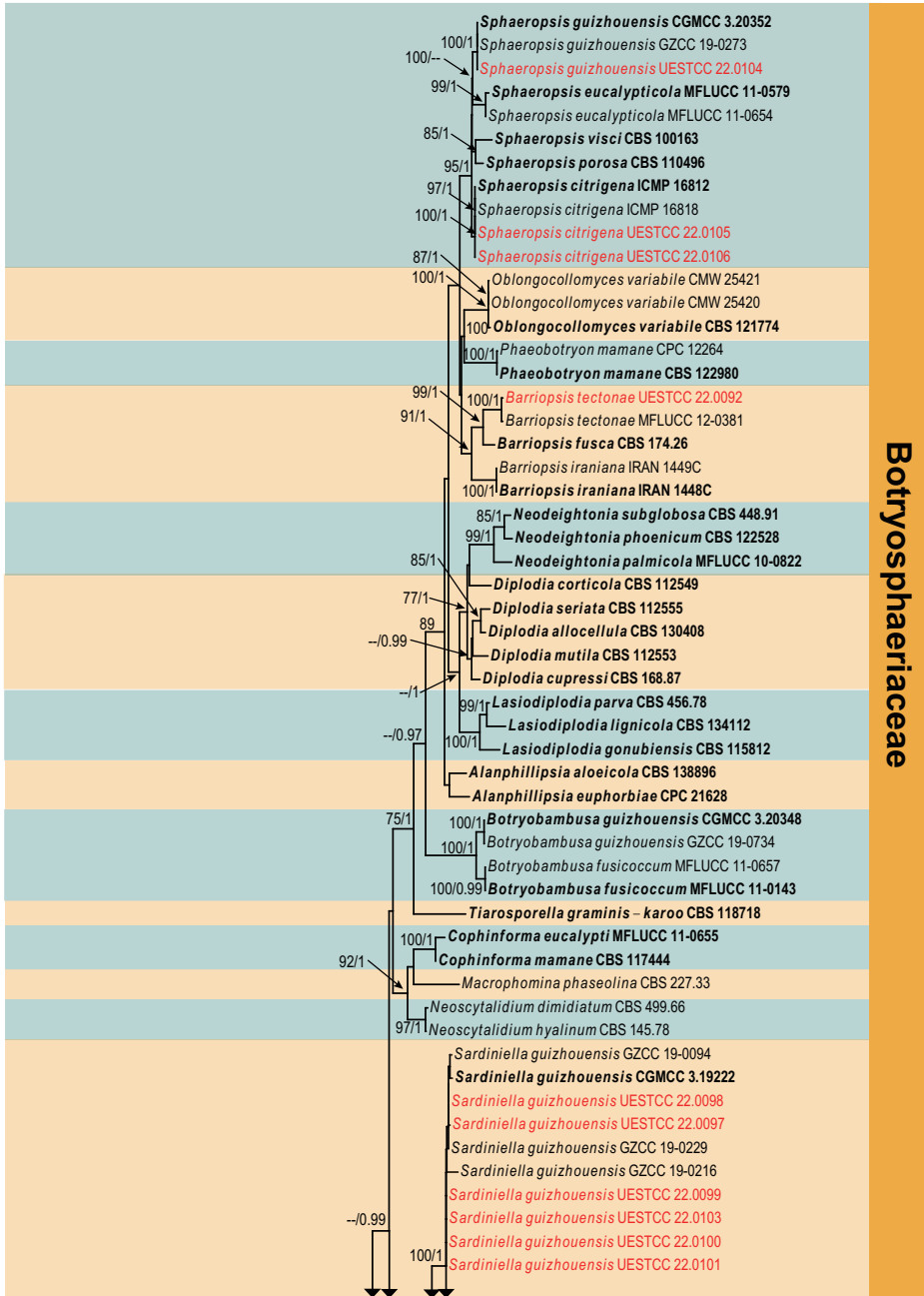


Figure 1. Phylogram generated from RAxML analysis based on combined ITS and *tefl* sequence data of *Botryosphaeriaceae* and *Aplosporellaceae* isolates. The tree was rooted to *Lecanosticta acicula* (LNPV 252). The ML ($\geq 75\%$) and BI ($\geq 95\%$) bootstrap supports are given near the nodes, respectively. Isolates from this study are marked in red and ex-type strains are marked in bold.

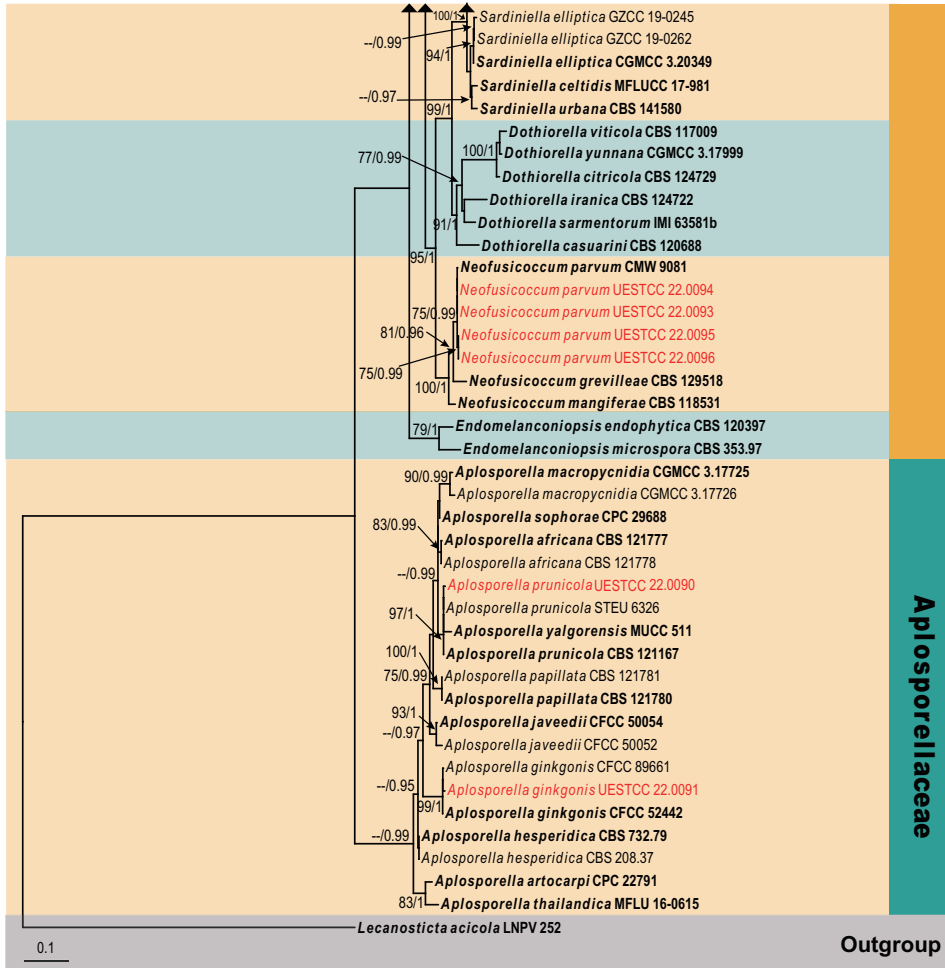


Figure 1. Continued.

Table 2. Alignment details and ML, BI analyses results of each phylogenetic tree constructed in this study.

Character	Overview phylogenetic tree	Botryosphaeria	Diplodia	Dothiorella	
Number of base pairs in each gene region (including the gaps after alignment)	ITS (603 bp), <i>tef1</i> (320 bp)	ITS (555 bp), <i>tef1</i> (315 bp)	ITS (537 bp), <i>tef1</i> (311 bp), <i>tub2</i> (381 bp)	ITS (523 bp), <i>tef1</i> (294 bp), <i>tub2</i> (427 bp)	
Number of isolates obtained in this study	17	12	11	9	
Number of taxa originated from GenBank	94	45	64	73	
Outgroup taxa	<i>Lecanosticta acicola</i> (LNPV252)	<i>Barriopsis iraniana</i> (IRAN1448C) and <i>Barriopsis iraniana</i> (IRAN1449C)	<i>Dothiorella dulcispinae</i> (CMW 36460) and <i>Dothiorella dulcispinae</i> (CMW 36462)	<i>Neofusicoccum luteum</i> (CBS 562.92) and <i>Neofusicoccum luteum</i> (CMW 41365)	
BI (model of each gene region)	ITS	GTR+I+G	SYM	K80+I+G	HKY+I+G
	<i>tef1</i>	GTR+I+G	HKY+G	GTR+G	GTR+G
	<i>tub2</i>	–	–	GTR+G	GTR+I+G

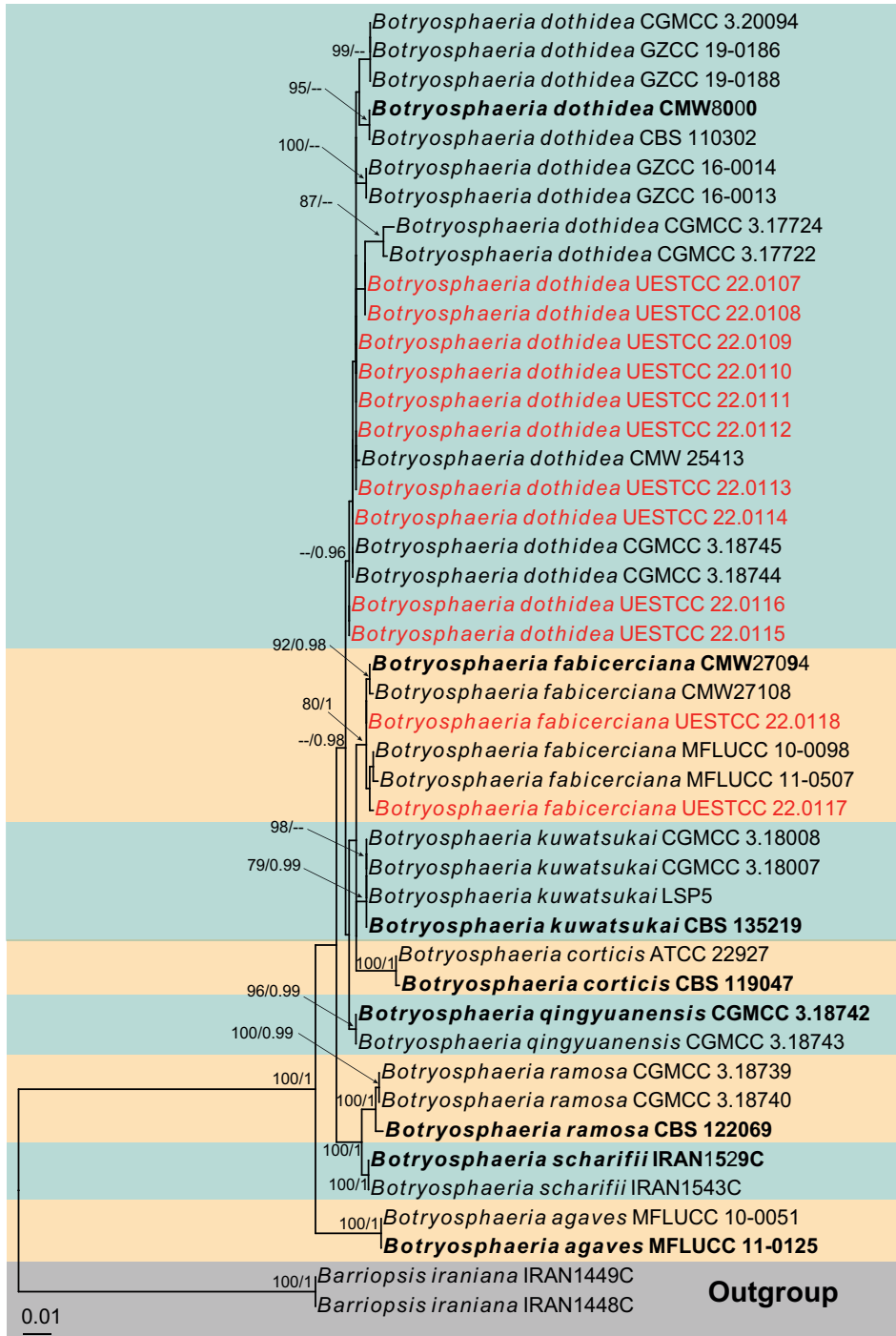


Figure 2. Phylogram generated from RAxML analysis based on combined ITS and *tef1* sequence data of *Botryosphaeria* isolates. The tree was rooted to *Barriopsis iraniana* (IRAN1448C and IRAN1449C). The ML ($\geq 75\%$) and BI ($\geq 95\%$) bootstrap supports are given near the nodes, respectively. Isolates from this study are marked in red and ex-type strains are marked in bold.

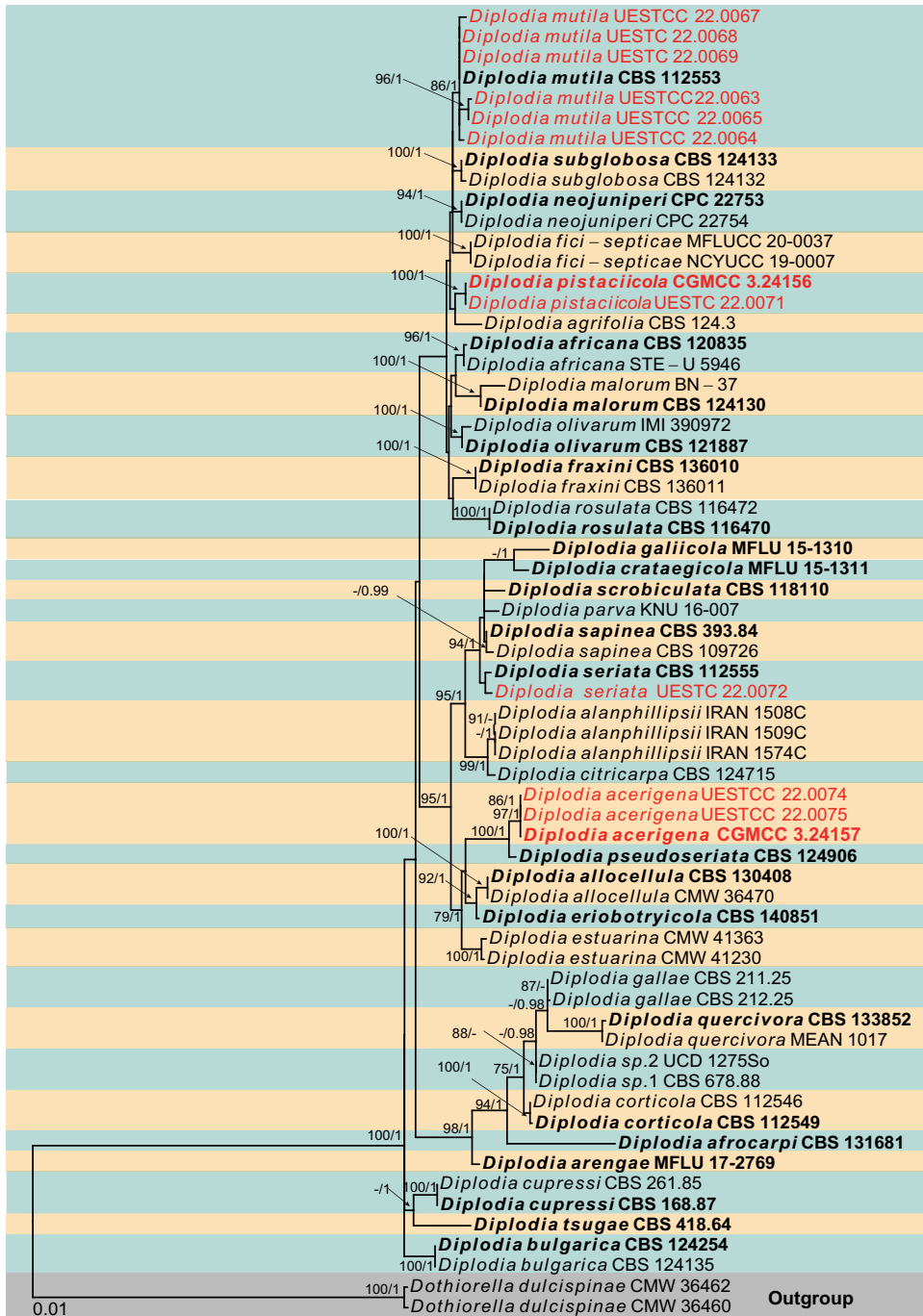


Figure 3. Phylogram generated from RAxML analysis based on combined ITS, *tef1* and *tub2* sequence data of *Diplodia* isolates. The tree was rooted to *Dothiorella dulcispinae* (CMW 36460 and CMW 36462). The ML ($\geq 75\%$) and BI ($\geq 95\%$) bootstrap supports are given near the nodes, respectively. Isolates from this study are marked in red and ex-type strains are marked in bold.

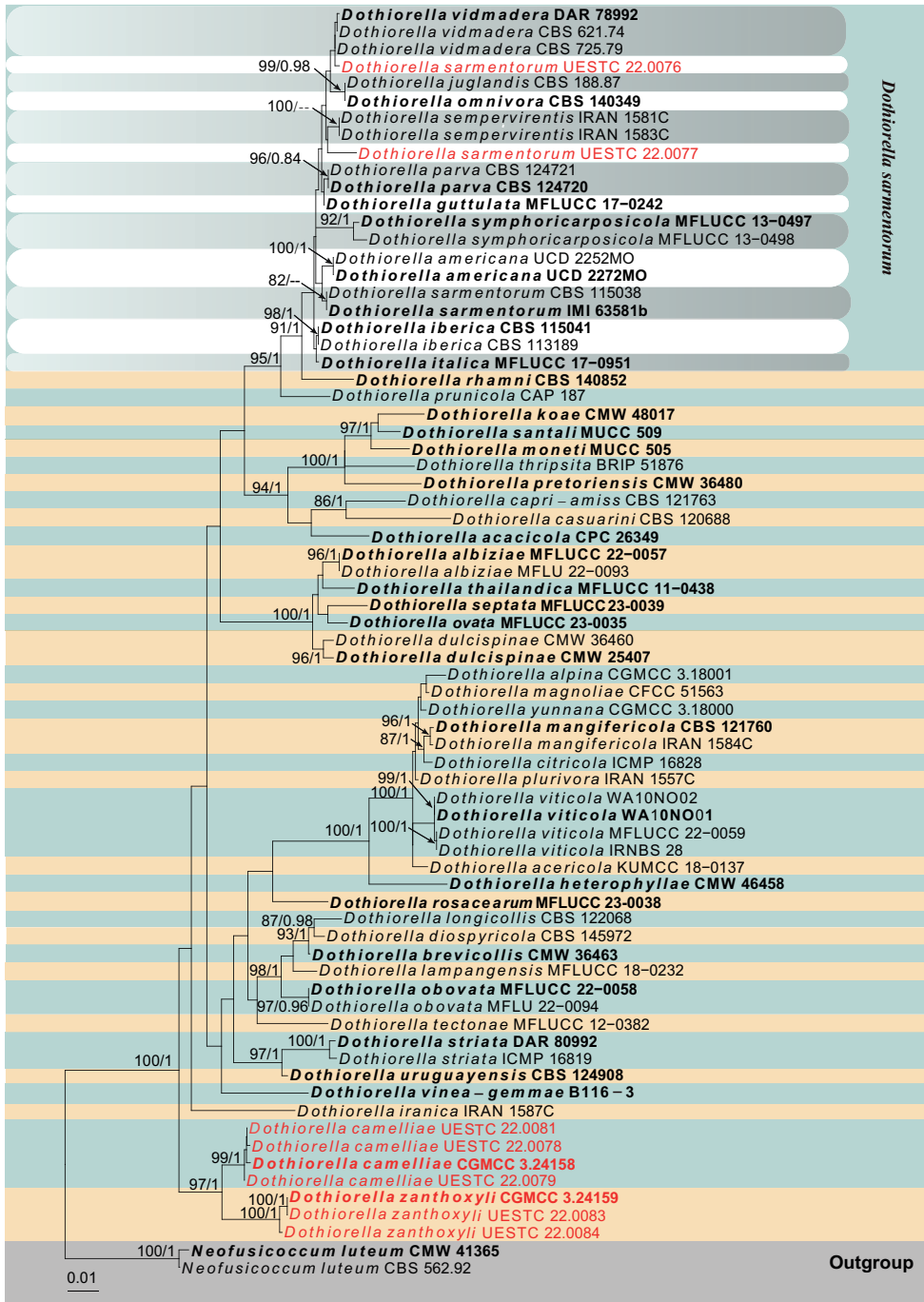


Figure 4. Phylogram generated from RAxML analysis based on combined ITS, *tef1* and *tub2* sequence data of *Dothiorella* isolates. The tree was rooted to *Neofusicoccum luteum* (CBS 562.92 and CMW 41365). The ML ($\geq 75\%$) and BI ($\geq 95\%$) bootstrap supports are given near the nodes, respectively. Isolates from this study are marked in red and ex-type strains are marked in bold.

Taxonomy

Aplosporella ginkgonis C.M. Tian, Z. Du & K.D. Hyde. *Mycosphere* 8(2): 1249 (2017).

MycoBank No: 552938

Fig. 5

Description. *Saprobic* on decaying branches of *Zanthoxylum bungeanum*. **Sexual morph:** Not observed. **Asexual morph:** Coelomycetous, *Conidiomata* 558–657 × 216–241 µm (\bar{x} = 235.5 × 228.5 µm, n = 10), immersed, partially erumpent when mature, multilocular, locules separated by pale brown cells of *textura angularis*. **Peridium** 65–106 µm wide, wall 6–10 cell-layers thick, outer layers composed of 3–4 layers of pale brown cells of *textura globulosa*, intermediate layers composed of dark brown cells of *textura angularis*, becoming pale brown towards the inner region. **Ostiole** 138–171 µm diam., central. **Conidiophores** reduced to conidiogenous cells. **Conidiogenous cells** 12–13 × 7.5–8 µm (\bar{x} = 12.5 × 8 µm, n = 20), holoblastic, hyaline, cylindrical to doliiform, smooth-walled. **Conidia** 17–20 × 6.5–7.5 µm (\bar{x} = 18.5 × 7 µm, n = 30), L/W ratio = 2.5, ellipsoidal to subcylindrical, with both ends rounded, initially hyaline, becoming dark brown, aseptate.

Culture characteristics. Colonies on PDA developing dense aerial mycelium with age, becoming white to gray-brown at the surface, and whitish to yellowish brown at the reverse, producing a brown pigment, with sinuate edges.

Material examined. CHINA, Sichuan Province, Yaan City, Hanyuan County, 29°16'51"N, 102°37'48"E, elevation 1,689 m, on dead branches of *Zanthoxylum bungeanum*, 30th October 2021, W.L. Li, HJ 511 (HUEST 22.0092), living culture UESTCC 22.0091.

Notes. *Aplosporella ginkgonis* was introduced by Du et al. (2017) and isolated from diseased branches of *Ginkgo biloba* and *Morus alba* from Gansu Province in China. One isolate (UESTCC 22.0091) obtained in this study from *Zanthoxylum bungeanum* is morphologically similar to the original description of *Aplosporella ginkgonis*, and the sequences data are identical to the previous data (99%–100%). We, thus, identify the new collection as *Aplosporella ginkgonis* and this is the first report from *Zanthoxylum bungeanum*.

Aplosporella prunicola Damm & Crous *Fungal Diversity* 27: 39 (2007).

MycoBank No: 504373

Fig. 6

Description. *Saprobic* on decaying branches of *Zanthoxylum bungeanum*. **Sexual morph:** Not observed. **Asexual morph:** Coelomycetous, *Conidiomata* 355–408 × 568.5–599 µm (\bar{x} = 381.5 × 584 µm, n = 10), immersed, partially erumpent when mature, multilocular, locules divided by pale brown cells of *textura angularis*.

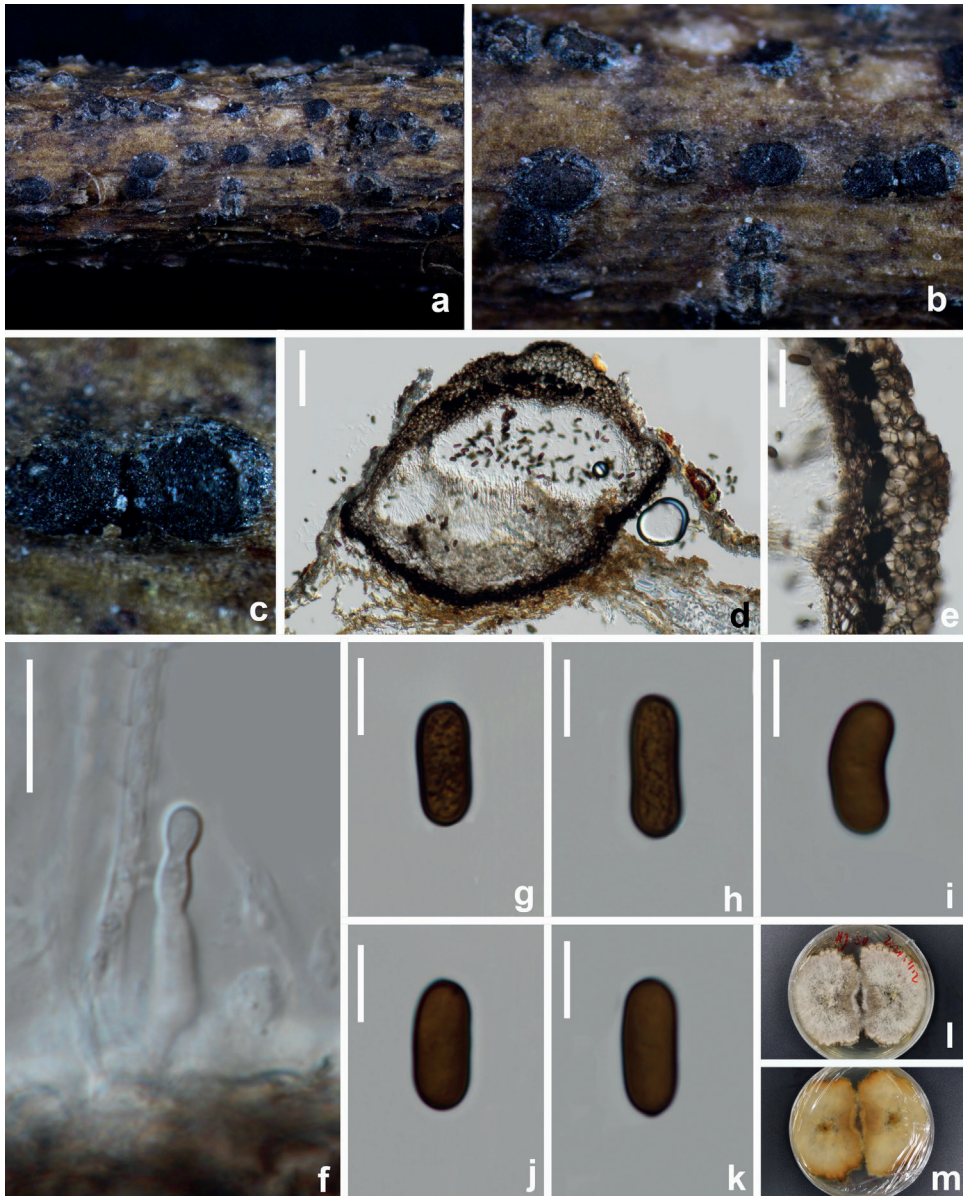


Figure 5. *Aplosporella ginkgonis* (HUEST 22.0092, new host record) **a–c** appearance of conidiomata on natural substrate **d** vertical section of conidioma **e** section of peridium **f** conidiogenous cells and developing conidia **g–k** brown aseptate conidia **l** upper view of the colony on PDA after 14 d **m** reverse view of the colony on PDA after 14 d. Scale bars: 100 μ m (**d**); 40 μ m (**e**); 10 μ m (**f–k**).

Peridium 107–122 μ m wide, composed of 3–5 layers of pale brown cells of *textura globulosa*. **Ostiole** 70–88 μ m diam., central. **Conidiophores** reduced to conidiogenous cells. **Conidiogenous cells** 6.5–10 \times 2–3 μ m (\bar{x} = 8 \times 2.5 μ m, n = 20), holoblastic, hya-

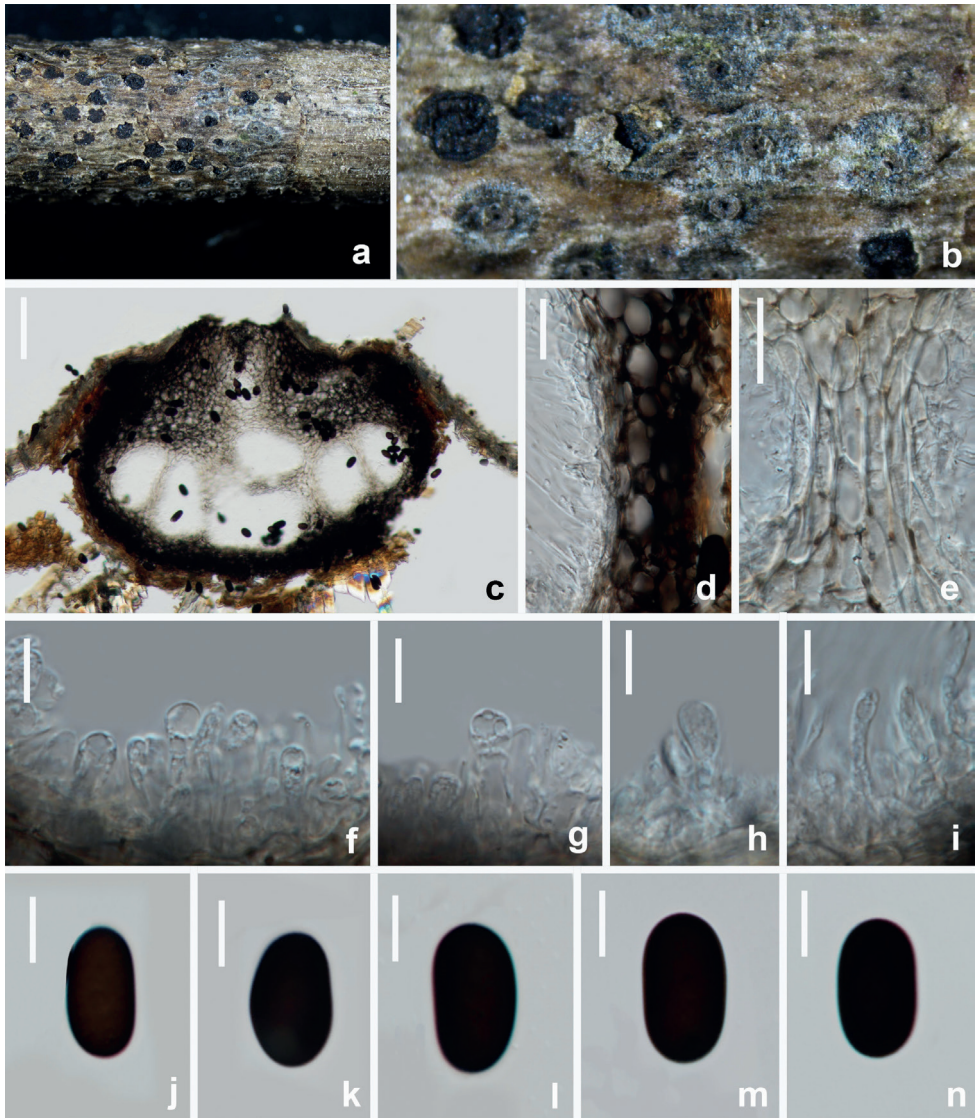


Figure 6. *Aplosporella prunicola* (HUEST 22.0091, new host record) **a, b** appearance of conidiomata on natural substrate **c** vertical section of multiloculate conidioma **d, e** section of peridium **f–i** conidiogenous cells and developing conidia **j–n** brown aseptate conidia. Scale bars: 100 μm (**c**); 20 μm (**d, e**); 10 μm (**f–n**).

line, cylindrical, smooth-walled. **Conidia** 20–23.5 \times 12–13.5 μm (\bar{x} = 21.5 \times 13 μm , n = 30), L/W ratio = 1.6, ellipsoidal to subcylindrical, with both ends broadly rounded, initially hyaline, becoming dark brown, aseptate, smooth.

Culture characteristics. Colonies on PDA after 7 d, becoming pale olivaceous-gray to olivaceous-black at the surface, and olivaceous black at the reverse, with irregular edges.

Material examined. CHINA, Sichuan Province, Yaan City, Hanyuan County, 29°16'51"N, 102°37'48"E, elevation 1,689 m, on dead branches of *Zanthoxylum bungeanum*, 30th October 2021, W.L Li, HJ 509 (HUEST 22.0091), living culture UESTCC 22.0090.

Notes. Our isolate UESTCC 22.0090 morphologically lines up with the description of *Aplosporella prunicola* provided by Damm et al. (2007) in having immersed to erumpent, multilocular conidiomata and brown, smooth-walled, ovoid to oblong conidia. The strain UESTCC 22.0090 is phylogenetically and morphologically similar to *A. yalgorensis* and *A. prunicola*, however, *A. yalgorensis* can be distinguished from other *Aplosporella* species by its pitted conidial walls. Thus, the strain UESTCC 22.0090 was identified as *A. prunicola* based on current evidence. This is the first time *A. prunicola* is reported from *Zanthoxylum bungeanum* in China.

***Diplodia acerigena* L.W. Li & Jian K. Liu, sp. nov.**

Mycobank No: 847163

Figs 7, 8

Etymology. The epithet “acerigena” refers to the host genus *Acer*, on which the holotype was collected.

Holotype. HKAS 125891.

Description. *Saprobic* on decaying branches of *Acer truncatum*. **Sexual morph:** *Ascomata* 304.5–321 × 217–260 (\bar{x} = 313 × 238.5 μ m, n = 20), more or less subglobose, solitary or gregarious, semi-immersed, medium brown to dark brown, unilocular, papillate, ostiolate. **Ostiole** 101–115 μ m diam., conical or circular, central, papillate, periphysate. **Peridium** 23–29 μ m wide, composed of 3–5 layers of dark brown cells of *textura angularis*. **Pseudoparaphyses** 3.5–5 μ m wide, hyaline, branched, septate. **Asci** 98–120 × 24–32.5 μ m (\bar{x} = 109 × 28 μ m, n = 30), (4–)8-spored, clavate, stipitate, irregularly bitunicate, apex rounded with an ocular chamber. **Ascospores** 24.5–31.5 × 13.5–16 μ m (\bar{x} = 28 × 14.5 μ m, n = 30), L/W ratio = 2, biseriate, broadly fusiform to oval, widest in the middle, both ends obtuse, hyaline, moderately thick-walled, smooth, becoming brown and 2-septate when aged. **Asexual morph:** Coelomycetous, pycnidia produced on mycelium in PDA. **Conidiomata** stromatic, mostly solitary, gray to black, globose to subglobose. **Paraphyses** 2–3.5 μ m wide, hyaline, subcylindrical, branched, septate. **Conidiophores** absent. **Conidiogenous cells** 9–12 × 3.5–5 μ m (\bar{x} = 10.5 × 4.5 μ m, n = 20), holoblastic, hyaline, cylindrical. **Conidia** 21–24 × 10–11 μ m (\bar{x} = 22.5 × 10.5 μ m, n = 30), L/W ratio = 2, aseptate, thick-walled, wall externally smooth, roughened on the inner surface, initially hyaline becoming dark brown, obovoid to ellipsoid, both ends broadly rounded. **Spermatogenous cells** 7–9.5 × 2.5–3.5 μ m (\bar{x} = 8 × 3 μ m, n = 20), discrete or integrated, hyaline, smooth, cylindrical, holoblastic or proliferating via determinate phialides with periclinal thickening. **Spermatia** 7–11.5 × 3–4 μ m (\bar{x} = 9 × 3.5 μ m, n = 30), hyaline, smooth, aseptate, rod-shaped with rounded ends.



Figure 7. The sexual morph of *Diplodia acerigena* (HKAS 125891, holotype) **a, b** appearance of ascomata on natural substrate **c** vertical section of ascoma **d** ostiole **e** section of peridium **f–h** asci with hyaline ascospores **i** asci with brown 2-septate ascospores **j, k** hyaline immature aseptate ascospores **l–n** mature brown 2-septate ascospores **o** germinated ascospore **p** upper view of the colony on PDA after 14 d **q** reverse view of the colony on PDA after 14 d. Scale bars: 100 μm (**c**); 10 μm (**d, e, j–o**); 20 μm (**f–i**).

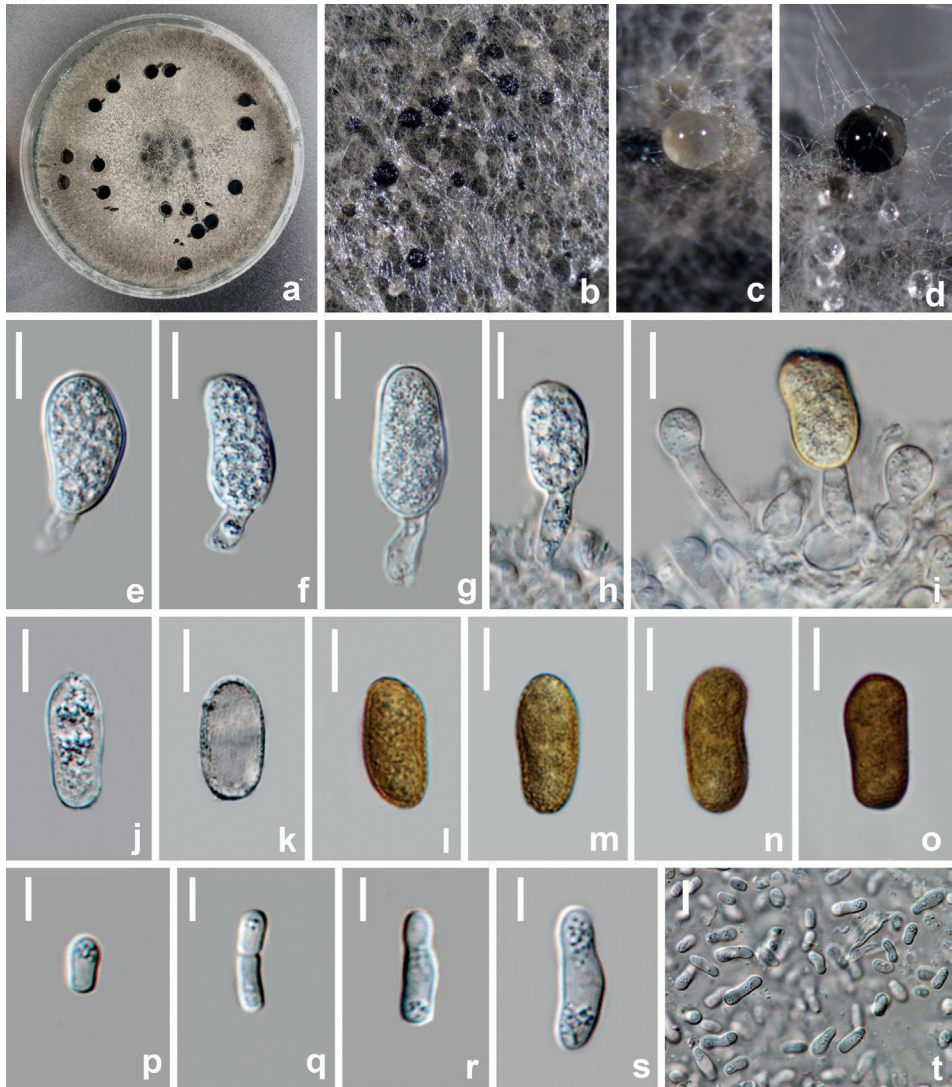


Figure 8. The asexual morph of *Diplodia acerigena* (HKAS 125891, holotype) **a–d** appearance of conidiomata on PDA **e–i** conidiogenous cells and developing conidia **j, k** hyaline immature conidia **l–o** mature brown aseptate conidia **p–t** Spermatogenous cells and Spermata. Scale bars: 10 μm (**e–o, t**); 5 μm (**p–s**).

Culture characteristics. Ascospores germinating on PDA within 12 h. Colonies growing on PDA, reaching a diam. of 4 cm after five days at 25 °C, effuse, velvety, with entire to slightly undulate edge. Surface initially white and later turning dark olivaceous from the surrounding of the colony and dark gray in reverse.

Material examined. CHINA, Sichuan Province, Chengdu City, Pidu District, 30°19'57"N, 103°59'47"E, elevation 442 m, on dead branches of *Acer truncatum* (Anacardiaceae), 19th March 2021, W.L Li, YBF 96 (HKAS 125891, holotype), ex-

type living culture UESTCC 22.0073 = CGMCC 3.24157; *ibid.*, YBF103 (HUEST 22.0075, paratype), living culture UESTCC 22.0074. Additional sequences: LSU: OQ164827 (CGMCC 3.24157), OQ164828 (UESTCC 22.0074).

Notes. Three isolates of *Diplodia acerigena* clustered closer to *Di. pseudoseriata* (CBS 124906) with high bootstrap support (ML/BI 100%/1). The asexual morph of *Diplodia pseudoseriata* was introduced by Pérez et al. (2010), collected and isolated from the *Blepharocalyx salicifolius* in Uruguay and its sexual morph has not been reported. The asexual morph of *Diplodia acerigena* differs from *Di. pseudoseriata* in having conidia which become 1-septate when aged. *Diplodia acerigena* shares similar sexual morph characters as of other *Diplodia* species by having immersed to semi-immersed pseudothecia, clavate asci, broadly fusiform to ovoid and hyaline ascospores. However, conidia of *Diplodia acerigena* become brown and septate when aged, which is rarely observed in any other sexual morph species of this genus.

***Diplodia mutila* (Fr.) Mont., Ann. Sci. nat., sér. 2, 1: 302. 1834.**

MycoBank No: 201741

Fig. 9

Sphaeria mutila Fr., Syst. Mycol. (Lundae) 2: 424. 1823. Basionym.

≡ *Physalospora mutila* (Fr.) N.E. Stevens, Mycologia 28: 333. 1936.

= *Botryosphaeria stevensii* Shoemaker, Canad. J. Bot. 42: 1299. 1964.

Description. *Saprobic* on decaying branches of *Camellia oleifera*. **Sexual morph:** Not observed. **Asexual morph:** Coelomycetous, **Conidiomata** 330–394 × 215–230 μm (\bar{x} = 362 × 223 μm, n = 10), immersed, erumpent, gregarious, dark brown to black, subglobose, unilocular. **Ostiole** 48.5–67 μm diam., central. **Peridium** 29–38 μm wide, thick-walled, outer and inner layers composed of 1–2 layers dark brown **textura angularis**, intermediate layers composed of 3–5 layers of hyaline cells of **textura angularis**. **Conidiophores** reduced to conidiogenous cells. **Conidiogenous cells** 8.5–12 × 3–5 μm (\bar{x} = 10 × 4 μm, n = 20), cylindrical, thin-walled, hyaline, holoblastic, indeterminate, proliferating at the same level to produce periclinal thickenings, or proliferating percurrently giving rise to 2–3 indistinct annellations. **Conidia** 19–21 × 9.5–11 μm (\bar{x} = 20 × 10.5 μm, n = 30), L/W ratio = 2, oblong, with broadly rounded apex and truncate base, thick-walled, wall externally smooth, roughened on the inner surface, hyaline, aseptate, becoming dark brown when aged.

Culture characteristics. Colonies on PDA initially olivaceous buff in the center of the colony and white at the edge, becoming olivaceous within 7 d on the surface, with smooth edge.

Materials examined. CHINA, Sichuan Province, Jiangyou City, Shuanghe County, 31°54'10"N, 104°55'57"E, elevation 657 m, on dead branches of *Camellia oleifera*,

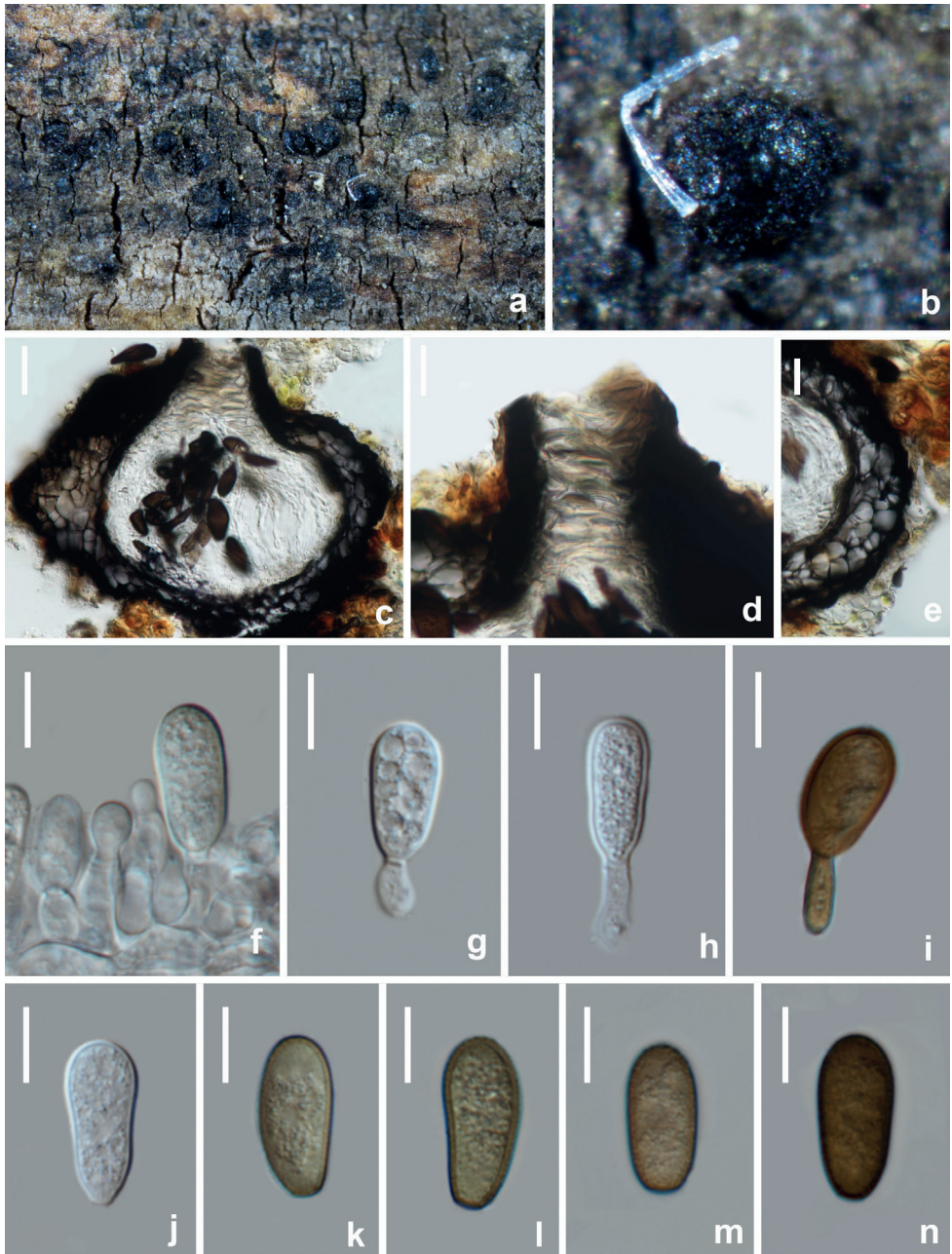


Figure 9. *Diplodia mutila* (HUEST 22.0069, new host record) **a, b** appearance of conidiomata on natural substrate **c** vertical section of conidioma **d** ostiole **e** section of peridium **f–i** conidiogenous cells and developing conidia **j** hyaline immature conidium **k–n** mature brown conidia. Scale bars: 40 μm (**c**); 20 μm (**d, e**); 10 μm (**f–n**).

11th July 2021, W.L Li, 286 (HUEST 22.0069), living culture UESTCC 22.0068; *ibid.*, 289 (HUEST 22.0068), living culture UESTCC 22.0067; *ibid.*, Guangyuan city, Qingchuan County, 32°40'38"N, 105°28'57"E, elevation 634 m, on dead branches of *Olea europaea*, 20th April 2021, W.L Li, 188 (HUEST 22.0065), living culture UESTCC 22.0064; *ibid.*, 257 (HUEST 22.0070), living culture UESTCC 22.0069; *ibid.*, on dead branches of *Vernicia fordii*, 20th April 2021, W.L Li, 238 (HUEST 22.0066), living culture UESTCC 22.0065; *ibid.*, Chengdu City, Pidu District, 30°49'27"N, 103°47'42"E, elevation 442 m, on dead branches of *Pistacia chinensis*, 5th March 2021, W.L Li, A61 (HUEST 22.0064), living culture UESTCC 22.0063. Additional sequences: LSU: OQ164832 (UESTCC 22.0063), OQ164830 (UESTCC 22.0064), OQ164831 (UESTCC 22.0065).

Notes. The phylogenetic tree show that six strains isolated from *Camellia oleifera*, *Olea europaea* and *Vernicia fordii* nested with *Diplodia mutila* (CBS 112553) with a moderate bootstrap support (ML/BI 86%/1). *Diplodia mutila*, the type of the genus, is a well-known and most commonly reported species. It has been recorded mainly from woody substrates, and it is known from more than 50 hosts (Batista et al. 2021). Morphologically, one of the isolates obtained in this study UESTCC 22.0068 shares similar conidia shape and size with *Di. mutila*, but hardly observed the mature conidia with septa. We identify these taxa as *Di. mutila* based on morphology and phylogeny evidences. This is the first report of *Di. mutila*, isolated from *Camellia oleifera*, *Olea europaea* and *Vernicia fordii*.

***Diplodia pistaciicola* L.W. Li & Jian K. Liu, sp. nov.**

Mycobank No: 847166

Fig. 10

Etymology. The epithet “*pistaciicola*” refers to the host genus *Pistacia*, on which the holotype was collected.

Holotype. HKAS 125890.

Description. *Saprobic* on decaying branches of *Pistacia chinensis*. **Sexual morph:** Not observed. **Asexual morph:** Coelomycetous, **Conidiomata** 353–441 × 274.5–316 µm (\bar{x} = 397 × 295 µm, n = 10), immersed, forming split-like opening on the host, solitary or gregarious, globose to subglobose, dark brown to black, unilocular, papillate, ostiolate. **Ostiole** 38–49.5 µm diam., conical or circular, centrally located. **Peridium** 42–60 µm wide, composed of thick walled, dark brown to hyaline cells of **textura angularis**. **Conidiophores** reduced to conidiogenous cells. **Conidiogenous cells** 10–14 × 3–4 µm (\bar{x} = 12 × 3.5 µm, n = 20), holoblastic, discrete, cylindrical, hyaline, smooth, indeterminate, arising from the inner cavity of the conidiomata. **Conidia** 24.5–27 × 11–13 µm (\bar{x} = 25.5 × 12 µm, n = 30), L/W ratio = 2.2, ellipsoid to obovoid, aseptate, hyaline, thick-walled, guttulate.

Culture characteristics. Conidia germinate on PDA within 12 h. Colonies growing on PDA, reaching a diameter of 4 cm after five days at 25 °C, effuse, velvety, with

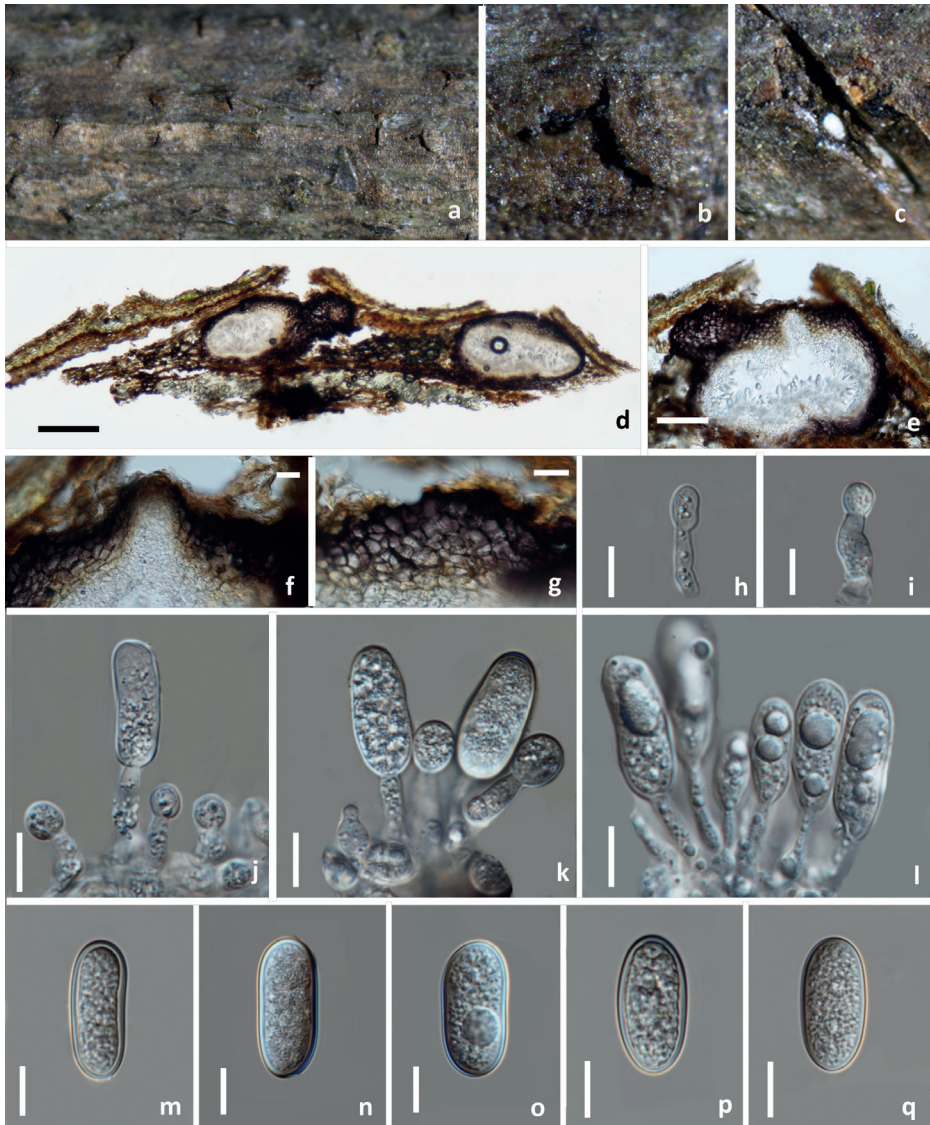


Figure 10. *Diplodia pistaciicola* (HKAS 125890, holotype) **a–c** appearance of conidiomata on natural substrate **d, e** vertical section of conidiomata/conidioma **f** ostiole **g** section of peridium **h–l** conidiogenous cells and developing conidia **m–q** hyaline aseptate conidia. Scale bars: 200 μm (**d**); 50 μm (**e**); 20 μm (**f, g**); 10 μm (**h–q**).

entire to slightly undulate edge. The early stage of the colony is white, later turning dark olivaceous and dark gray in reverse.

Material examined. CHINA, Sichuan Province, Chengdu City, Pidu District, 30°49'27"N, 103°47'42"E, elevation 442 m, on dead branches of *Pistacia chinensis* (Anacardiaceae), 5th March 2021, W.L Li, 049 (HKAS 125890, holotype), ex-type

living culture UESTCC 22.0070 = CGMCC 3.24156; *ibid.*, 049B (HUEST 22.0072 isotype), ex-isotype living culture UESTCC 22.0071. Additional sequence: LSU: OQ164833 (CGMCC 3.24156).

Notes. Phylogenetic analyses showed that two strains of *Diplodia pistaciicola* isolated from *Pistacia chinensis* are distinct but closely related to *Di. agrifolia* (CBS 124.30). The comparison of ITS, *tef1* and *tub2* of these two species indicate 5 bp (502), 3bp (224), 9 bp (425) differences, respectively. Morphologically, *Di. agrifolia* differs from *Di. pistaciicola* in producing two to three times larger ascomata than that of *Di. pistaciicola* (721–836 vs. 274.5–316 μm) and possessing smaller conidia (27–36.5 \times 14.5–17.8 μm vs. 24.5–27 \times 11–13 μm). In addition, conidia of *Di. pistaciicola* are hyaline, aseptate, rarely becoming pale brown and uniseptate with age, whereas conidia of *Di. agrifolia* are mostly dark brown and uniseptate before discharge from pycnidia.

***Diplodia seriata* De Not., Micr. Ital. Dec. 4: 6. (1942).**

MycoBank No: 180468

Fig. 11

Description. *Saprobic* on decaying branches of *Camellia oleifera*. **Sexual morph:** **Ascomata** 301–343 \times 293–340 (\bar{x} = 322 \times 316 μm , n = 10), more or less subglobose, solitary or gregarious, semi-immersed, medium brown to dark brown, unilocular, papillate, ostiolate. **Ostiole** 72–78 μm diam., conical or circular, central, papillate, periphysate. **Peridium** 33–44 μm wide, composed of dark brown, 4–6 layers of **textura angularis**. **Pseudoparaphyses** 2–2.5 μm wide, hyaline, branched, septate. **Asci** 112–141 \times 27.5–30 μm (\bar{x} = 126 \times 28.5 μm , n = 30), clavate, stipitate, bitunicate, containing eight, biseriate ascospores. **Ascospores** 31.5–32.5 \times 12–13.5 μm (\bar{x} = 32 \times 13 μm , n = 30), L/W ratio = 2.5, broadly fusiform to oval, widest in the middle, both ends obtuse, hyaline, moderately thick-walled, smooth, becoming brown when aged. **Asexual morph:** Not observed.

Culture characteristics. Ascospores germinate on PDA within 12 h. Colonies growing on PDA, reaching a diameter of 4 cm after five days at 25 °C, effuse, velvety, with entire to slightly undulate edge.

Material examined. CHINA, Sichuan Province, Jiangyou City, shuanghe County, 31°54'10"N, 104°55'57"E, elevation 656 m, on dead branches of *Camellia oleifera*, 10th June 2021, W.L Li, 288 (HUEST 22.0073), living culture UESTCC 22.0072.

Notes. The morphology of the taxa isolated from decaying woody oil plants is similar to *Diplodia seriata*. In the multi-gene phylogenetic analysis, our new collection clustered with the ex-type strain of *Di. seriata* (CBS 112555) with strong bootstrap support. *Diplodia seriata* has been isolated from a wide range of hosts (121 species) and has a worldwide distribution (reported in 46 countries) (Batista et al. 2021). This is the first report of *Di. seriata* isolated from *Camellia oleifera*.

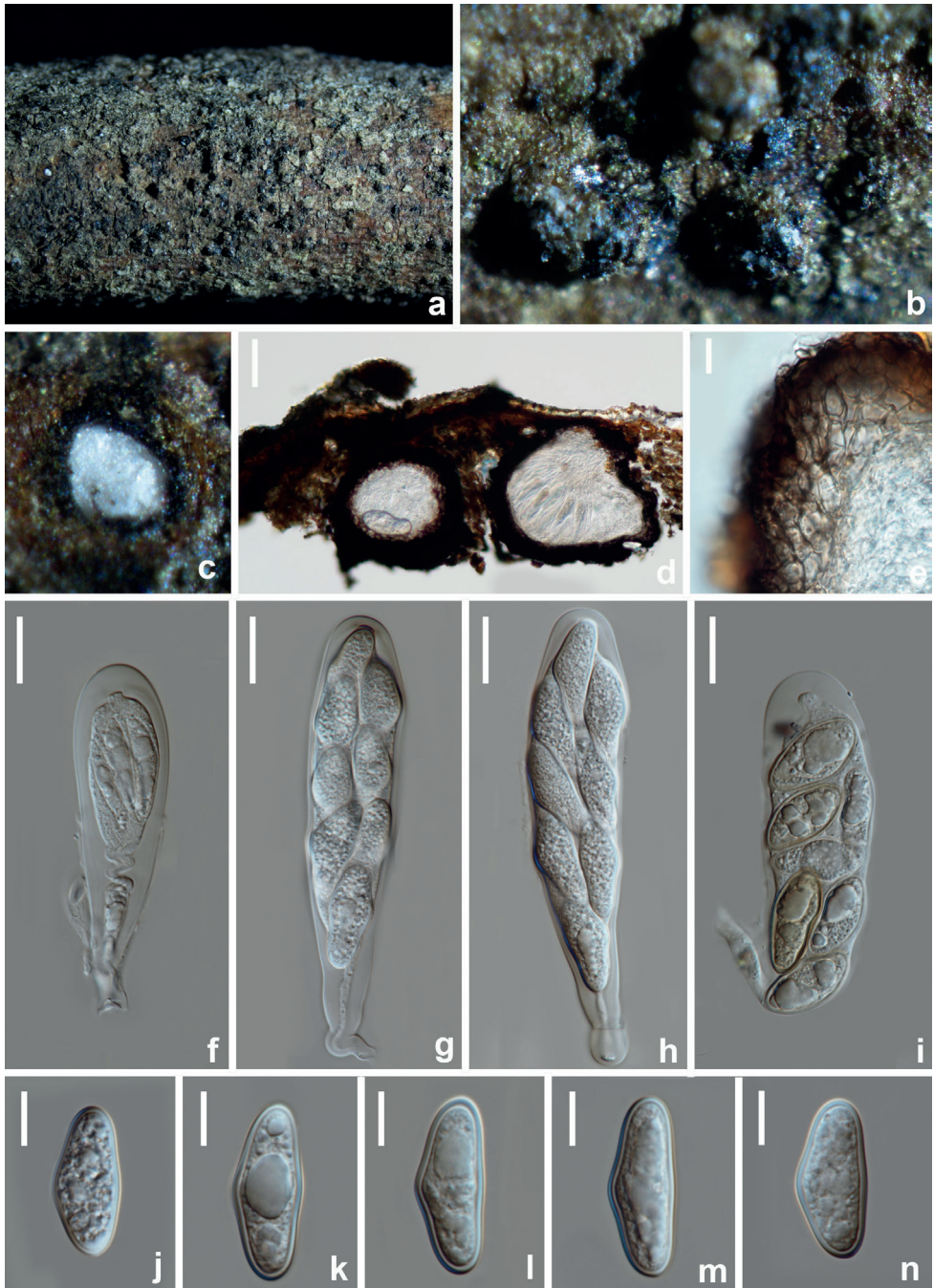


Figure 11. *Diploдия seriata* (HUEST 22.0073, new host record) **a-c** appearance of ascomata on natural substrate **d** vertical section of ascomata **e** section of peridium **f-i** asci **j-n** ascospores. Scale bars: 100 μm (**d**); 10 μm (**e, j-n**); 20 μm (**f-i**).

***Dothiorella camelliae* L.W. Li & Jian K. Liu, sp. nov.**

Mycobank No: 847167

Fig. 12

Etymology. The epithet “*camelliae*” refers to the host genus *Camellia*, on which the holotype was collected.

Holotype. HKAS 125892.

Description. *Saprobic* on decaying branches of *Camellia oleifera*. **Sexual morph:** **Ascomata** 199–222 × 237–269 μm (\bar{x} = 210.5 × 253 μm, n = 10), submerged in the substrate, partly erumpent at maturity, solitary or gregarious, dark brown to black, subglobose, multilocular or unilocular. **Ostiole** 17–37 μm diam., central. **Peridium** 35–43 μm wide, thick-walled, outer layers composed of 1–2 layers dark brown cells of *textura angularis*, becoming hyaline towards the inner region. **Pseudoparaphyses** 3–4 μm wide, hyaline, frequently aseptate. **Asci** 80–96 × 22–25 μm (\bar{x} = 88 × 23.5 μm, n = 30), stipitate, clavate, thick-walled, bitunicate, (6–)8-spored, irregularly biseriolate. **Ascospores** 21–25 × 9.5–12 μm (\bar{x} = 23 × 10.5 μm, n = 30), L/W ratio = 2, oblong, ovate to sub-clavate, (0–)1-septate, slightly constricted at the septum, hyaline to dark brown, moderately thick-walled, straight or inequilateral, basal cell tapering towards the acute end. **Asexual morph:** Not observed.

Culture characteristics. Ascospores germinate on PDA within 12 h. Colonies growing on PDA, reaching a diameter of 4 cm after five days at 25 °C, effuse, velvety, with entire to slightly undulate edge. Surface initially white and later turning dark olivaceous from the surrounding of the colony and dark gray in reverse.

Materials examined. CHINA, Sichuan Province, Leshan City, Wutongqiao District, 29°22'28"N, 103°45'49"E, elevation 383 m, on dead branches of *Camellia oleifera* (Theaceae), 23th July 2021, Z.P Liu, 351 (HKAS 125892, holotype), ex-type living culture UESTCC 22.0081 = CGMCC 3.24158; *ibid.*, 347 (HUEST 22.0081), living culture UESTCC 22.0080; *ibid.*, Shizhong District, 29°42'13"N, 103°52'25"E, elevation 356 m, on dead branches of *Paeonia suffruticosa*, 23th July 2021, W.L Li, A240 (HUEST 22.0080), living culture UESTCC 22.0079; *ibid.*, A234 (HUEST 22.0079), living culture UESTCC 22.0078. Additional sequences: LSU: OQ164834 (CGMCC 3.24158), OQ164835 (UESTCC 22.0079), OQ164836 (UESTCC 22.0078).

Notes. Four strains isolated from *Vernicia fordii* and *Camellia oleifera* occupy a basal position in the *Dothiorella* phylogenetic tree by forming a well-supported sub-clade sister to *Do. zanthoxyli* (ML/BI 97%/1, Fig. 4). The BLASTn searches of the ITS sequence of *Dothiorella zanthoxyli* resulted in 97% matches with *Neofusicoccum vitifusiforme* BRIP64010, the *tef1* showed 91.23% matches with *Do. symphoricarposicola* BL158, and the *tub2* BLASTn results indicated 96.53% similarity with *Do. uruguayensis* CBS 124908 and *Do. viticola* B116-3. *Dothiorella camelliae* can be distinguished from *Do. zanthoxyli* in the size of ascomata, ascus and L/W ratio of ascospores (Table 3). *Dothiorella camelliae* resembles the sexual morph of *Do. sarmentorum* in producing immersed to sub-immersed ascomata, clavate asci and ovate to sub-clavate, hyaline to

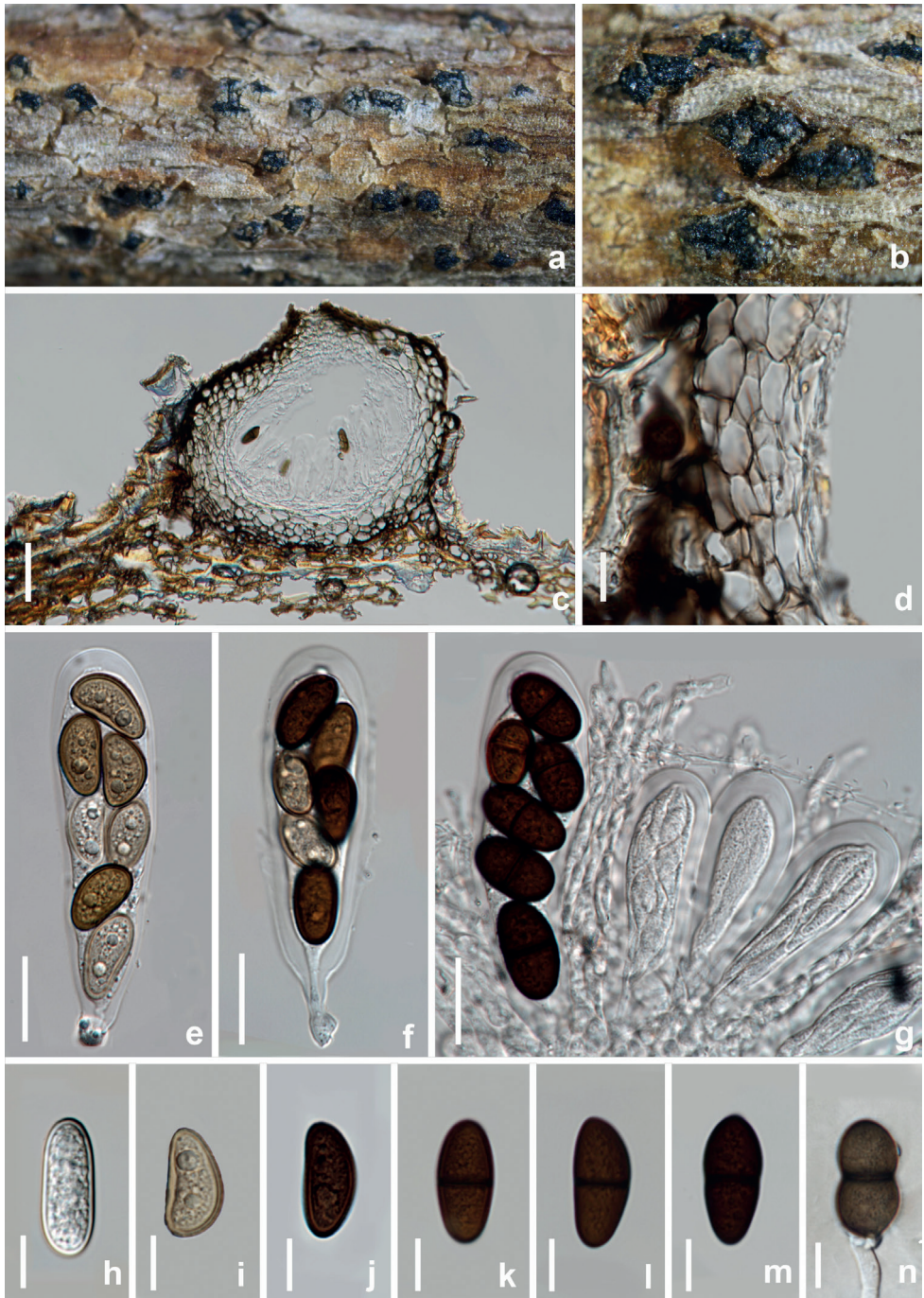


Figure 12. *Dothiorella camelliae* (HKAS 125892, holotype) **a, b** appearance of ascomata on natural substrate **c** vertical section of ascoma **d** section of peridium **e–g** asci **h–m** ascospores **n** germinated ascospore. Scale bars: 50 μm (**c**); 10 μm (**d, h–n**); 20 μm (**e–g**).

Table 3. A morphological comparison of the sexual morph of three *Dothiorella* species.

Taxa	Ascomata (µm)	Asci (µm)	Peridium (µm)	Ascospores		
				Size(µm)	Color	L/W ratio
<i>Dothiorella camelliae</i>	199–222 × 237–269	80–96 × 22–25	35–43	21–25 × 9.5–12	Hyaline to dark brown	2
<i>Dothiorella sarmentorum</i>	350–400	140–210 × 17–24	50–75	24.5–25.5 × 11.5–12.5	Dark brown	2.4
<i>Dothiorella zanthoxyli</i>	258–280 × 170–174	63.5–77 × 20–24.5	35–40	22.5–25 × 9.5–11	Hyaline to dark brown	2.6

brown conidia with (0–)1-septate. However, *Do. sarmentorum* morphologically can be distinguished from *Do. camelliae* in having larger ascomata (350–400 µm vs. 237–269 µm), thicker peridium (50–75 µm vs. 35–43 µm), and longer asci (140–210 µm vs. 80–96 µm) (Table 3). Phylogenetically, these two species reside in two distinct clades.

***Dothiorella sarmentorum* (Fr.) A.J.L. Phillips, J. Luque & A. Alves, Mycologia 97: 522. (2005).**

MycoBank No: 501403

Fig. 13

Sphaeria sarmentorum Fr., K. svenska Vetensk-Acad. Handl. 39: 107. 1818. Basionym.
 ≡ *Diplodia sarmentorum* (Fr.) Fr., Summ. veg. Scand. (Stockholm) 2: 417. 1849.
 = *Diplodia pruni* Fuckel, Jahrb. Nassauischen Vereins Naturk., 23–24: 169. 1870 [1869].
 = *Botryosphaeria sarmentorum* A.J.L. Phillips, J. Luque & A. Alves, Mycologia 97: 522. 2005.

Description. *Saprobic* on decaying branches of *Pistacia chinensis*. **Sexual morph:** Not observed. **Asexual morph: Conidiomata** 278–338 × 240–280 µm (\bar{x} = 308 × 260 µm, n = 10), immersed, erumpent, forming split-like opening on the host, gregarious, globose to subglobose, dark brown to black, unilocular or multilocular, papillate, ostiole. **Ostiole** 52–57 µm diam., conical or circular, centrally located. **Peridium** 28.5–44 µm, comprising 5–8 layers of thick-walled, dark brown to hyaline cells arranged in a *textura angularis*. **Conidiophores** reduced to conidiogenous cells. **Conidiogenous cells** 2.5–3.5 × 6–9 µm (\bar{x} = 3 × 7.5 µm, n = 20), holoblastic, discrete, cylindrical, hyaline, smooth, indeterminate, proliferating at the same level giving rise to periclinal thickenings, or rarely proliferating percurrently to form one or two close, indistinct annellations. **Conidia** 21.5–24 × 9–10 µm (\bar{x} = 22.5 × 9.5 µm, n = 30), L/W ratio = 2.4, ellipsoid to obovoid, with rounded ends, initially hyaline and aseptate becoming pigmented brown and 1-septate often while still attached to conidiogenous cell, brown walled, slightly constricted at the septum.

Culture characteristics. Conidia germinate on PDA within 12 h. Colonies growing on PDA, reaching a diameter of 4 cm after three days at 25 °C, effuse, velvety, with

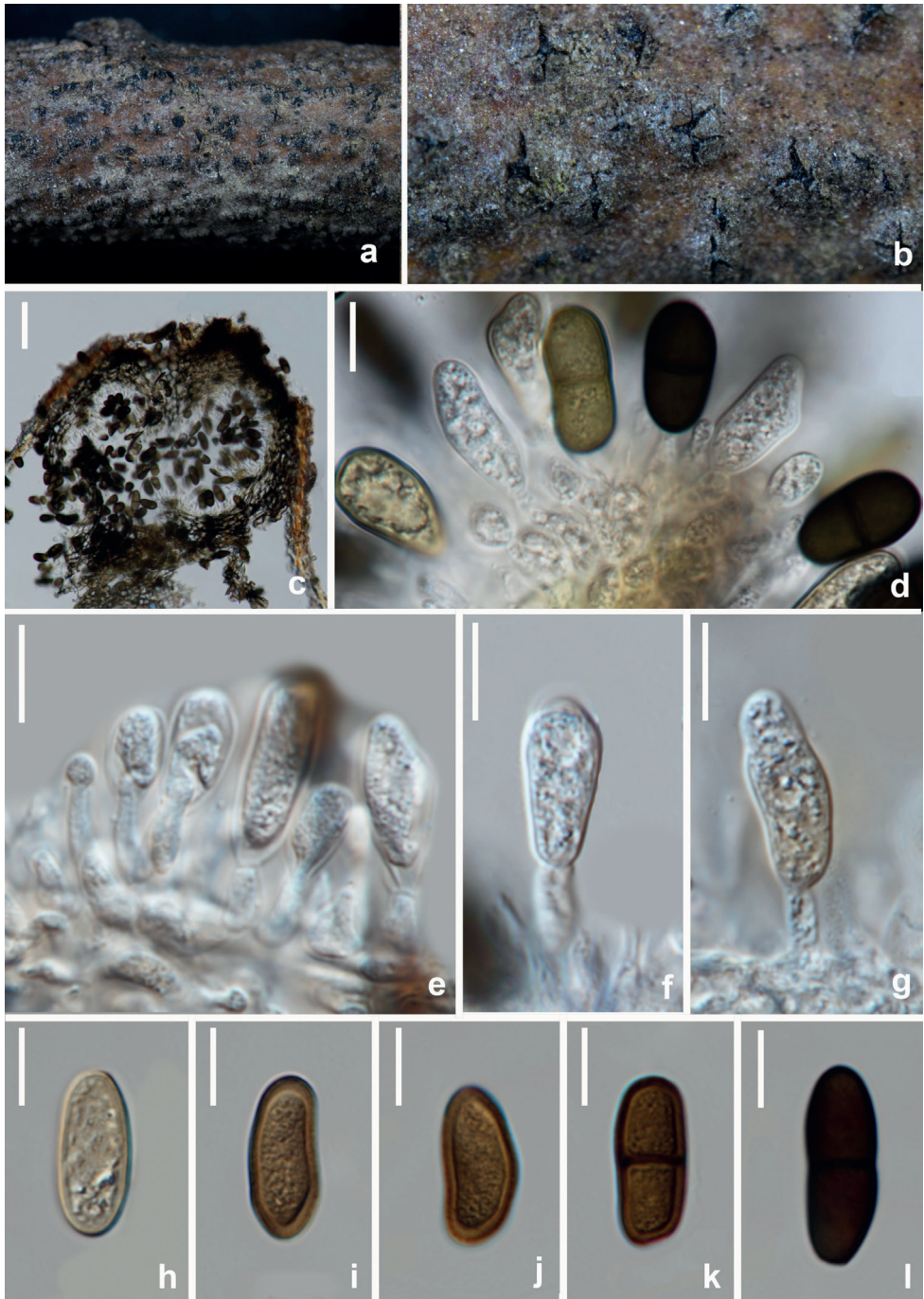


Figure 13. *Dothiorella sarmentorum* (HUEST 22.0077, new host record) **a, b** appearance of conidiomata on natural substrate **c** vertical section of conidioma **d–g** conidiogenous cells and developing conidia **h–l** brown conidia. Scale bars: 50 μm (**c**); 10 μm (**d–l**).

entire to slightly undulate edge. Surface initially white and later turning dark olivaceous from the surrounding of the colony and dark gray in reverse.

Materials examined. CHINA, Sichuan Province, Chengdu City, Pidu District, 30°19'57"N, 103°59'47"E, elevation 442 m, on dead branches of *Pistacia chinensis*, 19th March 2021, W.L Li, 072 (HUEST 22.0077), living culture UESTCC 22.0076; *ibid.*, Guangyuan City, Qingchuan County, 32°40'38"N, 105°28'57"E, elevation 638 m, 20th April 2021, W.L Li, A189 (HUEST 22.0078), living culture UESTCC 22.0077. Additional sequences: LSU: OQ164837 (UESTCC 22.0076), OQ164838 (UESTCC 22.0077).

Notes. *Dothiorella sarmentorum* was introduced by Phillips et al (2005) with both asexual and sexual morphs. Recently, nine *Dothiorella* species (*Do. californica*, *Do. iberica*, *Do. italica*, *Do. guttulata*, *Do. omnivora*, *Do. parva*, *Do. sempervirentis*, *Do. symphoricarpicola*, *Do. vidmadera*) were synonymized under *Do. Sarmentorum* by Zhang et al. (2021) based on phylogenetic analyses. Two isolates obtained in the present study clustered with the group of *Do. sarmentorum* taxa in the phylogenetic analyses (Fig. 4).

***Dothiorella zanthoxyli* L.W. Li & Jian K. Liu, sp. nov.**

MycoBank No: 847168

Fig. 14

Etymology. The epithet “*zanthoxyli*” refers to the host genus *Zanthoxylum*, on which the holotype was collected.

Holotype. HKAS 125893.

Description. *Saprobic* on decaying branches of *Zanthoxylum bungeanum*. **Sexual morph: Ascumata** 258–280 × 170–174 μm (\bar{x} = 269 × 172 μm, n = 10), submerged in the substrate, partly erumpent at maturity, solitary or gregarious, dark brown to black, subglobose, unilocular. **Ostiole** 42–44 μm diam., central. **Peridium** 35–40 μm wide, thick-walled, outer layers composed of 3–5 layers dark brown cells of *textura angularis*, becoming hyaline towards the inner region. **Pseudoparaphyses** 3–4.5 μm wide, hyaline, frequently aseptate. **Asci** 63.5–77 × 20–24.5 μm (\bar{x} = 70 × 22.5 μm, n = 30), short stipe, clavate, thick-walled, bitunicate, 8-spored, irregularly biseriate. **Ascospores** 22.5–25 × 9.5–11 μm (\bar{x} = 24 × 10 μm, n = 30), L/W ratio = 2.6, oblong, ovate to sub-clavate, (0–)1-septate, slightly constricted at the septum, hyaline to dark brown, moderately thick-walled, straight or inequilateral, basal cell tapering towards the acute end. **Asexual morph:** Not observed.

Culture characteristics. Ascospores germinate on PDA within 12 h. Colonies growing on PDA, reaching a diameter of 4 cm after five days at 25 °C, effuse, velvety, with entire to slightly undulate edge. Surface initially white and later turning dark olivaceous from the surrounding of the colony. Dark gray in reverse.

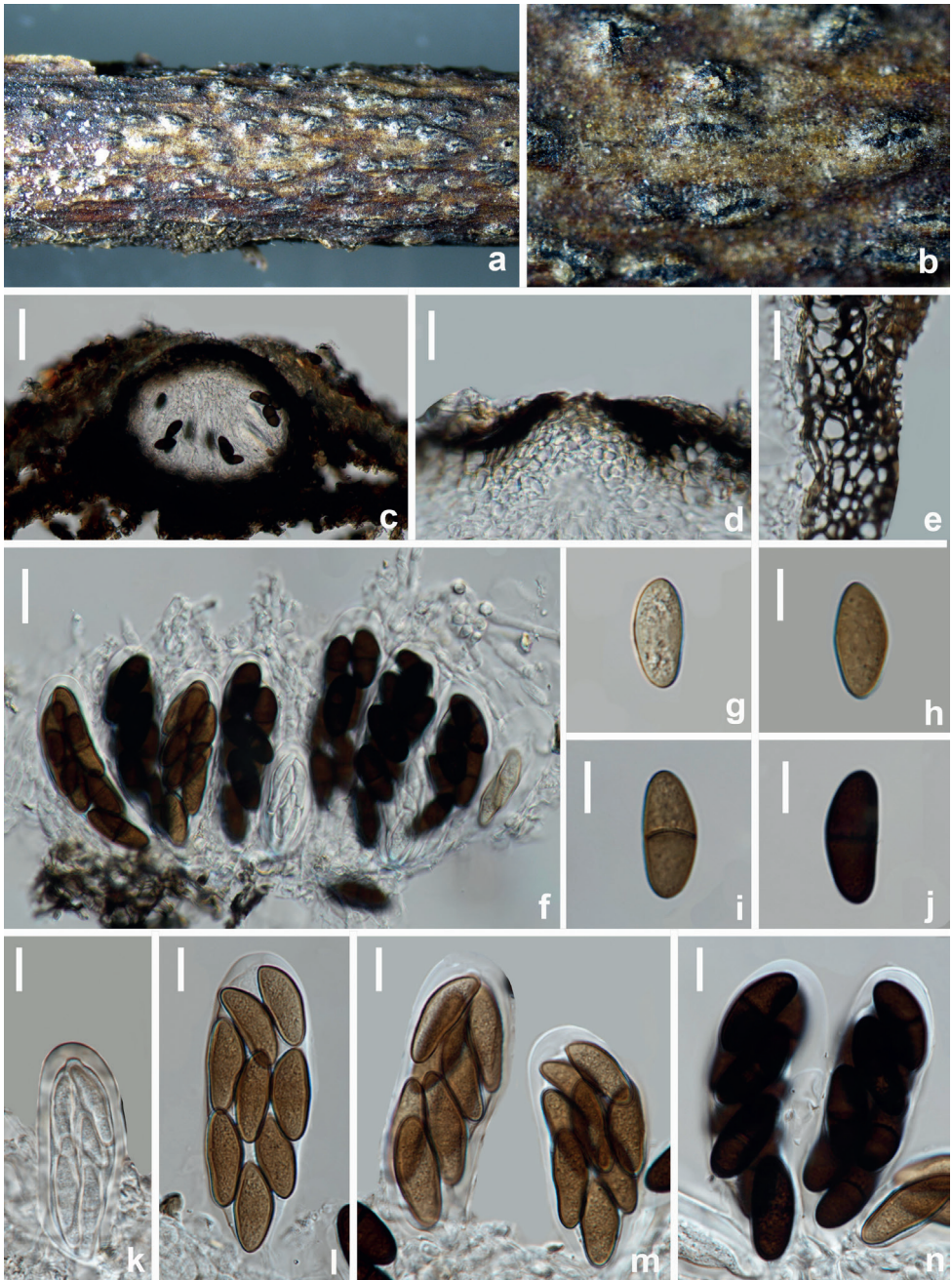


Figure 14. *Dothiorella zanthoxyli* (HKAS 125893, holotype) **a, b** appearance of ascomata on natural substrate **c** vertical section of ascoma **d** ostiole **e** section of peridium **f, k–n** asci **g–j** brown ascospores. Scale bars: 50 μm (**c**); 20 μm (**d–f**); 10 μm (**g–n**).

Materials examined. CHINA, Sichuan Province, Yanan City, Hanyuan County, 29°16'51"N, 102°37'48"E, elevation 1,689 m, on dead branches of *Zanthoxylum bungeanum* (Rutaceae), 30th October 2021, W.L Li, 504 (HKAS 125893, holotype), ex-type living culture UESTCC 22.0082 = CGMCC 3.24159; *ibid.*, 506 (HUEST 22.0084), living culture UESTCC 22.0083; *ibid.*, 507 (HUEST 22.0085), living culture UESTCC 22.0084. Additional sequences: LSU: OQ164839 (CGMCC 3.24159), OQ164840 (UESTCC 22.0083), OQ164841 (UESTCC 22.0084).

Notes. Three strains of *Dothiorella zanthoxyli* isolated from *Zanthoxylum bungeanum* correspond well with sexual morph of *Dothiorella* described by Phillips et al. (2013), but morphologically differ from other species (*Do. camelliae*, *Do. iberica* and *Do. sarmentorum*) in the size of ascomata and asci (Table 3). A comparison of ITS and *tef1* nucleotides shows that *Do. zanthoxyli* is significantly different from its sister species, *Do. camelliae* by 4/550 bp (0.72%) in ITS and 14/242 bp (5.8%) in *tef1*. In the phylogenetic analysis, these two species formed two distinct clades in *Dothiorella* (Fig. 4).

***Neofusicoccum parvum* (Pennycook & Samuels) Crous, Slippers & A.J.L. Phillips, Stud. Mycol. 55: 248. (2006).**

MycoBank No: 500879

Fig. 15

Fusicoccum parvum Pennycook & Samuels, Mycotaxon 24: 455. 1985. Basionym.
= *Botryosphaeria parva* Pennycook & Samuels, Mycotaxon 24: 455. 1985.

Description. *Saprobic* on decaying branches of *Idesia polycarpa*. **Sexual morph:** **Ascomata** 284–321 × 129–223 µm (\bar{x} = 302.5 × 176 µm, n = 10), pseudothecial, forming a botryose aggregation of up to 30, solitary or gregarious, stromatic, immersed, partially erumpent when mature, dark brown to black, more or less circular, multi-loculate, individual locules 143.5–161 µm diam, thick-walled. **Peridium** 59–78 µm diam., composed of several layers of thick-walled, pale brown cells of *textura angularis*. **Ostiole** 43.5–58 µm wide, circular, central, papillate. **Asci** 95–99 × 20–21.5 µm (\bar{x} = 97 × 20.5 µm, n = 30), (6–)8-spored, bitunicate, fissitunicate, cylindrical to clavate, apex rounded with an ocular chamber, sometimes short pedicellate. **Ascospores** 18.5–23 × 7–10.5 µm (\bar{x} = 20.5 × 9 µm, n = 30), L/W ratio = 3, fusoid to ovoid, with tapered ends and appearing spindle-shape, hyaline, aseptate, externally smooth, internally finely verruculose, biseriate in ascus. **Asexual morph:** Not observed.

Culture characteristics. Ascospores germinate on PDA within 12 h. Colonies growing on PDA, reaching a diam., of 7 cm after five days at 25 °C, effuse, velvety, with entire to slightly undulate edge. Surface initially white and later turning dark olivaceous from the surrounding of the colony and dark gray in reverse.

Materials examined. CHINA, Sichuan Province, Leshan City, Jingyan County, 29°30'27"N, 103°57'14"E, elevation 682 m, on dead branches of *Idesia polycarpa*, 23th

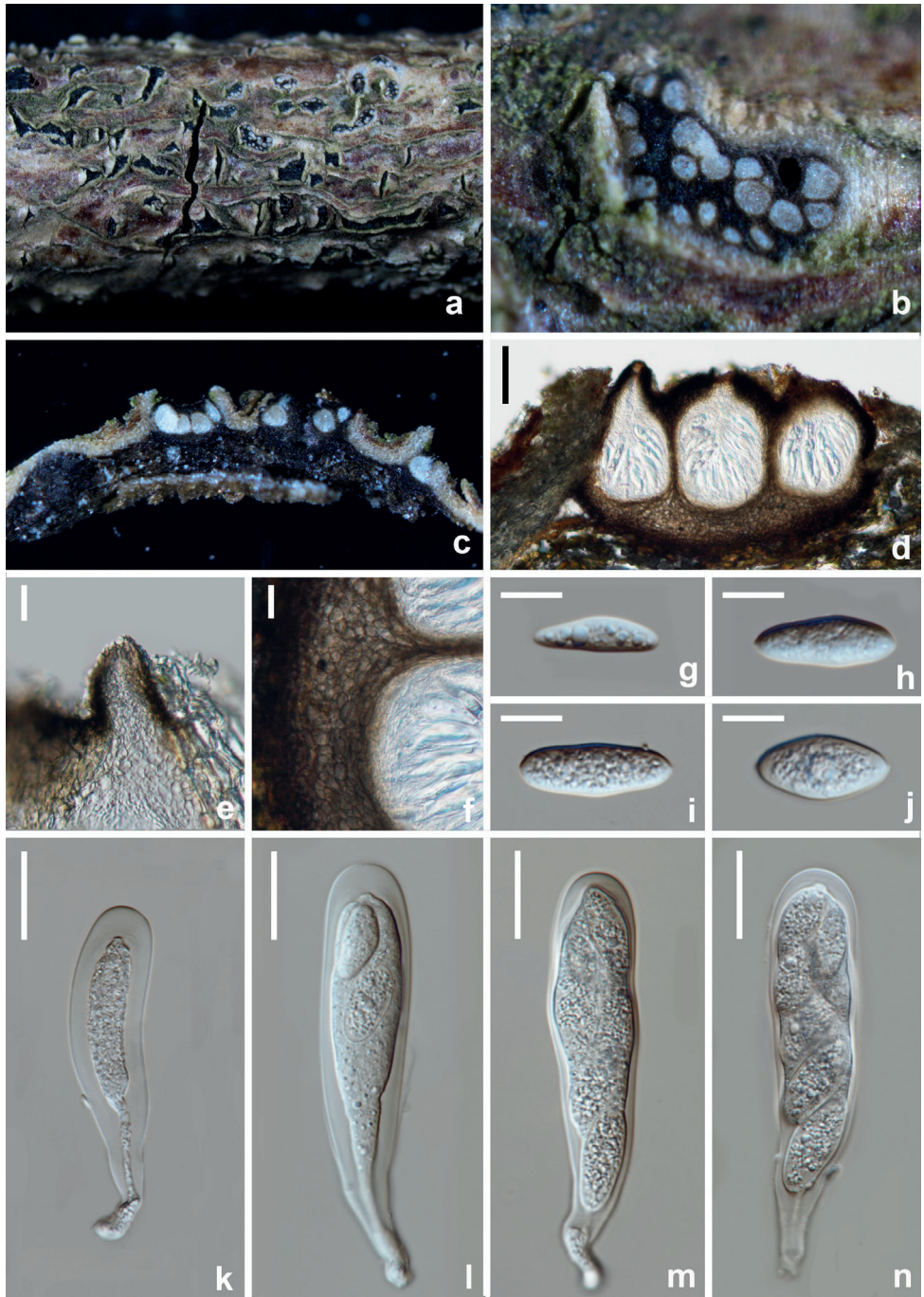


Figure 15. *Neofusicoccum parvum* (HUEST 22.0097, new host record) **a, b** appearance of ascomata on natural substrate **c, d** vertical section of ascomata **e** ostiole **f** section of peridium **g–j** ascospores **k, l** immature asci **m, n** mature asci. Scale bars: 100 μm (**d**); 25 μm (**e, f**); 10 μm (**g–j**); 20 μm (**k–n**).

July 2021, W.L. Li, STZ 327 (HUEST 22.0095), living culture UESTCC 22.0094; *ibid.*, STZ 359 (HUEST 22.0094), living culture UESTCC 22.0093; *ibid.*, Leshan City, Shizhong District, 29°42'13"N, 103°52'25"E, elevation 356 m, on dead branches of *Paeonia suffruticosa*, 23rd July 2021, W.L. Li, YMD 366 (HUEST 22.0096), living culture UESTCC 22.0095; *ibid.*, Guangyuan City, Qingchuan County, 32°40'38"N, 105°28'57"E, elevation 638 m, on dead branches of *Vernicia fordii*, 20th April 2021, W.L. Li, YT 175 (HUEST 22.0097), living culture UESTCC 22.0096.

Notes. The morphology of our collections obtained from decaying woody oil plants are similar to the original description of *Neofusicoccum parvum* (Crous et al. 2006). In the multi-gene phylogenetic analysis, these four isolates clustered together (ML/BI 75%/0.99) with the ex-type of *N. parvum*. *Neofusicoccum parvum* has a wide range of hosts and has a worldwide distribution (Phillips et al. 2013). This is the first report of *N. parvum* on *Idesia polycarpa*.

***Sardiniella guizhouensis* Y.Y. Chen & Jian K. Liu. Phytotaxa 508 (2): 190. (2021).**

MycoBank No: 558352

Fig. 16

Description. *Saprobic* on decaying branches of *Pistacia chinensis*. **Sexual morph:** Not observed. **Asexual morph:** **Conidiomata** 223–232 × 150–176 µm (\bar{x} = 227.5 × 163 µm, n = 10), dark brown to black, globose, submerged in the substrate, partially erumpent at maturity, ostiolate. **Ostiole** 28.5–45 µm diam., circular, central. **Peridium** 21–30 µm thick, composed of dark brown thick-walled cells of *textura angularis*, becoming thin-walled and hyaline towards the inner region. **Conidiophores** reduced to conidiogenous cells. **Conidiogenous cells** 6–9.5 × 3.5–5 µm (\bar{x} = 7.5 × 4 µm, n = 20), hyaline, short obpyriform to subcylindrical, holoblastic, indeterminate. **Conidia** 20.5–24 × 11.5–14 µm (\bar{x} = 22 × 13 µm, n = 30), L/W ratio = 1.6, ellipsoid to ovoid with both ends rounded, hyaline, aseptate, externally smooth, internally finely verruculose.

Culture characteristics. Conidia germinate on PDA within 12 h. Colonies growing on PDA, reaching a diameter of 7 cm after five days at 25 °C, effuse, velvety, with entire to slightly undulate edge. Surface initially white and later turning dark olivaceous from the surrounding of the colony and dark gray in reverse.

Material examined. CHINA, Sichuan Province, Chengdu City, Pidu District, 29°16'50.70"N, 102°37'47.53"E, elevation 442 m, on dead branches of *Pistacia chinensis*, 19th March 2021, W.L. Li, 047 (HUEST 22.0101), living culture UESTCC 22.0100; *ibid.*, 070 (HUEST 22.0102), living culture UESTCC 22.0101; *ibid.*, 071 (HUEST 22.0100), living culture UESTCC 22.0099; *ibid.*, 150 (HUEST 22.0098), living culture UESTCC 22.0097; *ibid.*, 151 (HUEST 22.0099), living culture UESTCC 22.0098; *ibid.*, A39 (HUEST 22.0103), living culture UESTCC 22.0102; *ibid.*, A40 (HUEST 22.0104), living culture UESTCC 22.0103. Additional

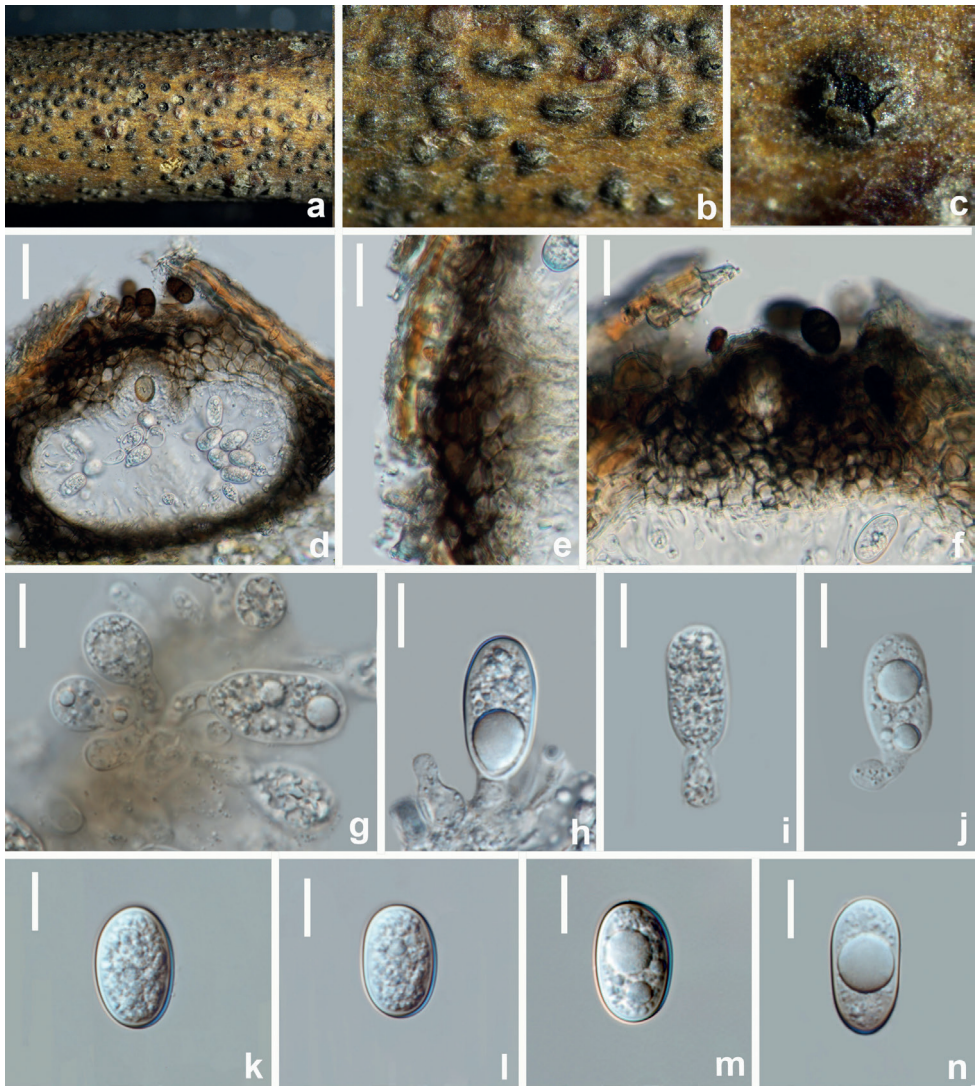


Figure 16. *Sardiniella guizhouensis* (HUEST 22.0100, new host record) **a–c** appearance of conidiomata on natural substrate **d** vertical section of conidioma **e** section of peridium **f** ostiole **g–j** conidiogenous cells and developing conidia **k–n** conidia. Scale bars: 40 μm (**d**); 20 μm (**e**, **f**); 10 μm (**g–n**).

sequences: LSU: OQ164842 (UESTCC 22.0100), OQ164843 (UESTCC 22.0101), OQ164844 (UESTCC 22.0099), OQ164845 (UESTCC 22.0097), OQ164846 (UESTCC 22.0098), OQ164847 (UESTCC 22.0102).

Notes. Seven isolates of our collection are morphologically similar to the original description of *Sardiniella guizhouensis* (Chen et al. 2021). The multi-gene phylogenetic

analysis showed that the newly obtained isolates clustered together with ex-type of *Sa. guizhouensis* (CGMCC 3.19222) and this is the first report of *Sa. guizhouensis* from *Pistacia chinensis*.

***Sphaeropsis citrigena* (A.J.L. Phillips, P.R. Johnst. & Pennycook) A.J.L. Phillips & A. Alves. Stud. Mycol. 76, 157. (2013).**

MycoBank No: 805463

Fig. 17

Description. *Saprobic* on decaying branches of *Camellia oleifera*. **Sexual morph:** *Ascomata* 219–252 × 216–241 μm (\bar{x} = 235.5 × 228.5 μm, n = 10), brown to black, solitary or aggregated, immersed, becoming erumpent, ostiolate. **Ostiole** 71–92 μm, central, relatively broad. **Peridium** 37.5–45 μm diam., composed of several layers of dark brown cells of *textura angularis*. **Pseudoparaphyses** 1.5–2 μm wide, hyaline, smooth, septate. **Asci** 93.5–107 × 28.5–33 μm (\bar{x} = 100 × 30.5 μm, n = 30), bitunicate, 8-spored, stipitate, thick-walled, with well-developed apical chamber. **Ascospores** 29–35 × 13–15 μm (\bar{x} = 32 × 14 μm, n = 30), L/W ratio = 2.3, yellowish brown to dark brown, ellipsoid to ovoid with both ends rounded, with an apiculus at either end, aseptate, externally smooth, internally finely verruculose, widest in middle to upper third. **Asexual morph:** Not observed.

Culture characteristics. Ascospores germinate on PDA within 12 h. Colonies growing on PDA, reaching a diam. of 7 cm after five days at 25 °C, effuse, velvety, with entire to slightly undulate edge. Surface initially white and later turning dark olivaceous from the surrounding of the colony and dark gray in reverse.

Materials examined. CHINA, Sichuan Province, Chengdu City, Pidu District, 31°54'10"N, 104°55'57"E, 656 m, on dead branches of *Camellia oleifera*, 10th June 2021, W.L Li, 285 (HUEST 22.0107), living culture UESTCC 22.0106; *ibid.*, on dead branches of *Acer truncatum*, 30°19'57"N, 103°59'47"E, elevation 442 m, 19th March 2021, W.L Li, A33 (HUEST 22.0106), living culture UESTCC 22.0105. Additional sequence: LSU: OQ164848 (UESTCC 22.0105).

Notes. The phylogenetic tree shows that two isolates of *Sphaeropsis* from our collection clustered together with the ex-type strain of *Sp. citrigena* (ICMP 16812) with high bootstrap support (ML/BI 100%/1). *Sphaeropsis citrigena* was first described as *Phaeobotryosphaeria citrigena* by Phillips et al. (2008), later transferred to *Sphaeropsis* based on morphological and phylogenetic analyses (Phillips et al. 2013). The new collection (UESTCC 22.0105) isolated from *Camellia oleifera* resembles *Sp. citrigena* isolated from *Citrus sinensis* (Phillips et al. 2013) in the shape of asci and ascospores, though their asci are somewhat smaller than those of *Sp. citrigena* (93.5–107 × 28.5–33 μm vs. 180–230 × 35–43 μm). In addition, there are no base pair differences in ITS and *tef1* sequences of these two strains. We, thus, identify the new collection as *Sp. citrigena* and this is the first record of *Sp. citrigena* from *Camellia oleifera*.

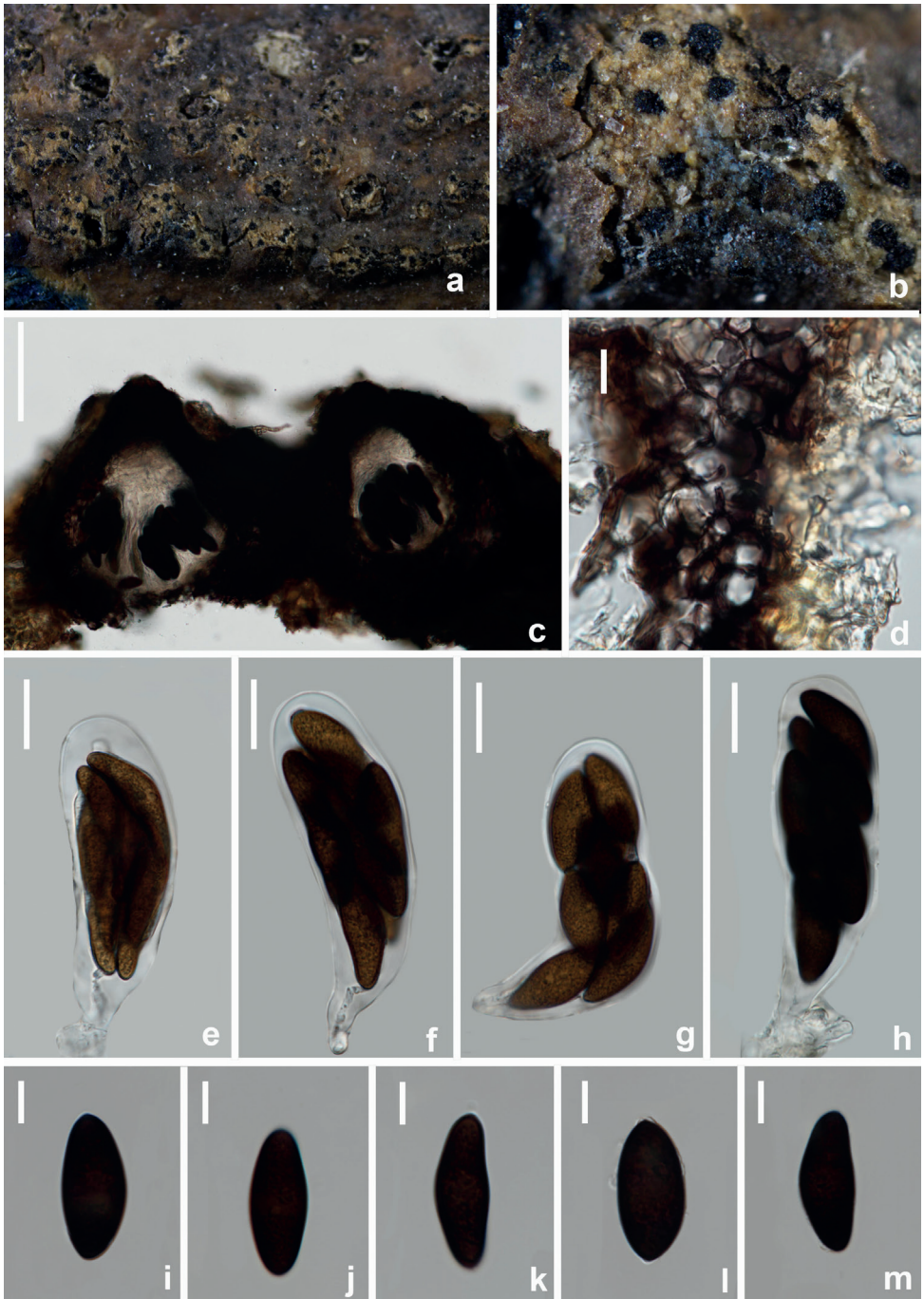


Figure 17. *Sphaeropsis citrigena* (HUEST 22.0107, new host record) **a, b** appearance of ascomata on natural substrate **c** vertical section of ascomata **d** section of peridium **e-h** mature asci **i-m** dark brown ascospores. Scale bars: 100 μm (**c**); 20 μm (**d-h**); 10 μm (**i-m**).

***Sphaeropsis guizhouensis* Y.Y. Chen, A. J. Dissanayake & Jian K. Liu., J. Fungi 7, 893. (2021).**

MycoBank No: 558475

Fig. 18

Description. *Saprobic* on decayed branched of *Camellia oleifera*. **Sexual morph:** *Ascstromata* 166–198 × 146.5–175 µm (\bar{x} = 182 × 160.5 µm, n = 20), initially immersed under host epidermis, becoming semi-immersed to erumpent, solitary or gregarious, uniloculate, black, globose to subglobose, membranous, ostiolate. **Ostiole** 75–80 µm wide, central, papillate, pale brown, relatively broad, periphysate. **Peridium** 23–27 µm wide, comprising 3–5 layers of relatively thick-walled, dark brown to black-walled cells arranged in a *textura angularis*. **Pseudoparaphyses** 2–2.5 µm diam., hyphae-like, numerous, embedded in a gelatinous matrix. **Asci** 87.5–135 × 28.5–35 µm (\bar{x} = 111 × 32 µm, n = 20), 8-spored, bitunicate, fissitunicate, cylindrical to clavate, sometimes short pedicellate, mostly long pedicellate, apex rounded with an ocular chamber. **Ascospores** 28.5–33 × 13–15 µm (\bar{x} = 30.5 × 14 µm, n = 20), overlapping uniseriate to biseriate, ellipsoidal to obovoid, pale brown to dark brown, septate, slightly wide at the center, minutely guttulate, smooth-walled. **Asexual morph:** Not observed.

Culture characteristics. Ascospores germinate on PDA within 12 h. Colonies growing on PDA, reaching a diam. of 7 cm after five days at 25 °C, effuse, velvety, with entire to slightly undulate edge. Surface initially white and later turning dark olivaceous from the surrounding of the colony and dark gray in reverse.

Material examined. CHINA, Sichuan Province, Chengdu City, Pidu District, on dead branches of *Pistacia chinensis*, 30°19'57"N, 103°59'47"E, elevation 442 m, 24th March 2021, W.L Li, 290 (HUEST 22.0105), living culture UESTCC 22.0104.

Notes. *Sphaeropsis guizhouensis* was introduced by Dissanayake et al. (2021) and isolated from an unknown host. One isolate obtained in the present study clustered with the ex-type isolate of *Sp. guizhouensis* (CGMCC 3.20352) in the phylogenetic analyses of combined ITS and *tefl* sequence data with high bootstrap support. A comparison of ITS and *tefl* shows that there are no base pair differences between the isolates of UESTCC 22.0104 and CGMCC 3.20352. The new collection is morphologically similar to *Sp. guizhouensis*, with immersed to erumpent, black ascstromata and biseriate, aseptate, ellipsoid to obovoid, thick-walled conidia. In addition, ascospores become brown and septate when aged. Considering similar morphology and strong molecular evidence, we identify UESTCC 22.0104 as *Sp. guizhouensis* and this is the first record of *Sp. guizhouensis* on *Camellia oleifera*.

Diversity of Botryosphaeriales fungi collected in this study

Based on the phylogenetic and morphological analyses, 50 Botryosphaeriales isolates collected from the five regions (Chengdu, Guangyuan, Leshan, Mianyang and Yaan City) in Sichuan Province were identified as 16 species. Of these, *Botryosphaeria dothidea* was the most prevalent species (20%), followed by *Sphaeropsis guizhouensis*

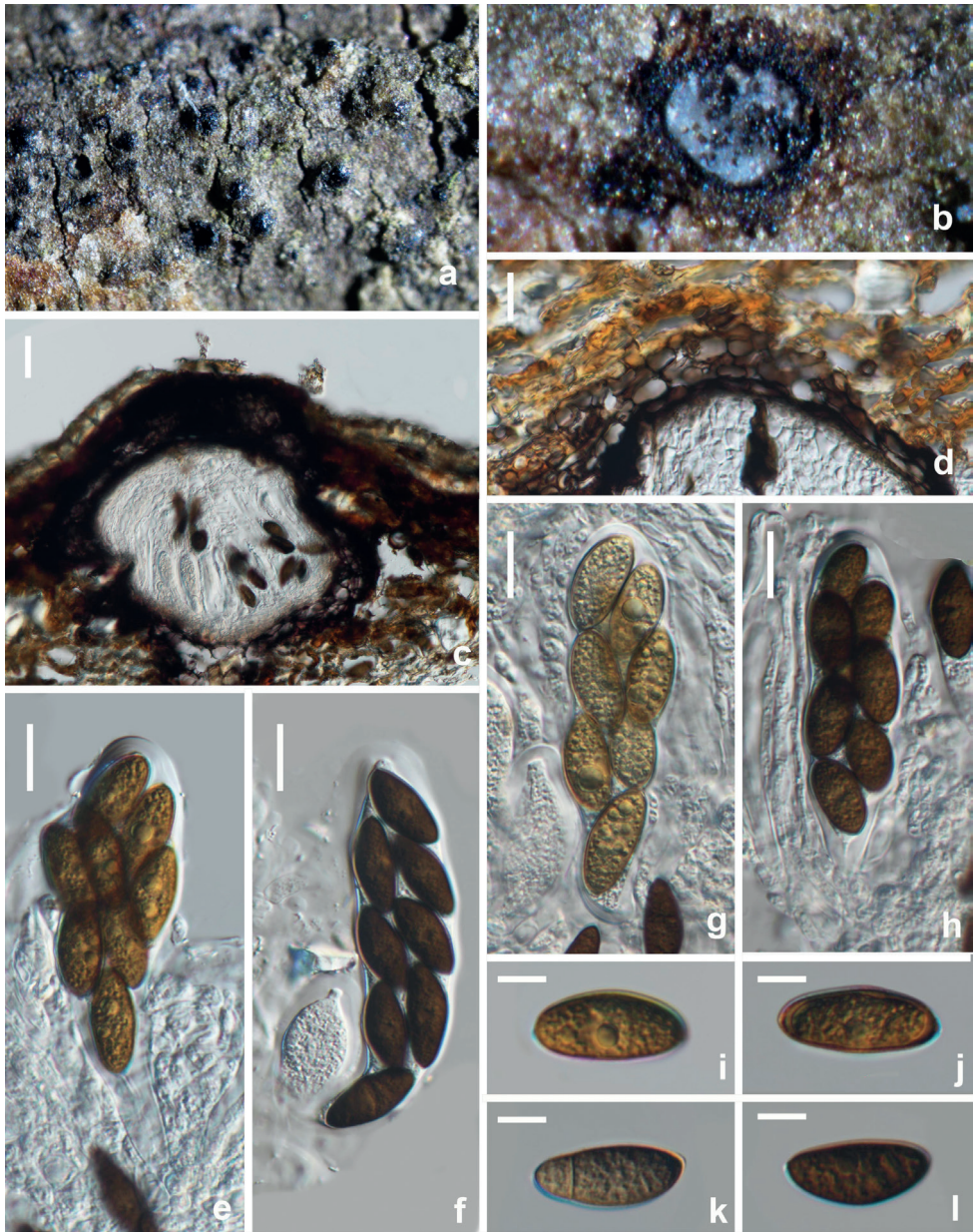


Figure 18. *Sphaeropsis guizhouensis* (HUEST 22.0105, new host record) **a, b** appearance of ascomata on natural substrate **c** vertical section of ascoma **d** section of peridium **e–h** mature asci **i–l** brown ascospores. Scale bars: 20 μ m (**c–h**); 5 μ m (**i–l**).

(14%) and *Diplodia mutila* (12%) (Fig. 19a). *Aplosporella ginkgonis*, *Barriopsis tectonae* and *Sphaeropsis guizhouensis* were identified only once. There are 14 isolates (28%) isolated from *Pistacia chinensis*, including *Di. acerigena*, *Di. mutila*, *Di. pistaciicola*,

including *Ba. tectonae*, *Bo. dothidea*, *Bo. fabicerciana*, *Di. mutila* and *Do. sarmentorum*. Relatively few strains were found on *Idesia polycarpa*, *Paeonia suffruticosa* and *Vernicia fordii*, as each host presents two species, respectively. As of final conclusion, *Bo. dothidea* were isolated from five hosts, *Di. mutila* were isolated from four hosts, *N. parvum* were isolated from three hosts, *Bo. fabicerciana*, *Di. acericola*, *Do. camelliae*, *Do. sarmentorum* and *Sp. citrigena* were isolated from two hosts, but several fungal isolates were only isolated from one host species, such as *A. prunicola*, *Sa. guizhouensis* and *Sp. guizhouensis* (Fig. 19b).

Discussion

In this study, 48 Botryosphaeriaceae isolates and two Aplosporellaceae isolates were obtained from woody oil plants in Sichuan Province, China, and they were identified as 16 species based on morphological characters and multi-gene phylogenetic analyses. These species included *Aplosporella prunicola*, *A. ginkgonis*, *Barriopsis tectonae*, *Botryosphaeria dothidea*, *Bo. fabicerciana*, *Diplodia acerigena*, *Di. mutila*, *Di. pistaciicola*, *Di. seriata*, *Dothiorella camelliae*, *Do. sarmentorum*, *Do. zanthoxyli*, *Neofusicoccum parvum*, *Sardiniella guizhouensis*, *Sphaeropsis citrigena* and *Sp. guizhouensis*. Of these, *Di. acerigena*, *Di. pistaciicola*, *Do. camelliae* and *Do. zanthoxyli* are introduced as novel species. Descriptions, illustrations and notes were provided for 13 species, and only sequences data were provided for the remaining three species viz. *Barriopsis tectonae*, *Botryosphaeria dothidea* and *Bo. fabicerciana* due to low specimen quality.

According to previous studies, *Barriopsis tectonae*, *Sardiniella guizhouensis*, *Sphaeropsis citrigena* and *Sp. guizhouensis* have limited geographical distribution. So far, *Barriopsis tectonae* has been reported from China, Thailand and South Africa (Doilom et al. 2014; Dissanayake et al. 2021). *Sardiniella guizhouensis* and *Sphaeropsis guizhouensis* were only found in China while *Sp. citrigena* was isolated from China, Colombia and New Zealand. It's worth noting that most of the species obtained from this study were also reported previously from Guizhou province (Dissanayake et al. 2021). Earlier studies have shown that the distribution of Botryosphaeriaceae species is influenced by the climate condition (Úrbez-Torres et al. 2006; Pitt et al. 2010; Li et al. 2020; Vivas et al. 2021). Thus, we speculate that the adjacent geographical location and similar climatic conditions may be important reasons for the similarity of fungal species isolated from the Sichuan and Guizhou provinces.

The remaining Botryosphaeriaceae species identified in this study are all well-known and reported from various geographic regions. *Botryosphaeria dothidea*, *Di. seriata* and *Ne. parvum* are recognized to be globally distributed while *Di. mutila* and *Do. sarmentorum* are founded only in the temperate and Mediterranean areas. In addition, these species have a broad host range. Batista et al. (2021) reported *Neofusicoccum parvum* from 223 hosts, *B. dothidea* from 403 hosts and *Di. seriata* from 121 hosts. *Diplodia mutila* and *Di. seriata* have previously been reported on *Olea europaea* in Uruguay (Hernández-Rodríguez et al. 2022). *Botryosphaeria dothidea* was recently isolated from diseased *Camellia oleifera* in China (Hao et al. 2022). In this study, *Bo. dothidea*,

Di. mutila and *Ne. parvum* occurred on most of the woody oil plants species we examined. However, some common genera e. g. *Lasiodiplodia*, *Neodeightonia* and *Phaeobotryon* have never been collected from this group of hosts (Fig. 19). The absence of these genera from there is likely a sampling effect.

Aplosporella (Aplosporellaceae) was introduced by Spegazzini (1880) with *A. chlo-rostroma* as the genetic type. In a previous study, *Aplosporella* represents anamorph lineage within the Botryosphaeriaceae. Slippers et al. (2013) later proposed the family Aplosporellaceae to accommodate *Aplosporella* and *Bagnisiella*. *Aplosporella* species are infrequently isolated in China. *Aplosporella ginkgonis*, isolated from Gansu Province, was first described by Du et al. (2017) while *Aplosporella macropycnidia* was reported in Yunnan Province. Subsequently, Jiang et al. (2021) isolated a new collection of *A. prunicola*. However, other species have not been recorded in China. Our study revealed new host records of *A. ginkgonis* and *A. prunicola*. Though the phylogenetic analyses indicated that *A. yalgorensis* and *A. prunicola* have a low genetic divergence (Taylor et al. 2008, in this study), *A. yalgorensis* is still considered as a different species as it differs from other *Aplosporella* species (including *A. prunicola*) by its pitted conidial walls.

Though there are more than 1,000 *Diplodia* epithets listed in Index fungorum (www. Index Fungorum. Accessed in November 2022), presently only 30 species are accepted in this genus based on phylogenetic analyses (Slippers et al. 2017; Wu et al. 2021). Holomorphic species in *Diplodia* are *Di. tsugae*, *Di. seriata*, *Di. mutila* and *Di. sapinea*. This study revealed two previously known *Diplodia* species, *Di. mutila* and *Di. seriata*, and two new species, *Di. acerigena* and *Di. pistaciicola*. Among them, *Di. acerigena* is a holomorphic species, as its sexual stage was observed on the dead branches of *Acer truncatum*, and the asexual stage produced on culture (PDA). However, the sexual morph of *Di. mutila* and *Di. pistaciicola*, as well as the asexual morph of *Di. seriata* have not been observed on woody oil plants.

Dothiorella was established by Saccardo with *Do. pyrenophora* as the type species (Saccardo 1880). Recently, *Dothiorella* encountered a series of revisions as many species in this genus have been reduced to synonymy, such as *Do. americana*, *Do. eriobotryae* and *Do. iberica* (Dissanayake et al. 2021; Zhang et al. 2021). So far, 31 species are valid in *Dothiorella*. Most of the species were reported as the asexual morph of *Dothiorella* and the sexual stage is rarely founded on nature (Dissanayake et al. 2016). Phillips et al. (2013) initiated a link of asexual-sexual morph for *Do. sarmentorum*, *Do. iberica* and *Do. vidmadera*. However, the latter two species were synonymized under *Do. sarmentorum* (Zhang et al. 2021). In this study, two new species *Do. camelliae* and *Do. zanthoxyli* are introduced based on their sexual morphs as well as strong molecular evidences. Besides, new collections of *Do. sarmentorum* is reported on *Pistacia chinensis* for the first time.

Multiple molecular systematic studies, mainly of pathogenic fungi of woody plants (Phillips et al. 2013; Slippers et al. 2013; Dissanayake et al. 2021; Zhang et al. 2021), have generated a robust phylogeny for Botryosphaeriaceae. However, the classification and identification of some species in this family remains a major challenge, due to the reasons 1) With the increase of the number of Botryosphaeriaceae species, morphological feature of inter-genera and inter-species is vague, 2) Some species occurred as asexual morph on nature and it is difficult to establish the link of asexual and sexual

morph, 3) In general, Botryosphaeriaceae species do not show an obvious host specialization, while some populations displayed a certain degree of host association. Thus, the traditional host-based classification system made taxonomic position confusion of some species. Therefore, collection of more fresh specimens is very important for better understanding the life cycle of Botryosphaeriaceae species, their host range (e. g. native plants) and potential pathogenicity.

Acknowledgements

Wen-Li Li thanks Tian Zhang for her help with sample collections and Yan-Peng Chen for the fungal diversity analysis.

This study was supported by the Joint Fund of the National Natural Science Foundation of China and the Karst Science Research Center of Guizhou province (Grant No. U1812401).

References

- Abdollahzadeh J, Zare R, Phillips AJ (2013) Phylogeny and taxonomy of *Botryosphaeria* and *Neofusicoccum* species in Iran, with description of *Botryosphaeria scharifii* sp. nov. *Mycologia* 105(1): 210–220. <https://doi.org/10.3852/12-107>
- Batista E, Lopes A, Alves A (2021) What do we know about Botryosphaeriaceae? An overview of a Worldwide Cured Dataset. *Forests* 12(3): e313. <https://doi.org/10.3390/f12030313>
- Braunsdorf C, Mailänder-Sánchez D, Schaller M (2016) Fungal sensing of host environment. *Cellular Microbiology* 18(9): 1188–1200. <https://doi.org/10.1111/cmi.12610>
- Capella-Gutiérrez S, Silla-Martínez JM, Gabaldón T (2009) trimAl: A tool for automated alignment trimming in large-scale phylogenetic analyses. *Bioinformatics* 25(15): 1972–1973. <https://doi.org/10.1093/bioinformatics/btp348>
- Carbone I, Kohn LM (1999) A method for designing primer sets for speciation studies in filamentous ascomycetes. *Mycologia* 91(3): 553–556. <https://doi.org/10.1080/00275514.1999.12061051>
- Chen SF, Morgan DP, Hasey JK, Anderson K, Michailides TJ (2014) Phylogeny, morphology, distribution, and pathogenicity of Botryosphaeriaceae and Diaporthaceae from English walnut in California. *Plant Disease* 98(5): 636–652. <https://doi.org/10.1094/PDIS-07-13-0706-RE>
- Chen YY, Dissanayake AJ, Liu JK (2021) Additions to Karst Fungi 5: *Sardiniella guizhouensis* sp. nov. (Botryosphaeriaceae) associated with woody hosts in Guizhou province, China. *Phytotaxa* 508(2): 187–196. <https://doi.org/10.11646/phytotaxa.508.2.7>
- Chomnunti P, Hongsanan S, Aguirre-Hudson B, Tian Q, Peršoh D, Dhama MK, Alias AS, Xu JC, Liu XL, Stadler M, Hyde KD (2014) The sooty moulds. *Fungal Diversity* 66(1): 1–36. <https://doi.org/10.1007/s13225-014-0278-5>
- Cloete M, Fourie PH, Damm U, Crous PW, Mostert L (2011) Fungi associated with die-back symptoms of apple and pear trees, a possible inoculum source of grapevine trunk

- disease pathogens. *Phytopathologia Mediterranea* 50: S176–S190. <https://www.jstor.org/stable/26458720>
- Crous PW, Slippers B, Wingfield MJ, Rheeder J, Marasas WF, Philips AJ, Alves A, Burgess T, Barber P, Groenewald JZ (2006) Phylogenetic lineages in the Botryosphaeriaceae. *Studies in Mycology* 55: 235–253. <https://doi.org/10.3114/sim.55.1.235>
- Crous PW, Müller MM, Sánchez RM, Giordano L, Bianchinotti MV, Anderson FE, Groenewald JZ (2015) Resolving *Tiarosporella* spp. allied to Botryosphaeriaceae and Phacidiaceae. *Phytotaxa* 202(2): 073–093. <https://doi.org/10.11646/phytotaxa.202.2>
- Damm U, Fourie PH, Crous PW (2007) *Aplosporella prunicola*, a novel species of anamorphic Botryosphaeriaceae. *Fungal Diversity* 27: 35–43.
- Dissanayake AJ, Phillips A, Li X, Hyde KD (2016) Botryosphaeriaceae: Current status of genera and species. *Mycosphere* 7(7): 1001–1073. <https://doi.org/10.5943/mycosphere/si/1b/13>
- Dissanayake AJ, Bhunjun CS, Maharachchikumbura SSN, Liu JK (2020) Applied aspects of methods to infer phylogenetic relationships amongst fungi. *Mycosphere* 11(1): 2653–2677. <https://doi.org/10.5943/mycosphere/11/1/18>
- Dissanayake AJ, Chen YY, Cheewangkoon R, Liu JK (2021) Occurrence and morpho-molecular identification of Botryosphaeriales species from Guizhou Province, China. *Journal of Fungi* 7(11): e893. <https://doi.org/10.3390/jof7110893>
- Doilom M, Shuttleworth LA, Roux J, Chukeatirote E, Hyde KD (2014) *Barriopsis tectonae* sp. nov. a new species of Botryosphaeriaceae from *Tectona grandis* (teak) in Thailand. *Phytotaxa* 176: 081–091. <https://doi.org/10.11646/phytotaxa.176.1.10>
- Du Z, Fan XL, Yang Q, Hyde KD, Tian CM (2017) *Aplosporella ginkgonis* (Aplosporellaceae, Botryosphaeriales), a new species isolated from *Ginkgo biloba* in China. *Mycosphere* 8(2): 1246–1252. <https://doi.org/10.5943/mycosphere/8/2/8>
- Farr D, Rossman A (2021) Fungal Databases, US National Fungus Collections, ARS, USDA, 2020.
- Glass NL, Donaldson GC (1995) Development of primer sets designed for use with the PCR to amplify conserved genes from filamentous ascomycetes. *Applied and Environmental Microbiology* 61(4): 1323–1330. <https://doi.org/10.1128/aem.61.4.1323-1330.1995>
- Gramaje D, Agustí-Brisach C, Pérez-Sierra A, Moralejo E, Olmo D, Mostert L, Damm U, Armengol J (2012) Fungal trunk pathogens associated with wood decay of almond trees on Mallorca (Spain). *Persoonia* 28(1): 1–13. <https://doi.org/10.3767/003158512X626155>
- Granata G, Faedda R, Sidoti A (2011) First report of canker disease caused by *Diplodia olivarum* on carob tree in Italy. *Plant Disease* 95(6): 776–776. <https://doi.org/10.1094/PDIS-12-10-0870>
- Hao Y, Liao K, Guo J, Jin C, Guo K, Chen M (2022) First report of *Botryosphaeria dothidea* causing leaf spot of *Camellia oleifera* in China. *Plant Disease* PDIS-06-22-1452-PDN. <https://doi.org/10.1094/PDIS-06-22-1452-PDN>
- Hernández-Rodríguez L, Mondino-Hintz P, Alaniz-Ferro S (2022) Diversity of Botryosphaeriaceae species causing stem canker and fruit rot in olive trees in Uruguay. *Journal of Phytopathology* 170(4): 264–277. <https://doi.org/10.1111/jph.13078>
- Jiang N, Fan XL, Tian CM (2021) Identification and characterization of leaf-inhabiting fungi from castanea plantations in China. *Journal of Fungi* 7(1): 64. <https://doi.org/10.3390/jof7010064>

- Jimenez Luna I, Besoain X, Saa S, Peach-Fine E, Cadiz Morales F, Riquelme N, Larach A, Morales J, Ezcurra E, Ashworth VETM, Rolshausen PE (2022) Identity and pathogenicity of Botryosphaeriaceae and Diaporthaceae from *Juglans regia* in Chile. *Phytopathologia Mediterranea* 61(1): 79–94. <https://doi.org/10.36253/phyto-12832>
- Katoh K, Rozewicki J, Yamada KD (2019) MAFFT online service: Multiple sequence alignment, interactive sequence choice and visualization. *Briefings in Bioinformatics* 20(4): 1160–1166. <https://doi.org/10.1093/bib/bbx108>
- Lazzizzera C, Frisullo S, Alves A, Lopes J, Phillips AJ (2008) Phylogeny and morphology of *Diplodia* species on olives in southern Italy and description of *Diplodia olivarum* sp. nov. *Fungal Diversity* 31: 63–71.
- Li GQ, Liu FF, Li JQ, Liu QL, Chen SF (2016a) Characterization of *Botryosphaeria dothidea* and *Lasiodiplodia pseudotheobromae* from English walnut in China. *Journal of Phytopathology* 164(5): 348–353. <https://doi.org/10.1111/jph.12422>
- Li P, Wu Z, Liu T, Wang Y (2016b) Biodiversity, phylogeny, and antifungal functions of endophytic fungi associated with *Zanthoxylum bungeanum*. *International Journal of Molecular Sciences* 17(9): e1541. <https://doi.org/10.3390/ijms17091541>
- Li GQ, Slippers B, Wingfield MJ, Chen SF (2020) Variation in Botryosphaeriaceae from *Eucalyptus* plantations in Yunnan Province in southwestern China across a climatic gradient. *IMA Fungus* 11(1): 1–49. <https://doi.org/10.1186/s43008-020-00043-x>
- Linaldeddu BT, Deidda A, Scanu B, Franceschini A, Serra S, Berraf-Tebbal A, Zouaoui Boutiti M, Ben Jamàa M, Phillips AJ (2015) Diversity of Botryosphaeriaceae species associated with grapevine and other woody hosts in Italy, Algeria and Tunisia, with descriptions of *Lasiodiplodia exigua* and *Lasiodiplodia mediterranea* sp. nov. *Fungal Diversity* 71(1): 201–214. <https://doi.org/10.1007/s13225-014-0301-x>
- Linaldeddu B, Maddau L, Franceschini A, Alves A, Phillips A (2016) Botryosphaeriaceae species associated with lentisk dieback in Italy and description of *Diplodia insularis* sp. nov. *Mycosphere* 7(7): 962–977. <https://doi.org/10.5943/mycosphere/si/1b/8>
- Liu JK, Chomnunti P, Cai L, Phookamsak R, Chukeatirote E, Jones EBG, Moslem M, Hyde KD (2010) Phylogeny and morphology of *Neodeightonia palmicola* sp. nov. from palms. *Sydowia* 62(2): 261–276.
- Liu JK, Phookamsak R, Doilom M, Wikee S, Li YM, Ariyawansha H, Boonmee S, Chomnunti P, Dai DQ, Bhat JD, Romero AI, Zhuang WY, Monkai J, Jones EBG, Chukeatirote E, Ko Ko TW, Zhao YC, Wang Y, Hyde KD (2012) Towards a natural classification of Botryosphaeriales. *Fungal Diversity* 57(1): 149–210. <https://doi.org/10.1007/s13225-012-0207-4>
- Nylander JA (2004) MrModeltest v2, Program distributed by the author, Evolutionary Biology Centre. Uppsala University, Uppsala.
- Olmo D, Armengol J, León M, Gramaje D (2016) Characterization and pathogenicity of Botryosphaeriaceae species isolated from almond trees on the island of Mallorca (Spain). *Plant Disease* 100(12): 2483–2491. <https://doi.org/10.1094/PDIS-05-16-0676-RE>
- Panahandeh S, Mohammadi H, Gramaje D (2019) Trunk disease fungi associated with *Syzygium cumini* in Iran. *Plant Disease* 103(4): 711–720. <https://doi.org/10.1094/PDIS-06-18-0923-RE>

- Pérez CA, Wingfield MJ, Slippers B, Altier NA, Blanchette RA (2010) Endophytic and canker-associated Botryosphaeriaceae occurring on non-native *Eucalyptus* and native Myrtaceae trees in Uruguay. *Fungal Diversity* 41(1): 53–69. <https://doi.org/10.1007/s13225-009-0014-8>
- Phillips AJ, Alves A, Correia A, Luque J (2005) Two new species of *Botryosphaeria* with brown, 1-septate ascospores and *Dothiorella* anamorphs. *Mycologia* 97(2): 513–529. <https://doi.org/10.1080/15572536.2006.11832826>
- Phillips AJ, Alves A, Pennycook S, Johnston P, Ramaley A, Akulov A, Crous PW (2008) Resolving the phylogenetic and taxonomic status of dark-spored teleomorph genera in the Botryosphaeriaceae. *Persoonia* 21: 29–55. <https://doi.org/10.3767/003158508X340742>
- Phillips AJ, Alves A, Abdollahzadeh J, Slippers B, Wingfield MJ, Groenewald JZ, Crous PW (2013) The Botryosphaeriaceae: Genera and species known from culture. *Studies in Mycology* 76: 51–167. <https://doi.org/10.3114/sim0021>
- Pitt WM, Huang R, Steel CC, Savocchia S (2010) Identification, distribution and current taxonomy of Botryosphaeriaceae species associated with grapevine decline in New South Wales and South Australia. *Australian Journal of Grape and Wine Research* 16(1): 258–271. <https://doi.org/10.1111/j.1755-0238.2009.00087.x>
- Rambaut A (2006) 2006–2009. FigTree: tree figure drawing tool. Version 1.3. 1. University of Edinburgh.
- Rannala B, Yang ZH (1996) Probability distribution of molecular evolutionary trees: A new method of phylogenetic inference. *Journal of Molecular Evolution* 43(3): 304–311. <https://doi.org/10.1007/BF02338839>
- Rathnayaka AR, Chethana KT, Phillips AJ, Jones EG (2022) Two new species of Botryosphaeriaceae (Botryosphaeriales) and new host/geographical records. *Phytotaxa* 564(1): 8–38. <https://doi.org/10.11646/phytotaxa.564.1.2>
- Ronquist F, Teslenko M, Van Der Mark P, Ayres DL, Darling A, Höhna S, Larget B, Liu L, Suchard MA, Huelsenbeck JP (2012) MrBayes 3.2: Efficient Bayesian phylogenetic inference and model choice across a large model space. *Systematic Biology* 61(3): 539–542. <https://doi.org/10.1093/sysbio/sys029>
- Saccardo PA (1880) *Conspectus generum fungorum Italiae inferiorum nempe ad Sphaeropsideas, Melanconieas et Hyphomyceteas pertinentium systemate sporologico dispositorum*. *Michelia* 2: 1–38.
- Schoch CL, Shoemaker RA, Seifert KA, Hambleton S, Spatafora JW, Crous PW (2006) A multigene phylogeny of the Dothideomycetes using four nuclear loci. *Mycologia* 98(6): 1041–1052. <https://doi.org/10.1080/15572536.2006.11832632>
- Sivanesan A (1984) *The bitunicate ascomycetes and their anamorphs*. J. Cramer.
- Slippers B, Boissin E, Phillips AJ, Groenewald JZ, Lombard L, Wingfield MJ, Postma A, Burgess T, Crous PW (2013) Phylogenetic lineages in the Botryosphaeriales: A systematic and evolutionary framework. *Studies in Mycology* 76: 31–49. <https://doi.org/10.3114/sim0020>
- Slippers B, Crous PW, Jami F, Groenewald JZ, Wingfield MJ (2017) Diversity in the Botryosphaeriales: Looking back, looking forward. *Fungal Biology* 121(4): 307–321. <https://doi.org/10.1016/j.funbio.2017.02.002>

- Spegazzini C (1880) Fungi argentini. *Pugillus tertius* (Continuacion). *Anales de la Sociedad Científica Argentina* 10: 145–168.
- Stamatakis A (2006) RAxML-VI-HPC: Maximum likelihood-based phylogenetic analyses with thousands of taxa and mixed models. *Bioinformatics* 22(21): 2688–2690. <https://doi.org/10.1093/bioinformatics/btl446>
- Taylor K, Barber PA, Hardy GESJ, Burgess TI (2008) Botryosphaeriaceae from tuart (*Eucalyptus gomphocephala*) woodland, including descriptions of four new species. *Mycological Research* 113: 337–353. <https://doi.org/10.1016/j.mycres.2008.11.010>
- Theissen F, Sydow H (1918) Vorentwürfe zu den Pseudosphaeriales. *Annales Mycologici* 16: 1–34.
- Thynne E, McDonald MC, Evans M, Wallwork H, Neate S, Solomon PS (2015) Re-classification of the causal agent of white grain disorder on wheat as three separate species of *Eutiarospora*. *Australasian Plant Pathology* 44(5): 527–539. <https://doi.org/10.1007/s13313-015-0367-2>
- Úrbez-Torres J, Leavitt G, Voegel T, Gubler W (2006) Identification and distribution of *Botryosphaeria* spp. associated with grapevine cankers in California. *Plant Disease* 90(12): 1490–1503. <https://doi.org/10.1094/PD-90-1490>
- Vaidya G, Lohman DJ, Meier R (2011) SequenceMatrix: Concatenation software for the fast assembly of multi-gene datasets with character set and codon information. *Cladistics* 27(2): 171–180. <https://doi.org/10.1111/j.1096-0031.2010.00329.x>
- Vilgalys R, Hester M (1990) Rapid genetic identification and mapping of enzymatically amplified ribosomal DNA from several *Cryptococcus* species. *Journal of Bacteriology* 172(8): 4238–4246. <https://doi.org/10.1128/jb.172.8.4238-4246.1990>
- Vivas M, Mehl JW, Wingfield MJ, Roux J, Slippers B (2021) Botryosphaeriaceae on *Syzygium cordatum* across a latitudinal gradient in South Africa. *Fungal Biology* 125(9): 718–724. <https://doi.org/10.1016/j.funbio.2021.04.006>
- White TJ, Bruns T, Lee S, Taylor JW (1990) Amplification and direct sequencing of fungal ribosomal RNA genes for phylogenetics. In: Innis MA, Gelfand DH, Sninsky JJ, White TJ (Eds) *PCR Protocols: a Guide to Methods and Applications*. New York. <https://doi.org/10.1016/B978-0-12-372180-8.50042-1>
- Wu N, Dissanayake AJ, Chethana KT, Hyde KD, Liu JK (2021) Morpho-phylogenetic evidence reveals *Lasiodiplodia chiangraiensis* sp. nov. (Botryosphaeriaceae) associated with woody hosts in northern Thailand. *Phytotaxa* 508(2): 142–154. <https://doi.org/10.11646/phytotaxa.508.2.3>
- Xiao XE, Wang W, Crous PW, Wang HK, Jiao C, Huang F, Pu ZX, Zhu ZR, Li HY (2021) Species of Botryosphaeriaceae associated with citrus branch diseases in China. *Persoonia* 47(1): 106–135. <https://doi.org/10.3767/persoonia.2021.47.03>
- Yang T, Groenewald JZ, Cheewangkoon R, Jami F, Abdollahzadeh J, Lombard L, Crous PW (2017) Families, genera, and species of Botryosphaeriales. *Fungal Biology* 121(4): 322–346. <https://doi.org/10.1016/j.funbio.2016.11.001>
- Zhang M, Zhang Y, Geng Y, Zang R, Wu H (2017) First report of *Diplodia seriata* causing twig dieback of English walnut in China. *Plant Disease* 101(6): 1036–1036. <https://doi.org/10.1094/PDIS-04-16-0458-PDN>

Zhang W, Groenewald JZ, Lombard L, Schumacher RK, Phillips AJL, Crous PW (2021) Evaluating species in Botryosphaerales. *Persoonia* 46: 63–115. <https://doi.org/10.3767/persoonia.2021.46.03>

Supplementary material I

Taxa and GenBank accession numbers of sequences used in this study

Authors: Wen-Li Li, Rui-Ru Liang, Asha Dissanayake, Jian-Kui Liu

Data type: table (excel document)

Copyright notice: This dataset is made available under the Open Database License (<http://opendatacommons.org/licenses/odbl/1.0/>). The Open Database License (ODbL) is a license agreement intended to allow users to freely share, modify, and use this Dataset while maintaining this same freedom for others, provided that the original source and author(s) are credited.

Link: <https://doi.org/10.3897/mycokeys.97.103118.suppl1>